Tetrahedron Vol. 38, No. 10, pp. 1339 to 1388, 1982
Printed in Great Britain.

0040-4020/82/101339-50$25.00/0

TETRAHEDRON REPORT NUMBER 126

STRUCTURE AND REACTIVITY IN ORGANOMETALLIC CHEMISTRY. AN APPLIED MOLECULAR ORBITAL APPROACH

THOMAS A. ALBRIGHT
Department of Chemistry, University of Houston, Houston, TX 77004, U.S.A.

(*Received in U.S.A.* 19 *August* 1981)

CONTENTS

I. INTRODUCTION

Organometallic chemistry is a very young field on the time-scale of chemistry. Its growth has been confined primarily to the last twenty years. I take here the perhaps overly restrictive definition that organometallic compounds are those that contain at least one transition metal–carbon bond. Thus, the field is a hybrid of organic and coordination chemistry. Much of its interest has been in the ability of complexes to function as homogeneous catalysts.[1] Transition metals confer unique and sometimes very unusual reactivity patterns on coordinated organic molecules.[2] Metals also stabilize such reactive organic molecules as cyclobutadiene, trimethylenemethane, and vinyl alcohol. But apart from these synthetic concerns are also geometric ones. Organometallic molecules present to the chemist a tremendously diverse array of structures that are at the same time beautiful and bewildering. Two relatively simple examples are illustrative. Ferrocene **1** was first proposed a σ-bonded structure by Kealy and Pauson[3] in 1951. The correct π-bonded structure was given in the next year by Wilkinson, Rosenblum, Whiting and

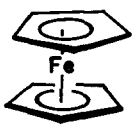

1

2

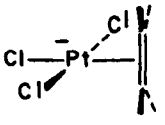

3

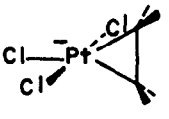

4

Woodward[4] and for the isoelectronic cobalt cation by Fischer and Pfab.[5] The X-ray structure[6] of ferrocene shows that in the solid state all Fe–C distances are nearly equivalent. The use of two vertical lines emanating from iron in **1** is taken to indicate this. One could have explicitly drawn ten Fe–C bonds. Now, organic chemists draw lines between atoms not only to indicate connectivity but also bond order. Herein lies the dilemma, are there ten bonds to iron, two as in **1**, or more difficult to visualize but perhaps more accurate, six? There are a variety of Cp_2ML_n complexes **2** (Cp = cyclopentadienyl) where the Cp rings are bent back and n = 1 – 3. Such compounds are used, for example, in the Ziegler–Natta polymerization process[7] and hydrozirconation.[8] What metals and number of ligands, L, are active? One has the intuitive feeling that the electronic structure of **2** should somehow be related to ferrocene. Another large class of organometallic compounds are π-bonded olefins. The first organometallic compound, **3**, was reported by Zeise in 1827.[9] Are these best represented as π complexes **3**, or metallocyclopropanes **4**? This has been the subject of active controversy for a number of years, We

have a good idea of the electronic factors behind rotational barriers and what should be the equilibrium conformation in organic chemistry. The situation in organometallic chemistry appears on the surface to be more confusing. The barriers for rotation about the metal–olefin axis in analogs of **3** is in the medium range—10–15 kcal/mol.[10] The barrier in the tetrahedrally-based **5** where $L = PR_3$, etc. is extremely

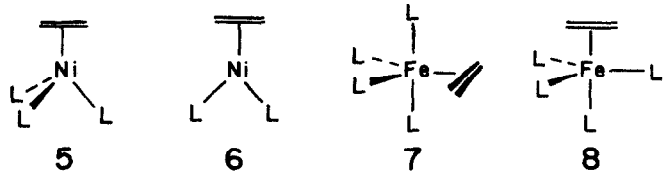

5 **6** **7** **8**

small,[11] probably less than 5 kcal/mol. That in **6** is large—upwards of 20 kcal/mol.[12] We shall see in detail later that the barrier for rigid rotation in **7**(L = CO, etc.) is approximately 30 kcal/mol while that in the related **8** drops to nearly zero. Finally, the process which equivalences ligands in **7** is probably geometrically complicated. Distortion of the arrangement of ligands and rotation operate in concert. It is clear that for this most elementary type of "reaction", internal rotation, not only the metal (or more accurately, the number of d electrons formally assigned to the metal) but also the number of other ligands and their geometrical arrangement play decisive roles in setting the barrier size. The same comment applies to other reactions—we *cannot* forget the other ligands and view the metal as a black-box, supplying or withdrawing electrons from the organic piece.

In this review, a qualitative method for viewing the electronic structure of organometallic molecules will be featured. It is not my intention to review all of the theoretical work in this area, and there has been a considerable amount done.[13] Rather I want to concentrate on one particular method for viewing the electronic structure of organometallic compounds. This approach is called the fragment molecular orbital method.[14] The idea behind it is that the important, valence orbitals of a molecule can be constructed from the valence orbitals of its constituent fragments. For example, the molecular orbitals of the ethylene-ML_n molecules, **3–8**, can be developed by interacting the valence orbitals of the ML_n fragments with the π and π^* orbitals of ethylene. Once we develop a catalogue of ML_n orbitals for common types, and we shall spend considerable time doing this, the varieties of molecules and types of problems that can be treated are endless. This approach uses delocalized molecular orbitals and, therefore, it initially sidesteps questions such as how many bonds there are to iron in **1**. We shall see that the outcome of this analysis will shed some light on the question. With localized or valence bond approach such questions need to be dealt with from the start. Let me emphasize again that the fragment orbital method is not the only way in which the electronic structure of organometallic or inorganic molecules have been approached nor is it particularly new.[14,15] However, it is a very powerful and conceptually easy method for understanding many problems in the organometallic field.

A key step in this approach is the development of a catalog of the important valence orbitals for ML_n fragments. A way for this to be done is illustrated in Chart 1. An octahedral ML_6 molecule **9** will be our

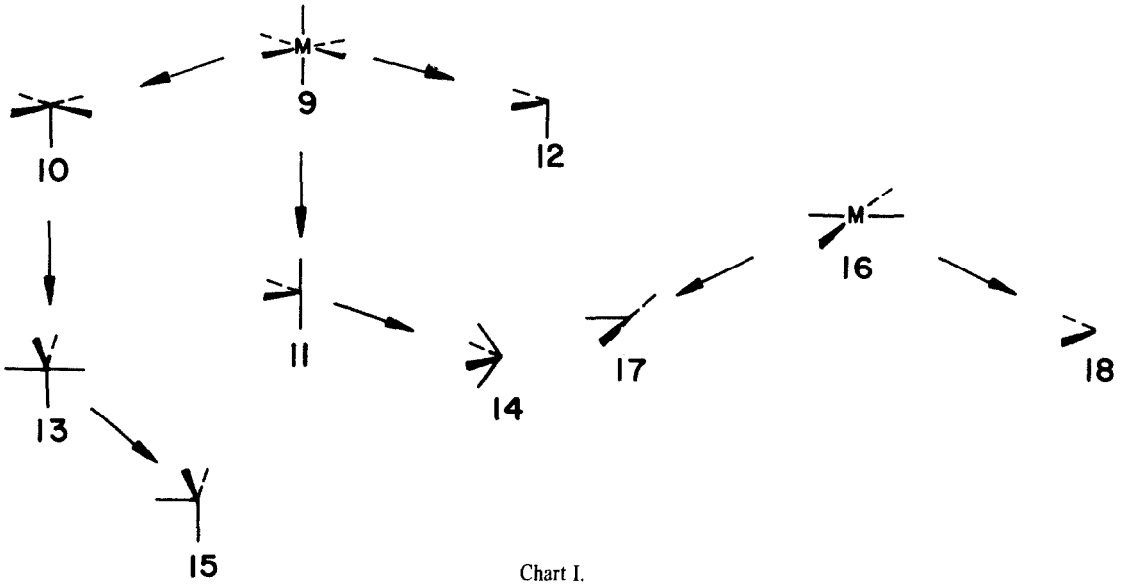

Chart I.

starting point. The orbitals of a $C_{4v}ML_5$ fragment, **10**, can be derived quite simply by taking those of ML_6 and considering the perturbation encountered by removing one ligand. Removal of two *cis* ligands from ML_6 gives a $C_{2v}ML_4$ fragment, **11**, and removal of three gives a $C_{3v}ML_3$, **12**. Distortion of two *trans* ligands in ML_5, **10**, leads to the orbitals of a trigonal bipyramidal, D_{3h}, ML_5, **13**. Likewise, the $C_{2v}ML_4$ orbitals can be distorted to a $C_{4v}ML_4$ fragment, **14**. Finally, the orbitals of a $C_{3v}ML_4$ fragment, **15**, can be derived by removing one ligand from a trigonal bipyramid. In the same way, the orbitals of a $C_{2v}ML_3$ group, **17**, and $C_{2v}ML_2$, **18**, can be obtained by way of a square-planar ML_4 starting point. Now, the orbitals of our parent molecules, the octahedral ML_6 and square-planar ML_4, are very well-known.[2] By the term valence orbitals I mean those mainly d in character. But before we develop the valence orbitals of these fragments and elaborate upon them. there are two other concepts which must be clarified—electron counting and the principles of orbital interaction.

II. PRINCIPLES OF ORBITAL INTERACTION, ELECTRON COUNTING, AND THE 18 ELECTRON RULE

The ideas behind what happens when two orbitals interact[16] can be shown in a simplified way for the interaction of two s orbitals, ϕ_i and ϕ_j, say with differing electronegativities. When ϕ_i and ϕ_j interact,

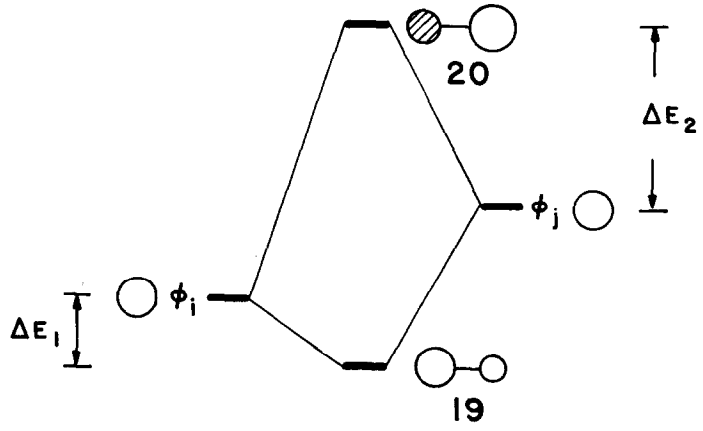

perturbation theory tells us that one combination, lowered in energy, is bonding, **19**, and the other combination, pushed to higher energy, is antibonding, **20**. Each molecular orbital most resembles that starting orbital closest to it in energy. Therefore, **19** is concentrated more on ϕ_i and **20** is more heavily weighted on ϕ_j. As the energy of ϕ_i and ϕ_j move closer to one another, **19** and **20** become more delocalized. The amount of energy, ΔE_1, by which ϕ_i is lowered upon interaction with ϕ_i has the form:

$$\Delta E_1 \propto \frac{|H_{ij}|^2}{\epsilon_j^0 - \epsilon_j^0}. \tag{1}$$

Here ϵ_i^0 and ϵ_j^0 are the energies of the starting orbitals ϕ_i and ϕ_j, respectively. H_{ij}, the matrix element of the perturbation of ϕ_i by ϕ_j, has a direct relationship with the overlap between ϕ_i and ϕ_j, S_{ij}. When S_{ij} is large H_{ij} also is large. The same relationship can be established for ΔE_2, the amount of energy that ϕ_j is destabilized by ϕ_j (the order of the subscripts in the denominator of eqn (1) is inverted). There are two important points contained within eqn (1). As the overlap between ϕ_i and ϕ_j is increased (H_{ij} increases) so too does the magnitude of ΔE_1 and ΔE_2. There is an inverse dependence on the energy difference between ϕ_i and ϕ_j—the denominator of eqn (1). ΔE_1 (and ΔE_2) becomes larger as ϕ_i and ϕ_j approach each other in energy. It is for this reason that qualitative molecular orbital theory concentrates so heavily on valence orbitals—the few highest occupied and lowest unoccupied molecular orbitals (HOMO's and LUMO's, respectively). Interaction between pairs of these will produce the smallest denominator in eqn (1) and consequently the greatest interactions. If there are one or two electrons involved in the union of ϕ_i and ϕ_j, then they will populate **19**. A stabilization in the thermodynamic sense (and usually kinetic sense, as well) is introduced. It really makes no difference whether we say that the electrons initially came from ϕ_i, ϕ_j, or both. The occupancy of the final molecular orbital, **19**, is what is important. If we put four electrons into the system, then both **19** and **20** are filled. It will not be derived here,[17] but $|\Delta E_2| > |\Delta E_1|$. Therefore, with four electrons there is a net repulsion between the two interacting groups. This istuation commonly arises when non-bonded atoms approach each other too

closely. So a $4e^-$, 2 orbital repulsion is the molecular orbital equivalent of a steric effect. With three electrons in two orbitals it is difficult to decide whether a net stabilization or destabilization results. That will depend on the actual values of S_{ij} and $\epsilon_i^0 - \epsilon_j^0$. Now these principles have been illustrated for the interaction of two atomic orbitals. But it makes no difference in actual fact what these starting orbitals are. They could just as well have been molecular orbitals from fragments. Our principal concerns will be the evaluation of the numerator in eqn (1) by symmetry considerations and the denominator by a consideration of the few valence orbitals. Before we see this in action there is still one concept to be clarified—that of electron counting.

Most stable, diamagnetic organometallic compounds possess a total of 18 electrons around the transition metal. In other words, the sum of the d electrons and the electrons formally assigned to coordinate bonds from the surrounding ligands should be 18. This is the essence of the 18-electron rule. Its derivation can be constructed in several ways. A transition metal will have 5nd (n is the principal quantum number), 3(n + 1)p and 1(n + 1)s orbitals with which to bond the surrounding ligands. These 9 orbitals will then house a total of 18 electrons for the complex to be saturated. The 18 electron rule in this sense is a restatement of the Lewis-octet rule taking into consideration the "extra" ten electrons that can go into the five d-based orbitals. We can probe into this a little deeper. Consider there to be n ligands positioned in a *spherical* arrangement about a transition metal. Figure 1 shows how in principle the

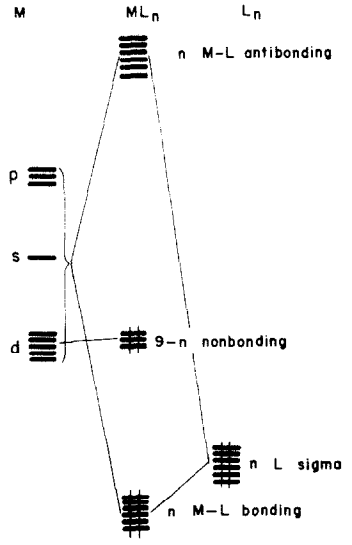

Fig. 1. Orbital interaction diagram for an ML_n complex.

molecular orbitals of this ML_n complex can be elaborated. On the left side are the 9 orbitals brought by the metal. On the right side of the Figure are n ligand based orbitals. These are normally at lower energy than the metal based ones, but this is of no real concern. It is normally the case that the symmetry adapted linear combinations[18] of these n ligand orbitals will find symmetry matches with the 9 metal based ones. Therefore, there will be n metal–ligand bonding orbitals which are filled and mainly of ligand character. There are also n metal–ligand antibonding orbitals empty and at high energy. Finally, there will be 9n-nonbonding orbitals at the metal to be filled at an intermediate energy. Because d orbitals are more noded than those of the s or p type, the nonbonded ones are of (or mainly of) d character. There are a total $n + (9 - n) = 9$ orbitals to be filled or $9 \times 2 = 18$ electrons to be placed in the bonding and nonbonding orbitals which will give a saturated complex. The ligand orbitals at the bottom right of Fig. 1 are either of the σ donor type or filled π orbitals. The ligands then are treated in a formal sense as Lewis bases. The electrons from the remaining 9n-nonbonding orbitals can formally be assigned to the metal. The case explicitly shown in Fig. 1 is a d^6 complex.

The pattern presented in Fig. 1 will hold for most cases. Of course, the n M-L bonding orbitals will not all come at the same energy nor will the nonbonding orbitals. Often one will see a continuum of orbitals in these regions. A major difference arises when a square-planar ML_4, trigonal ML_3, or linear ML_2 complex is considered. In each of these cases the ligand donor set will not match the symmetry of one p orbital on the metal in the first two examples and two p orbitals in the third. This is illustrated

in **21–23**. **21–23** are very high-lying, clearly not at the same energy as the d-based nonbonding orbitals (refer to Fig. 1), and it would not be advantageous to put electrons in them. Therefore, square planar

21 **22** **23**

ML_4 and trigonal ML_3 complexes will be thermodynamically stable with 16 electrons and linear ML_2 with 14 electrons. All are coordinatively unsaturated and reminiscent of the situation in BR_3 and other main-group compounds of this type.

As far as the mechanics of electron counting goes, I will use the following convention: all ligands will be considered as Lewis bases. Therefore, all of the ligands shown in **24** are two electron donors. Note that hydrides and alkyl groups are classified as anionic two electron donors rather than neutral one

$$CO,\ PR_3,\ H^-,\ CH_3^-,\ S\text{-}R^-,\ Cl^-,$$
$$SR_2,\ CNR,\ CR_2$$

24

electron donors. Polyenes are counted so that all bonding (and nonbonding) π orbitals are filled. Some representative examples are given in **25**. The number of electrons formally donated to the metal is given

6 6 6 4 2 2

25

beneath each structure. In these examples some care must be taken to fix the connectivity of the metal to the polyene. For example, a benzene complex will donate six electrons only if the metal is η^6 (bonded to all six carbon atoms). If the benzene was η^4, then four electrons would be donated and two electrons donated for an η^2 complex. All three examples are known. The number of d electrons assigned to the metal is then set by adding the number of charges at the ligands and subtracting the sum from the total charge on the molecule. This will give the formal charge (oxidation state) at the metal. The number of d electrons is equal to the number of d electrons of the metal in the zero oxidation state minus the oxidation state of the metal. To count the number of electrons associated with the metal one adds the d electrons to the number of electrons donated by the ligand set. Ferrocene **1**, contains two Cp^- groups and the molecule is neutral. Iron, therefore, in in the +2 oxidation state and since Fe(O) is d^8 it will be a d^6 complex. Each Cp^- group contributes six electrons so $6+6+6=18$ electrons assigned to the metal. The Zeise salt complex **3**, will be Pt(+2) and, therefore, d^8. There are a total of $2+2+2+2+8=16$ electrons associated with the metal. The molecule falls into the square-planar category with a very high-lying, empty p orbital on platinum, **21**, not involved (in a first approximation) in the bonding. Other examples will be illustrated later.

The formal way we have assigned electrons in **24** and **25** is certainly not unique. For example, alkyl groups and halogens could be counted as one electron, *neutral* donors. The cyclopropenyl system could be utilized as a four electron, anionic polyene. The total electron count will stay the same no matter what convention is used, since the formal oxidation state at the metal is adjusted. The virtue in assigning the numbers of electrons and charges to the ligands in **24** and **25** is that the number of d electrons left at the metal will correspond to the number of electrons in the 9-n nonbonding levels of Fig. 1.

What we have done here is to barely outline the principles of electron counting. Some ligands are particularly difficult cases. For example, the nitrosyl (NO) group could be treated as a two electron,

cationic system isoelectronic to CO or as a four electron, anionic one. The former way is taken to imply a linear coordination mode for NO. The latter formalism is used for a complex with a M–N–O angle less than 180°. There are also ambiguities for handling ligands which bridge two or more metals and how one treats metal–metal bonds in dimers and clusters. The interested reader is directed elsewhere.[2a,19]

III. THE OCTAHEDRAL ML_6 AND SQUARE-PLANAR ML_4 SYSTEMS

The orbitals of octahedral ML_6 can easily be constructed. For the time being L will be a σ donor ligand only. Linear combinations[18] of the σ donor orbitals are taken and these are interacted with the 9 orbitals of the transition metal. This is shown in Fig. 2. The e_g, t_{1u}, and a_{1g} donor orbitals find symmetry matches with the metal s, p, and three of the five d levels. The donor orbitals are stabilized by this interaction giving the molecular $1a_{1g}$, $1t_{1u}$, and $1e_g$ levels. In turn the metal centered $2e_g$, $2a_{1g}$, and $2t_{1u}$

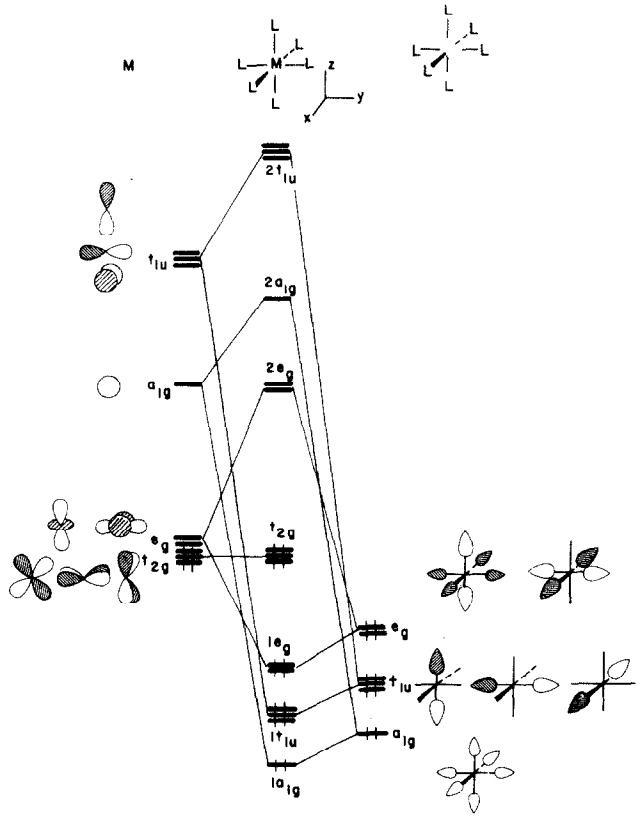

Fig. 2. The orbitals of octahedral ML_6.

orbitals are destabilized. This leaves a set of three metal d orbitals of t_{2g} symmetry which find no ligand combination to interact with. A stable complex would be one where t_{2g} is filled, i.e. a d^6 complex which then has 18 electrons. Notice that $1a_{1g} + 1t_{1u} + 1e_g$ correspond to n M–L bonding orbtials of Fig. 1. t_{2g} is the 9-n nonbonding orbitals. The valence orbitals which we shall concentrate on will be derived from t_{2g}, $2e_g$, and sometimes $2a_{1g}$, $2a_{1g}$ and $2t_{1u}$ will be used in that when the symmetry of the octahedron is broken by the reductive process in Chart 1, metal s and p can mix into $2e_g$, for example. In other words, $2t_{1u}$ and $2a_{1g}$ will provide a mechanism for the hybridization of the valence orbitals.

How does this picture change when the ligands also possess π orbitals? A good example would be carbonyl ligands in $Cr(CO)_6$–a d^6, 18 electron complex. The carbonyl ligand has two orthogonal π and π^* orbitals, **26**. Taking linear combinations of the 12π and $12\pi^*$ sets produces, among others, a combination

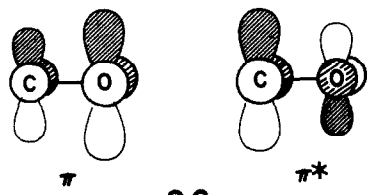

26

of t_{2g} symmetry in each case. These will interact with the nonbonding metal t_{2g} in Fig. 2 as shown in **27a**. The π set is stabilized by bonding to metal t_{2g}. Likewise, π will mix into $2t_{2g}$ which is primarily metal

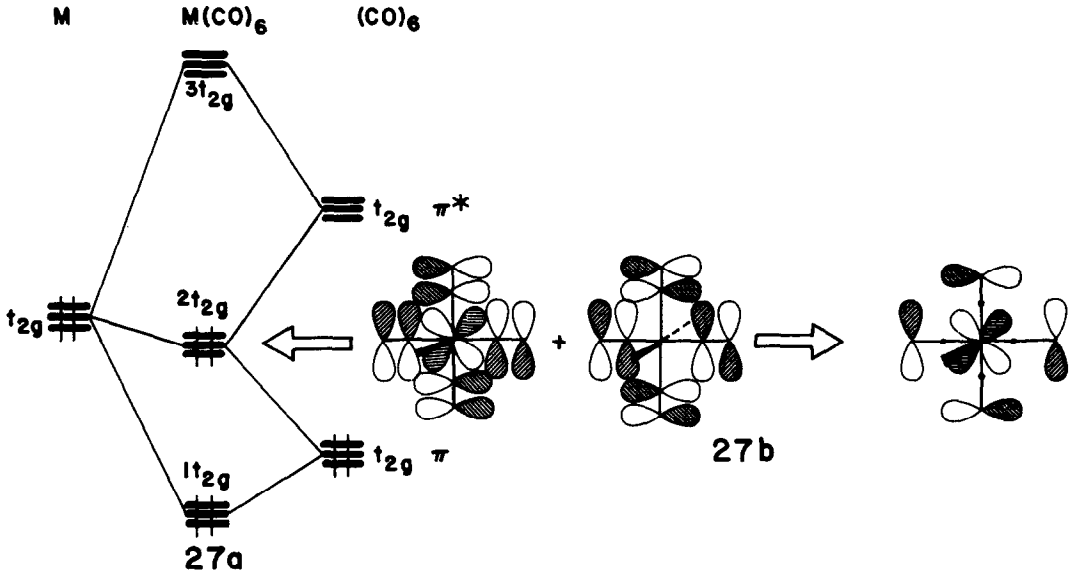

centered in an antibonding manner. However, π^* mixes into $2t_{2g}$ in a bonding way. This is diagrammed for one component in **27b**. The situation here is analogous to the allyl π system: $1t_{2g}$ is the bonding level, $2t_{2g}$ is nonbonding, and $3t_{2g}$ is antibonding. The density on carbon in $2t_{2g}$ is greatly reduced just as a node develops at the central carbon in the nonbonding orbital of the allyl system. **27** contains all the elements for any π donor or π acceptor ligand. In the extreme cases π donor ligands would have filled, relatively high-lying π orbitals which would destabilize at least one component of $2t_{2g}$. Examples would include the halogens and amido groups. A superlative π acceptor would possess an empty π orbital-stabilizing t_{2g}. A case in point would be the carbene ligand. In a formal way it has a filled σ donor orbital and an orthogonal empty p orbital **28**, available for backbonding to metal t_{2g}. Depending on its relative energy

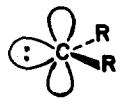

28

and overlap with t_{2g} the interaction can be very large. In that case a good bit of electron density is transferred from t_{2g} to the carbene and the ligand becomes nucleophilic. Other times the interaction is not so strong and the carbene is electrophilic.[20] Many ligands have both π acceptor and π donor functions. The propensity of the ligand will lie on the acceptor side if the π^* levels lie at low energy, such is the case for CO. Notice that overlap factors also favor this for CO. The π orbital in **27** is localized more on oxygen than carbon. π^* is concentrated more on carbon. Because CO coordinates to the metal at carbon; the overlap of t_{2g} to π^* is greater than that to π. A detailed theoretical investigation of π acceptor and π donor effects for several ligands has been given by Ziegler and Rauk.[21]

Our other starting point, the $D_{4h}ML_4$ system, is a little more complicated. Figure 3 shows how the molecular orbitals for it are constructed. The four ligand combinations, $a_{1g}+e_u+b_{1g}$, find symmetry matches with four metal orbitals and are stabilized giving the $1a_{1g}$, e_u, and $1b_{1g}$ molecular levels. Notice that there are two metal orbitals of a_{1g} symmetry—z^2 and s. $1a_{1g}$ is mainly ligand a_{1g} bonding with respect to z^2. Additionally, some metal s mixes into $1a_{1g}$ in a bonding manner. The $2a_{1g}$ molecular orbital is primarily z^2 with ligand a_{1g} mixed in an antibonding way. However, s is mixed into the orbital *bonding* with respect to ligand a_{1g}. This is diagrammed in **29**. $3a_{1g}$ is primarily metal with z^2 and ligand a_{1g} antibonding. This three orbital pattern of bonding, "nonbonding", and antibonding occurs quite frequently. We have already seen another example for the π and π^* levels of CO combining with the metal t_{2g} set in **27**. We are left with three metal orbitals, b_{2g} and e_g, at low energy which find no symmetry match with the ligand set and one very high-lying metal p orbital, a_{2u}, which is also nonbonding.

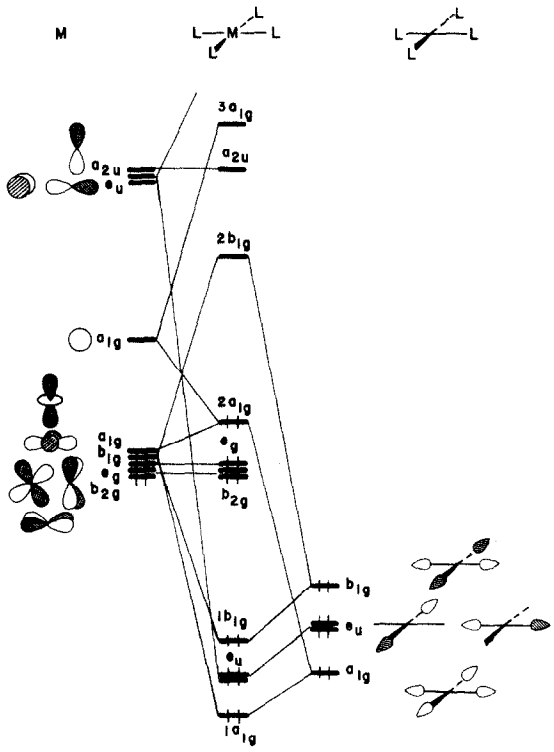

Fig. 3. Orbital interaction diagram for a $D_{4h}ML_4$ complex.

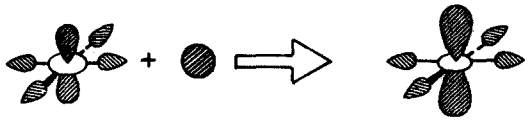

29

$b_{2g} + e_g + 2a_{1g}$ are identifiable with the 9n-orbitals of Fig. 1. A stable compound would be d^8, a 16 electron complex. π acceptors and π donors will interact with e_g and b_{2g} with the same pattern that was developed for the t_{2g} set in ML_6. This parallelism between d^6, 18 electron ML_6 and d^8, 16 electron ML_4 will be exploited in subsequent material.

IV. ML_5 AND C_{2v} ML_3 FRAGMENTS

After a rather lengthy diversion we are back at a point where the orbitals of organometallic fragments can be developed. Recall from Scheme 1 that our method will be to examine what happens when one or more ligands are removed from the benchmark molecules, octahedral ML_6 and square-planar ML_4. The ML_6 to $C_{4v}ML_5$ transformation[23] is shown in Fig. 4. At the left are the valence, metal centered orbitals of a d^6 ML_6 molecule. When one ligand is removed nothing much happens to what was the t_{2g} set, now in C_{4v} symmetry, e and b_2. If the ligand removed was a π-acceptor, then the energy of the e set would go up slightly. But the shape of e and b_2 remain identical to what they were in the octahedron. Furthermore, one component of e_g, $x^2 - y^2$ (see the coordinate system at the top of Fig. 4), is also unaffected by the perturbation giving a high-lying orbital of b_1 symmetry. The other component of e_g, z^2, is markedly altered. Removing the ligand loses one antibonding interaction between the metal and ligand. That orbital, a_1, then goes down in energy. It is also hybridized by mixing some metal s and z from $2a_{1g}$ and one component of $2t_{1u}$ (see Fig. 2). These higher-lying orbitals will mix into z^2, **30**, in such a way to reduce the antibonding between the metal and its surrounding ligands. This is diagrammed in **31**. Notice that it is the bonding of metal s and z to the ligand components in **30** that determines the phase relationship. The resultant orbital, **32**, is hybridized out away from the remaining ligands, toward the missing one. This will be a general phenomena that we will find in the fragment orbitals.

A $C_{4v}ML_5$ fragment will then have a nest of three "t_{2g} like" orbitals and a highly directional orbital of

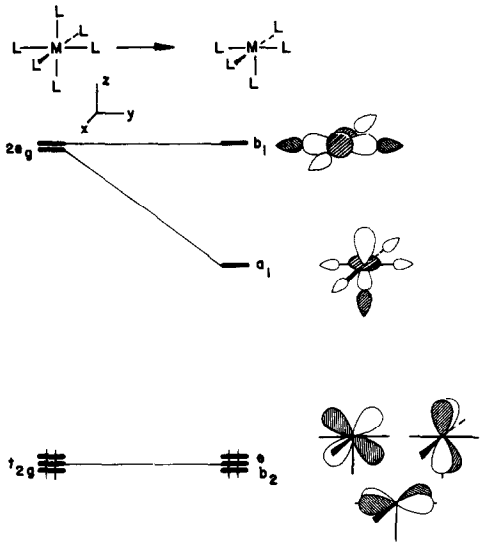

Fig. 4. Derivation of the orbitals for a $C_{4v}ML_5$ fragment.

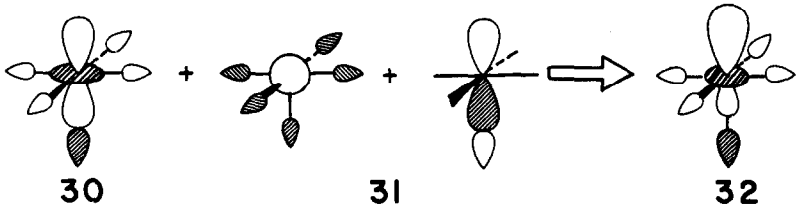

a_1 symmetry. In a d^6 complex such as $Cr(CO)_5$ the a_1 orbital would be empty. $Cr(CO)_5$ itself has been experimentally studied by matrix isolation spectroscopy.[23] A square-pyramidal geometry was determined to be the ground state. Hay[24] has carried out an extensive series of *ab initio* molecular orbital calculations on the ground and number of excited electronic states in $Cr(CO)_5$. The influence of π and σ donors on stabilizing the $d^6M(CO)_4X$ system has also been developed.[25] The $d^7Mn(CO)_5$ molecule where there is one electron in a_1 has also been investigated.[26,27] $Mn(CO)_5$ is then not unlike the methyl radical. This is an analogy we will pursue in a later section.

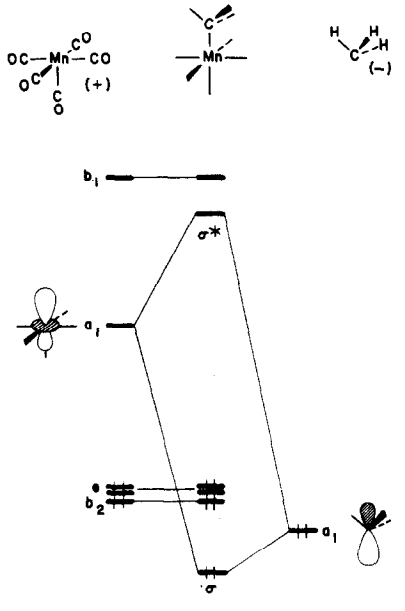

Fig. 5. Construction of the molecular orbitals of $CH_3Mn(CO)_5$.

Let us construct the orbitals of $CH_3Mn(CO)_5$ from the valence orbitals of a $d^6Mn(CO)_5^+$ fragment and CH_3^-. This is done in Fig. 5. The valence orbitals of $Mn(CO)_5^+$ are on the left of this figure. On the right is a hybridized lone pair orbital of the methyl anion. This finds a strong overlap with the a_1 orbital of $Mn(CO)_5^+$ to form a bonding, σ, orbital which is filled and an empty antibonding combination, σ^*. The octahedral splitting pattern of three below two is restored. A common rearrangement reaction, carbonyl insertion, has been extensively studied experimentally[28] and theoretically[29] for $CH_3Mn(CO)_5$. Here the methyl group migrates to a coordinated carbonyl group to form an acyl complex, **33**. The evolution of

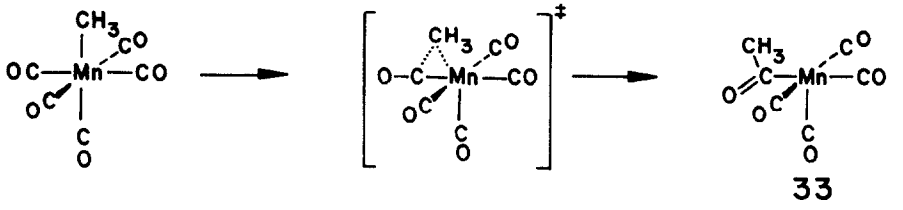

33

the orbitals from $CH_3Mn(CO)_5$ to **33** can easily be followed. **34** shows the σ and σ^* orbitals of $CH_3Mn(CO)_5$ along with a high-lying mainly carbonyl η^* orbital. This is one member of $3t_{2g}$—see **27a**. As

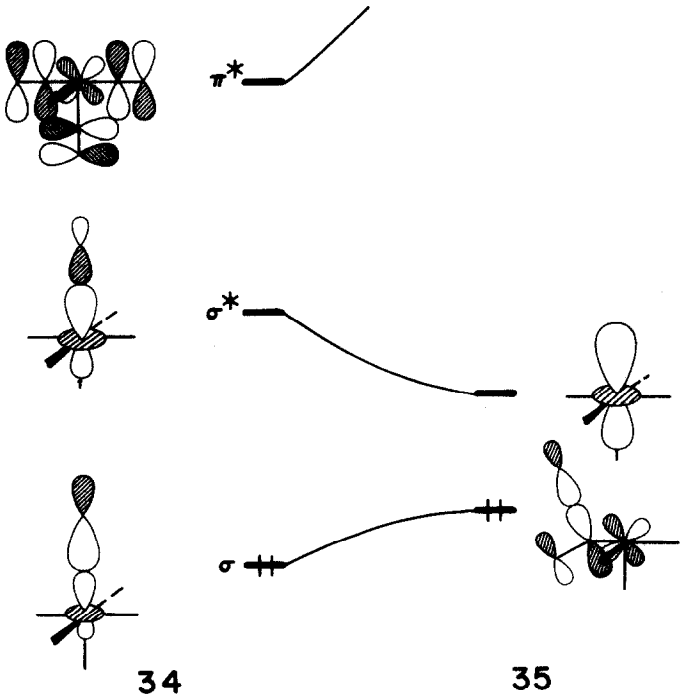

34 **35**

the methyl group migrates its overlap with a_1 hybrid decreases that causes σ to go up in energy. Likewise, the antibonding σ^* orbital drops in energy becoming the empty a_1 hybrid in the $16e^-$ intermediate, **33**. The σ orbital is prevented by rising too high in energy by mixing π^* into itself. That leads to the formation of a methyl-acyl σ bond. The acyl complex **33** is then set up to coordinate another ligand. There are several strategies that can be developed[29] to modify the activation energy for carbonyl insertion. One way would be to make the carbonyl based π^* level lie at lower energies. The mixing of π^* into σ then increases because the denominator of the perturbation expression in eqn (1) becomes smaller. This could be done by prior coordination of a Lewis acid to the carbonyl, as in **36**. Another approach would be to replace a *trans* or *cis* carbonyl with NO, as in **37** or **38**. The higher elec-

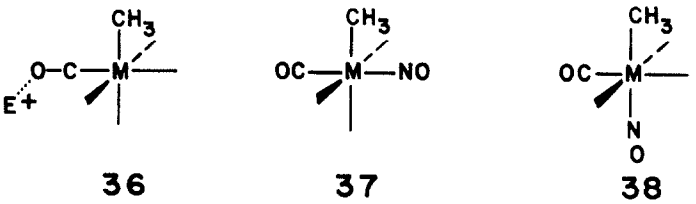

36 **37** **38**

tronegativity of nitrogen compared to carbon makes π^* in **34** lie at lower energies. Electronegativity modifications of the migrating alkyl group and metal can also influence the activation energy.[29]

Much larger systems can be treated in a similar way. One example is $M_2(CO)_{10}H^-$, where M = Cr, Mo, W. This series has been structurally investigated by Peterson, Dahl, Koetzle, Williams, Bau *et al.*[30] Instead of a linear array **39** with an M–H–M angle of 180°, bent geometries **40** are found. The degree

39 **40**

of bending is variable depending upon packing forces. The orbitals can easily be constructed from the interaction of the in-phase and out-of-phase combinations of a_1 hybrids on a d^6 $M(CO)_5$ with the bridging hydride s orbital-**41**. σ and σ^* levels are formed along with a nonbonding one, labelled n. Bending the M–H–M core on going from **39** and **40** is done in a peculiar manner. Perhaps the easiest way to visualize

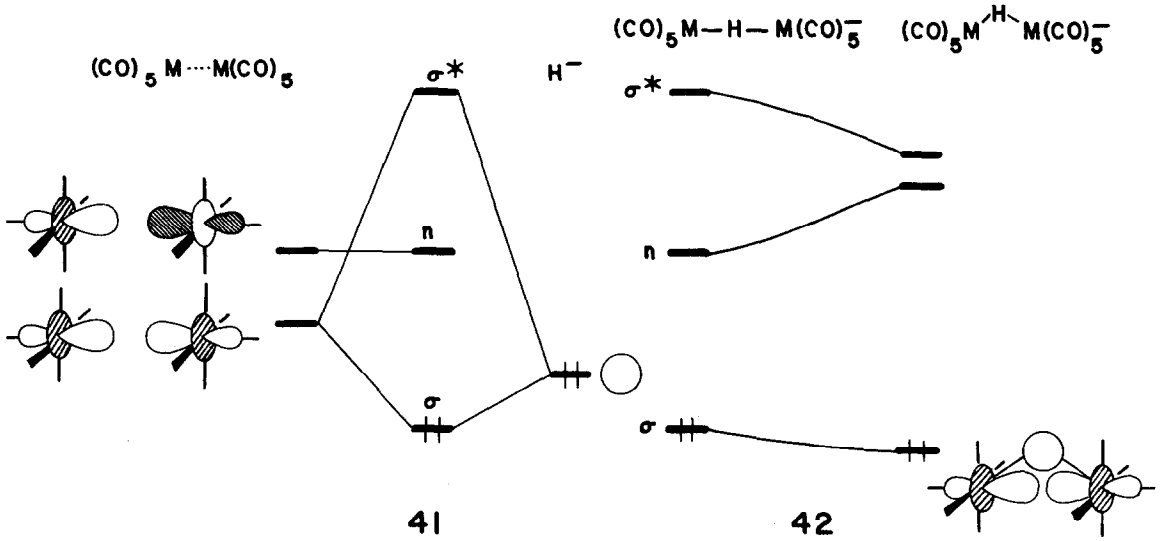

41 **42**

the deformation is by allowing the hydride to move upwards away from the M–M vector and at the same time bringing both $M(CO)_5$ units closer to each other. The energetic consequences of this distortion on the energies of the three orbitals are shown in **42**. When the M–M distance becomes smaller both σ and σ^* go down in energy since they are derived from the bonding combination of a_1 hybrids. The resultant filled σ-orbital is shown on the right side of **42**. Likewise, n will go up in energy. Counteracting this is the fact that as a M–H–M angle decreases the overlap between hydride s and the two a_1 orbitals diminishes. The hydride moves toward a nodal plane. Therefore, the downward slope of σ is quite gentle and a variety of geometries is expected. There are a couple of ways to modify the M–H–M angle. Notice that we have kept the carbonyls in an eclipsed conformation for the two $M(CO)_5$ units. Had they been staggered, less steric interaction will occur in the bent geometry and the molecule should be able to bend to a greater degree. This is indeed the case.[30] If a larger amount of a s character (and z) is mixed into a_1, then less overlap is lost between the bridging hydride and a_1 as the M–H–M angle is made smaller. That angle formed by the two nodal planes of a_1 becomes smaller. Referring back to **30–32** we can see that the energy difference between **30** and **31** sets the amount of mixing. σ donors stronger than CO substituted *trans* to the bridging hydride will destabilize **30** more than that orbital derived from a_{1g} in **30**. Since the energy difference becomes smaller, there should be a greater amount of s character mixed into a_1. This sort of bonding situation is a very typical one found for 3-center-2-electron systems. It can be traced back all the way to H_3^+! Putting one or two more electrons into the system would fill the n level and we would predict a linear geometry with, perhaps, not much stability. In fact, this is the transition state for

electron transfer reactions. The electronic requirements for electron transfer reactions built up along the lines of **41** and **42** have been beautifully analyzed by Burdett.[31]

Removing one ligand from a d^8 square-planar ML_4 complex yields a pattern very similar to that in ML_5. The orbitals for a $C_{2v}ML_3$ fragment are so constructed in Fig. 6. On the left are the metal centered

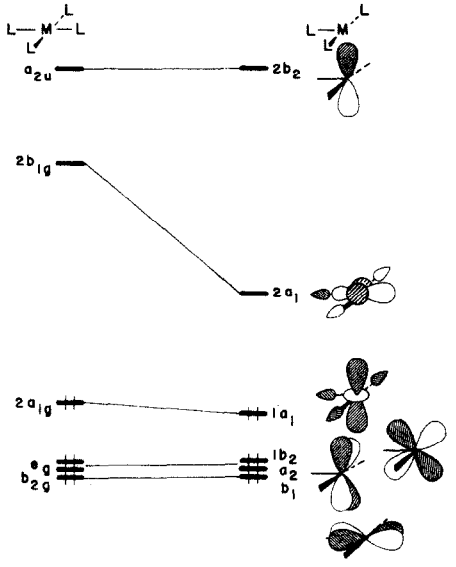

Fig. 6. Construction of the valence orbitals of a $C_{2v}ML_3$ fragment.

orbitals of the starting d^8ML_4 complex (see Fig. 3). Three levels, $e_g + b_{2g}$, are unaffected by the perturbation. $2a_{1g}$ goes down slightly in energy; one of the rather small ligand antibonding interactions to the torus of z^2 is lost. The major change occurs with $2b_{1g}$. Removing one antibonding ligand lowers the energy of that orbital significantly. There is again mixing of metal s and p into $2a_1$ making the orbital become hybridized out away from the remaining ligands. This is shown by **43**. Notice that in ML_5 there

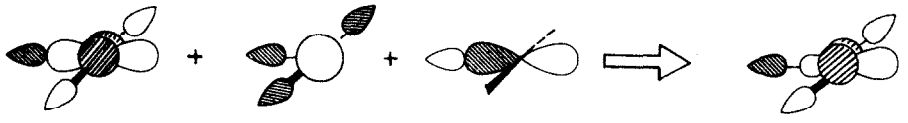

43

were three filled orbitals mainly of d character. In ML_3 there are four. The "extra" fragment orbital is $1a_1$. In ML_5 with the addition of two ligands it is destabilized, becoming b_1. One should also recall that we have started with a 16 electron ML_4 complex. The non-bonding, empty metal p orbital, a_{2u}, is carried into our fragment set.

Those fragment orbitals in Fig. 6 are appropriate for any ligand set of σ donors. π effects can be introduced in a manner identical to that presented for ML_5. Most commonly there will be one or more halogens (a π donor) as ligands, they will destabilize b_1, a_2 and $1b_2$, not all to the same extent, but rather depending upon the number of antibonding interactions. For example, in the MCl_3 fragment b_1 will lie at highest energy being destabilized by all three π-donors, see **44**. The a_2 orbital will lie lower with two antibonding interactions, **45**, and $1b_2$ at lowest energy with one, **46**.

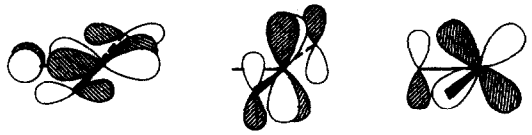

44 **45** **46**

It is easy to see how to build the molecular orbitals of a CH_3–ML_3 molecule from CH_3^- and d^8ML_3 fragments. The significant interaction will occur between the lone pair on CH_3^- and $2a_1$. The square-planar splitting pattern is restored. Let us instead develop the orbitals for Zeise's salt **3**. This is done in Fig. 7 for an "upright" conformation.[32] On the left the ordering of levels for the $PtCl_3^-$ fragment have

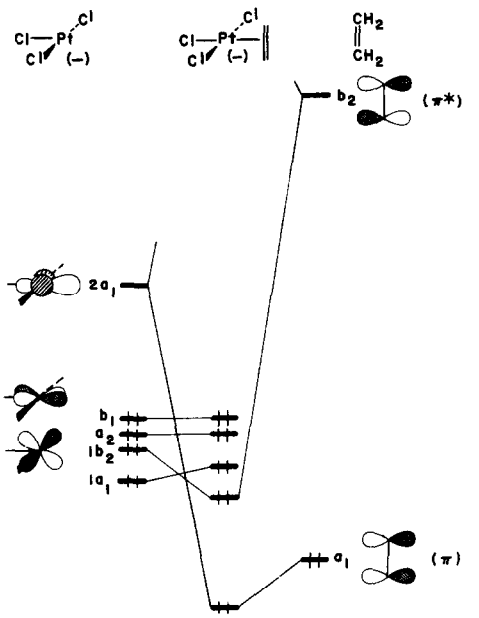

Fig. 7. Orbital interaction diagram for Zeise's salt.

been reordered, reflecting the π-donor influences of Cl in **44–46**. On the right side are the π and π^* orbitals of ethylene. The π orbital finds a good overlap with the $2a_1$ hybrid orbital. The bonding combination is sketched in **47**. In this conformation $1b_2$ is stabilized by ethylene π^*, **48**. The other

47 **48**

orbitals of $PtCl_3^-$ are essentially unaffected. Electron density from the filled ethylene π orbital is transferred to the empty $2a_1$ orbital. In the opposite direction, electron density from the metal $1b_2$ orbital is donated to the empty π^*. This is the Dewar–Chatt–Duncanson model[33] of metal–olefin bonding. The amount of forward and back donation will be very sensitive to the method and parameters (basis sets, etc.) used, as well as the partitioning scheme employed.[32b] We can say with some certainty that both effects are important. If π-acceptor groups were substituted on the olefin the energies of π and π^* drop. That will make for a stronger $1b_2 + \pi^*$ interaction since the energy gap between the two fragment orbitals decreases. This also requires that the $2a_1 + \pi$ interaction will diminish. On the other hand, the substitution of π-donors on ethylene raises the energy of π and π^* so that $2a_1 + \pi$ becomes stronger and $1b_2 + \pi^*$ is weaker. We will return to this general treatment in a later section. Had the orbital diagram for Zeise's salt been developed for the in-plane conformation, **49**, little would have changed. The $2a_1 + \pi$

49 **50** **51**

combination is essentially invariant to rotation. Rotating the olefin by 90° does, however, change the symmetry of π^* to b_1. π^* now interacts with the b_1 level as shown in **50**. Recalling that the energy of b_1

is a little higher than $1b_2$ because of Cl π-donor effects would lead us to suspect that the in-plane conformation, **49**, might be of lower energy than the upright one displayed in Fig. 7. This is in fact not true. The in-plane conformation suffers from steric repulsion between the *cis*-chlorines and the ethylene. Several four-electron, two orbital repulsions can be highlighted as the principle causes of the energy difference.[32a] It is also easy to see that if there are steric problems with **49**, then geometrical optimization will be important in setting the magnitude of the barrier. In particular the *cis*-chlorines should bend back away from ethylene and, perhaps, one will find an elongation of the Pt–olefin bond length. These effects are found both from calculations[32] and in an X-ray structure of **51**[34] where one π system is geometrically constrained to lie in-plane. Between the upright and in-plane conformations π^* will interact in a smoothly continuous fashion with a combination of metal $1b_2$ and b_1. The calculated barrier at the *ab initio* level of 15 kcal/mol is in good agreement with experimental values.[35]

To pursue the analogy between a d^6ML_5 and d^8ML_3 fragment, the orbitals of an ethylene–$Cr(CO)_5$ molecule can be constructed. **52** points to the salient features. Ethylene π and the a_1 hybrid form

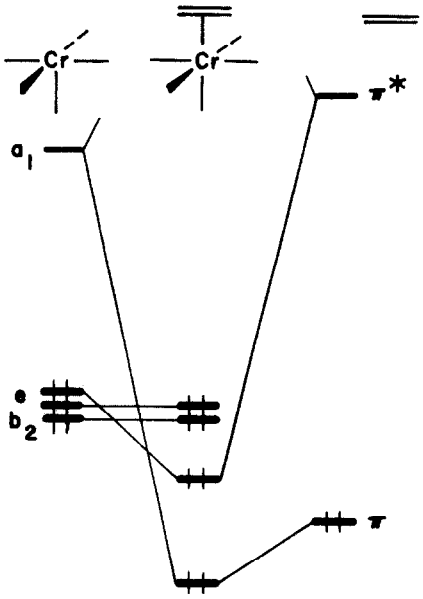

52

a bonding combination. One component of the e set finds a match with π^*. The same electronic picture as in Zeise's salt emerges. There are additional electronic factors which give rise to a rotational barrier for this class of compounds.[32a,36] The analogy can be carried much further. For example, the ligand lying *trans* to X in ML_5X and ML_3X complexes often has a different M–L bond length than the others. This *trans* influence has a common electronic origin in octahedral and square-planar complexes.[37] The electronic features of the olefin insertion reaction,[38] **53**, are very similar to step **54** in the olefin hydrogenation catalytic cycle.[39]

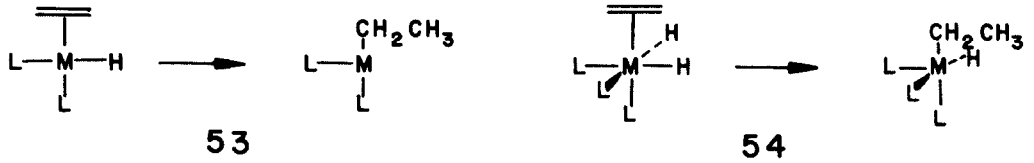

53 54

Another conceptually useful analogy pairs the ethylene ligand with a carbene. Both contain a filled orbital of a_1 symmetry, **55**, and an empty orbital of b_2 (or b_1) symmetry, **56**. Carbene complexes of both d^6-ML_5 and d^8-ML_3 complexes are known.[40] Their electronic structure follows directly from what has been presented for the olefin complexes. The notion that the barrier in Zeise's salt is set by steric rather

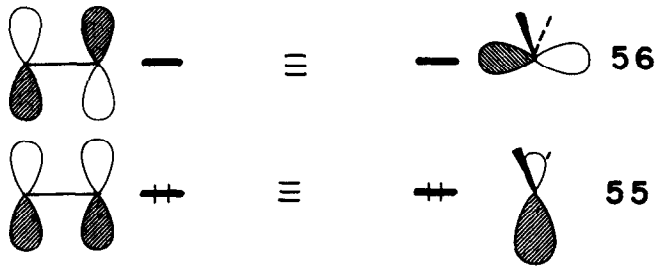

than electronic factors is further supported by carbene–ML_3 complexes. Conformation **57** is analogous to the upright geometry; the p orbital on the carbene interacts with $1b_2$. The experimentally observed structures are of types **58**[41] which correspond to the in-plane conformation of Zeise's salt. Now **57** is the more sterically encumbered geometry.

57 **58**

V. THE $C_{2v}ML_4$ AND ML_2 FRAGMENTS

Removing two *cis* ligands from an octahedral complex will generate a $C_{2v}ML_4$ fragment, **59**. From

59

what we have learned about ML_5 it might be anticipated that there will be two hybrid orbitals formed, pointing towards the missing ligands. Figure 8 shows this decomposition. The three members of the t_{2g}

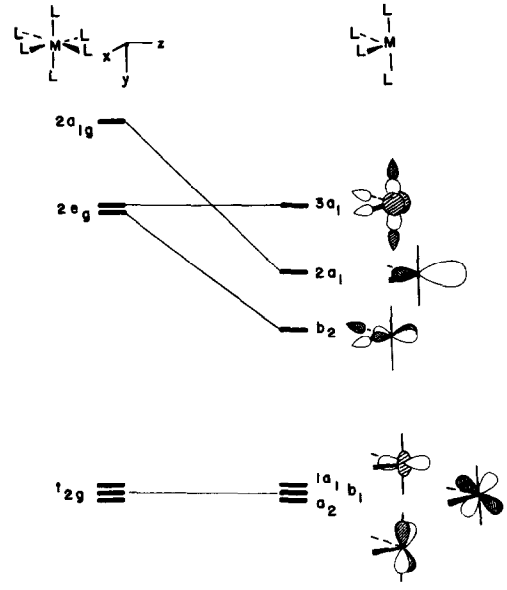

Fig. 8. Construction of the valence orbitals of a $C_{2v}ML_4$ fragment from octahedral ML_6.

set will again not be affected much. There might be slight changes due to π effects. If the two ligands removed were π acceptors, then $1a_1 + b_1 + a_2$ would go to slightly higher energy. One member of e_g is also kept at constant energy ($3a_1$). The other component, b_2, will be stabilized greatly. It had started as a pure d function, **60**, losing one-half of the antibonding interactions to the ligands. A lowering of the

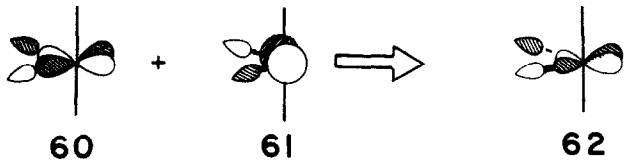

60 61 62

symmetry from O_h to C_{2v} allows one component of $2t_{1u}$ (see Fig. 2), **61**, to mix in a bonding way with respect to the ligand lone-pairs in **60**. For convenience, we have changed the coordinate system to that shown at the top of Fig. 8. **60** is then xz. Metal x mixes into it to produce **62** which is hybridized out away from the ligands. The a_{1g} orbital in ML_6 is also stabilized greatly. Removal of the two ligands reduces the amount of antibonding by one-third. Again metal z (from one member of $2t_{1u}$) mixes into the orbital producing $2a_1$. Notice that there has been a slight reshuffling of the d orbitals in $1a_1$ and $3a_1$. $1a_1$ in the octahedral complex using the "natural" coordinate system of Fig. 2 was xy. It is now in the coordinate system of Fig. 8 z^2. Likewise, $3a_1$ was z^2, it is now an x^2-y^2. Part of this is due to the change in coordinates. The other part comes about by changing the ligand field. Irrespective of the coordinate system $1a_1$ and $3a_1$ (or for that matter, $2a_1$) have the same symmetry. They remix somewhat during the perturbation process.

One idea that can be readily exploited by this fragment analysis is that certain metal complexes have an anisotropic electronic environment. Take the d^8-ML_4 fragment, for example. The three lower orbitals, $a_2+b_1+1a_1$, along with the higher lying b_2 orbital would be filled. The asymmetry comes about from the b_2-b_1 difference. b_2 lies at higher energy. It is also hybridized, whereas b_1 is not. Therefore, if a ligand with a π-acceptor orbital is brought up to the d^8ML_4 fragment that orbital will preferentially interact with b_2 rather than b_1. Our probe ligand will again be ethylene. Figure 9 shows an interaction diagram for ethylene–$Fe(CO)_4$ in two possible conformations, **63** and **64**. In both conformations the π level of

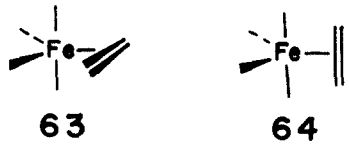

63 64

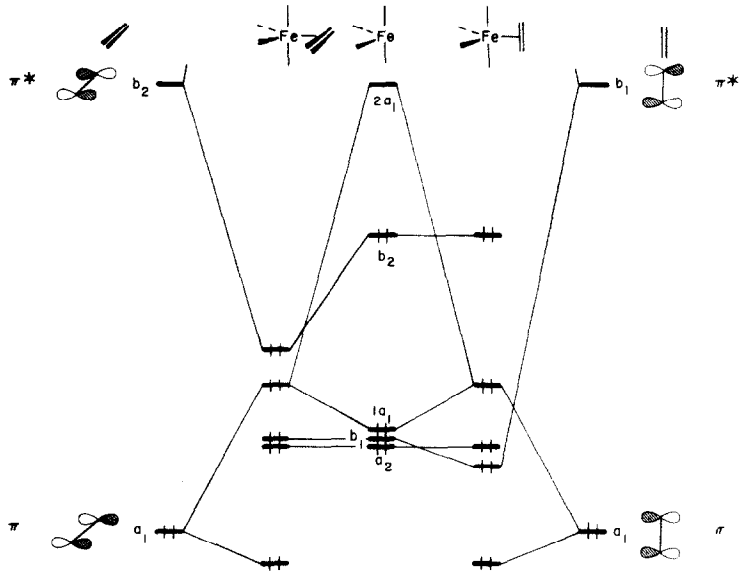

Fig. 9. Interaction diagram for ethylene–$Fe(CO)_4$ in two possible conformations.

ethylene interacts with $1a_1$ and $2a_1$. That produces three molecular orbitals, the lower two shown in Fig. 9 are filled. The important point is that essentially those fragment orbitals are cylindrically symmetrical. Therefore, the overlap between them and the energies of the resultant molecular orbitals are invariant with respect to the conformation. The $Fe(CO)_4$ a_2 orbital is nonbonding in both conformations. This

leaves us with the b_1, b_2 pair on $Fe(CO)_4$ and π^* of ethylene. In conformation **63** where the olefin lies in the equatorial plane π^* is of b_2 symmetry. Its overlap with b_2 of $Fe(CO)_4$ is large and with the small energy gap between them they form a strong bonding combination. The $Fe(CO)_4$ b_1 level is nonbonding. When the ethylene is rotated by 90° to **64** the π^* orbital now is of b_1 symmetry. It forms a bonding combination with b_1 of $Fe(CO)_4$. The b_2 level is left non-bonding. Which conformation is more stable? A decision can be made easily by comparing the stabilization inherent in the $\pi^* + b_2$ interaction in **63** vs $\pi^* + b_1$ in **64**. The b_2 level is closer in energy to π^* than b_1 is. Furthermore, b_2 is hybridized out towards ethylene; b_1 is not. That hybridization in turn creates a larger overlap with π^*. Therefore, both factors for the stabilization energy of equation (1) make the $\pi^* + b_2$ interaction better than $\pi^* + b_1$ and conformation **63** is expected to be more stable than **64**. The energy difference is actually calculated to be about 30 kcal/mol at the extended Huckel[32a] and *ab initio*[42] levels. All structures of olefin–$Fe(CO)_4$ complexes are of type **63** where the olefin is oriented in the equatorial plane.[43]

We could have come to this result in a slightly different fashion. The orbitals of a trigonal-bipyramidal, $D_{3h}ML_5$ system can be constructed in many ways. Linear combinations of the five σ-donor orbitals could be interacted with the atomic levels of M. This is analogous to our derivation of the molecular orbitals in ML_6 and square-planar ML_4. Alternatively, the orbitals of the $C_{2v}ML_4$ fragment (Fig. 8) could be interacted with one σ donor function of a_1 symmetry from L. From Fig. 8 it is easy to see that b_1, a_2, and b_2 are left non-bonding. The $1a_1$ and $2a_1$ levels of ML_4 interact with the a_1 donor function to provide three molecular orbitals. The one at low energy is mainly of donor character with $1a_1$ (and $2a_1$) mixed in a bonding fashion. The middle molecular orbital is the donor orbital antibonding with respect to $1a_1$ and bonding to $2a_1$. This level is actually pushed up in energy to the non-bonding b_2 of $Fe(CO)_4$. In other words, the antibonding of L to $1a_1$ is significant. The resultant splitting pattern is shown in **65**. We have relabelled the molecular orbitals according to D_{3h} symmetry of the molecule and filled the levels appropriate for a d^8 complex. That d orbital which was $3a_1$ in Fig. 8 stays empty at very

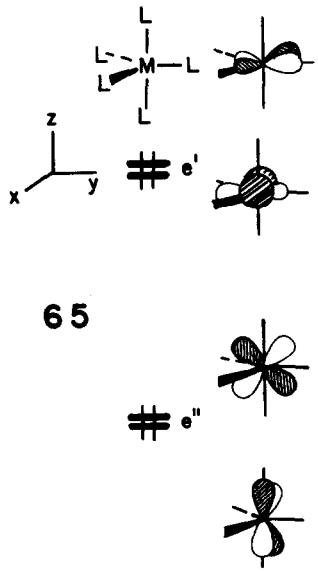

65

high energy. Yet another way to derive **65** would be to take the $C_{4v}ML_5$ fragment, **66**, and distort it in the sense shown. Referring back to Fig. 4 for the orbitals of a $C_{4v}ML_5$ system we see that b_2 and one member of the e set (*yz* in the coordinate system at the top of the Figure) are unaffected by the distortion. The other component of e (*xz*) will be destabilized. As the two *trans* ligands move upwards they start to overlap with *xz*. That will lower the energy of the orbital which is donor-based. However, the *xz* level is destabilized since the ligand lone pairs will enter into this orbital in an antibonding fashion. This is shown in **67**. Finally, the a_1 level will be stabilized slightly. The lone pairs of the two *trans* ligands move into the nodal plane of this orbital which is primarily z^2. The three methods for the development of the splitting pattern in **65** work equally well. In general, there may be advantages for doing the problem with one particular method. For example, looking at the variation of orbital energies with respect to a distortion coordinate, i.e. a Walsh diagram,[44] which we have done in **67**, focuses on the interrelationships between the molecular orbitals of two different molecular geometries and the points

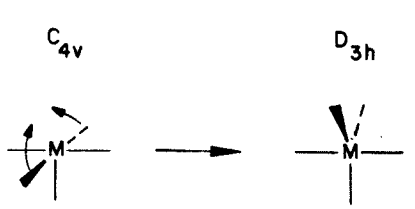

66

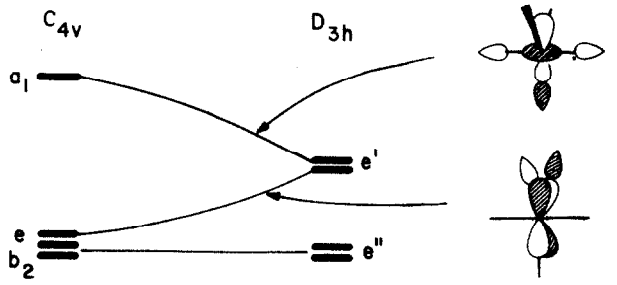

67

between them. But, back to ethylene–Fe(CO)$_4$. Taking the carbonyls just as four σ-donors and the filled π level of ethylene will generate a splitting pattern like that present in **65**. Two filled levels will be at high energy and two at lower energy. Perhaps one component of e'—mainly $x^2 - y^2$ will lie a little lower in energy than the other component does since ethylene is not as strong of a σ-donor compared to CO. The important point is that there are two "lonepairs" on Fe which have the correct symmetry to interact with the empty ethylene π^* orbital. The xy component of e' since it is hybridized and lies at high energy will be more stereochemically active towards the π^* acceptor probe than the yz component of e''. This leads to the same conformational prediction as before, namely, geometry **63** should be more stable than **64**. Two or three olefins would use both components of e' for back bonding rather than e''. Therefore, the structure of tris–olefin–ML$_2$ complexes should be and is[45] that in **68** rather than the sterically much less encumbered **69**.

68 69

There remains one unsettling point in all of this. It was mentioned that **63** is calculated to be ~30 kcal/mol more stable than **64** for ethylene–Fe(CO)$_4$. However, NMR measurements in substituted olefin complexes put that barrier in the 10–15 kcal/mol region.[46] A resolution of this discrepancy can be advanced once one thinks about why the calculations gave such a high barrier in the first place. The energy and hybridization differences between b_1 and b_2 (see Figs. 8 and 9) are at the heart of this problem. If there is a way to equivalence b_1 and b_2, then the ethylene π^* acceptor level will not discriminate between them. The way to do this for the ML$_4$ fragment is shown in **70**. The two equatorial

70

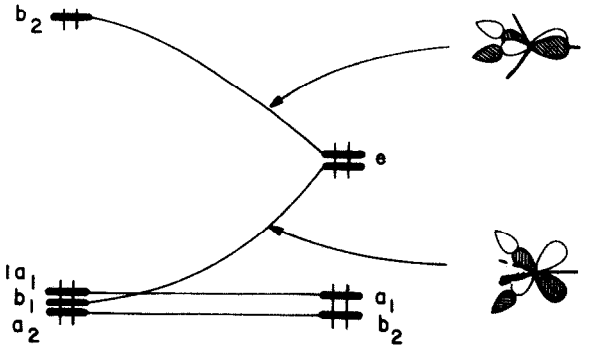

71

groups spread out and in doing so the equatorial ligand σ-donors move towards the nodal plane of b_2. That means that the energy of b_2 drops and the amount of x mixing into xz (for the coordinate system—see Fig. 8) decreases. This is indicated by the Walsh diagram in **71**. Concommitant with this motion is the bending of the two axial groups towards each other. The two axial donors move off from the nodal plane of yz and enter antibonding. Metal y is mixed into b_1 in a bonding way with respect to the ligand donor orbitals to partially alleviate the antibonding, but the energy of b_1 rises. When the two

trans L–M–L angles are equal, at the right side of **71**, the ML_4 fragment has C_{4v} symmetry. The b_1 and b_2 levels become equivalent—an e set. So ethylene rotation in a square-pyramidal complex should be relatively facile. A 1,1-disubstituted olefin complex, **72**, would accomplish a net rotation to **73** not with

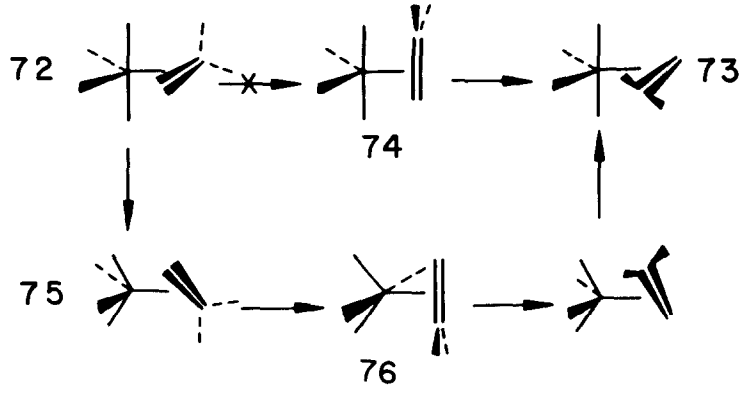

rigid rotation via the high energy **74**. But rather, olefin rotation is accompanied by the pseudorotation sequence in **70** to a square-pyramidal structure **75** where the olefin has rotated 45° from that in **72**. Continuing the pseudorotation–rotation itinerary generates a new trigonal-bipyramidal structure **76** and ultimately **73**.

The bonding in any polyene–ML_4 complex can be constructed by interacting the π levels of the polyene with the orbitals of a C_{2v} or $C_{4v}ML_4$ fragment. Following the example set by ethylene–$Fe(CO)_4$ in Fig. 9, one can develop analogous situations for other acyclic polyene complexes. It turns out that conformation **77** will always be more stable than a geometry where the ML_4 unit has been rotated by 90°

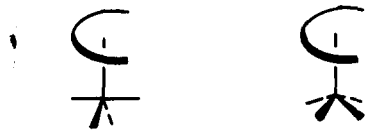

with respect to the polyene.[47] The $b_1 - b_1$ difference in a $C_{2v}ML_4$ fragment will always be exploited. In other words, the b_2 level will find a very good match, in terms of energy, with the HOMO or LUMO (depending upon whether b_2 is formally filled or empty) polyene π orbital. That interaction will be the dominant one and will set the conformation. Furthermore, rotation about the polyene-M axis should be accompanied by a pseudorotation of the other ligands. The transition state will then be **78** where the ML_4 unit has been rotated by 45° and is approximately a square pyramidal unit.[47]

Allene–$Fe(CO)_4$ complexes undergo a rapid fluxional process, **79–80**, which equivalences both π-faces of the allene.[48] Although the mechanism of this rearrangement has not been investigated theoretically, there are a couple of points that can be predicted. The dominant interaction between

79 **80**

ethylene and $Fe(CO)_4$ was the $b_2 + \pi^*$ one. The same will be true for the allene complex. **81** shows that

81 **82**

interaction along with the π^* orbital of the uncomplexed side of the olefin for **79**. If we assume that the mechanism of the **79–80** exchange proceeds via a structure where the $Fe(CO)_4$ group is bound only to the central allene carbon, then the allene must rotate about its axis by 45°. That could have been anticipated since the two π faces of the allene are orthogonal. Also, in order that bonding is maintained with the b_2 orbital of $Fe(CO)_4$, there must be a 90° rotation about the allene–Fe axis. The geometry is indicated in **82**. Both π^* orbitals of allene (in reality this will be a linear combination of them) interact with b_2 at the transition state—see **82**. Notice that if the allene were chiral, then the fluxional motion would not racemize the complex. In other ML_n complexes of allenes a rotation about one of the C–C bonds may occur in concert with the slipping motion.[49] This would lead to racemization.

The valence orbitals of a $C_{2v}ML_2$ fragment are developed in Fig. 10. The molecular orbitals of a

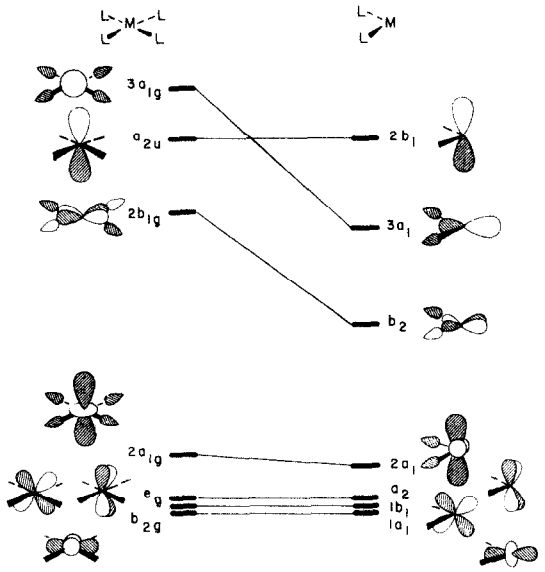

Fig. 10. Derivation of the orbitals of a $C_{2v}ML_2$ fragment from the molecular orbitals of ML_4.

$D_{4h}ML_4$ molecule that we constructed in Fig. 3 are displayed on the left side. Removing two *cis* ligands leaves the e_g and a_{2u} levels totally unaffected. $2a_{1g}$ and b_{2g} intermix a little since the symmetry of both becomes a_1 in the fragment. Half of the antibonding in $2b_{1g}$ is lost when the two ligands are removed. Furthermore, metal p is mixed into the orbital in a bonding way with respect to the two remaining ligands. That resultant b_2 level is much like b_2 from the $C_{2v}ML_4$ fragment. Finally, some of the antibonding in $3a_{1g}$ is reduced and metal p is mixed into the orbital giving $3a_1$. Just like in the $C_{4v}ML_5$ and $C_{3v}ML_3$ systems there is a correspondence between the orbitals of $C_{2v}ML_2$ and $C_{2v}ML_4$ (in Fig. 8). Both have a set of three orbitals at low energy of $a_1 + b_1 + a_2$ symmetry. There are additionally two orbitals at higher energy, $a_1 + b_2$, which are derived from the two vacant sites where ligands have been removed. The ML_2 unit has one additional orbital, $2a_1$. That orbital (along with $2b_1$ in Fig. 10) is destabilized when two axial ligands are added to form a $C_{2v}ML_4$ fragment.

A $d^{10}Ni(PR_3)_2$ fragment would have b_2 as the HOMO analogous to the HOMO of d^8 $Fe(CO)_4$. So too, the bonding and conformational preference of ethylene–$Ni(PR_3)_2$ is very similar to our ethylene–$Fe(CO)_4$ case study. An interaction diagram for a d^{10} ethylene–ML_2 complex is sketched in **83** for the "in-plane" conformation. The π orbital of ethylene interacts with $1a_1$ and $3a_1$ of ML_2 to produce three molecular orbitals. The lower two are filled. There is a strong interaction between b_2 of ML_2 and π^*. The bonding combination is occupied. Finally, b_1, a_2, and $2a_1$ of ML_2 are essentially nonbonding. It is easy to see that an "out of plane" conformation, **84**, will not be as stable as the in-plane one shown in **83**. In **84** the π^* orbital is of b_1 symmetry. Therefore, it interacts with the ML_2 b_1 orbital, **85**. For the in-plane conformation π^* interacts with b_2—**86**. The a_1 levels are cylindrically symmetric, so the molecular orbitals of a_1 symmetry remain constant in energy upon rotation. The argument becomes identical to the one developed for ethylene–$Fe(CO)_4$. Is there greater stabilization in the $b_1 + \pi^*$ combination, **85**, or the $b_2 + \pi^*$, **86**? b_2 lies higher and, therefore, closer in energy to π^* than b_1. The hybridization contained within b_2 also makes its overlap with π^* greater than that with b_1. So, again both the energy gap and

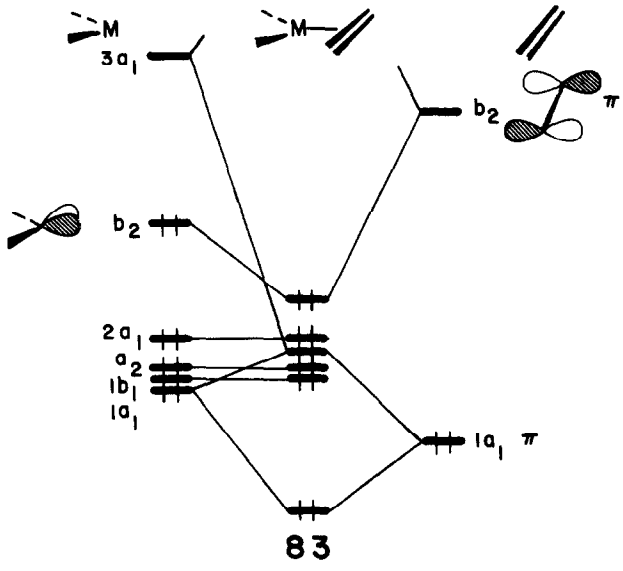

83

84 85 86

overlap factors make **86** a stronger interaction than **85** and, consequently, the inplane conformation is more stable. There is no good way for the ML_2 group to alter its geometry so that b_1 becomes equivalent to b_2 during rotation in ethylene–ML_2. Therefore, the rotational barrier is quite large, ~20–25 kcal/mol.[12,32a]

Before we go on to other polyene–ML_2 complexes, let us take an aside for a moment to present a model of metal–olefin binding and its ramifications. We have analyzed four cases in some depth. Each system, and this is true in general for any ML_n fragment, had an empty orbital of a_1 symmetry, **87**. That will interact with the filled π orbital of ethylene. There will also always be a filled orbital of b_2 (or b_1)

87 88 89 90

symmetry, **88**, available for backbonding to ethylene-π^*. This is the essence of the Dewar–Chatt–Duncanson model.[33] But, are these compounds better represented as olefin π complexes, **89**, or as metallocyclopropanes, **90**? Let us take the metallocyclopropane structure as being represented by two localized M–C σ bonds, **91**. These must be symmetry adapted by taking in-phase and out-of-phase combinations of them. The resultant, symmetry correct, orbitals are given by **92** and **93**. **92** is readily

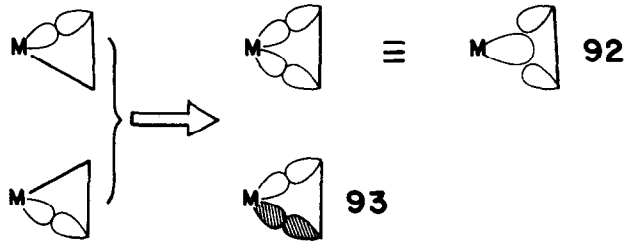

91

identifiable with $a_1 + \pi$ and **93** with b_2 (or b_1) with π^*. So, in this sense the π-olefin and metallocyclopropane pictures are equivalent. One might push the argument a little further. A consequence of the metallocyclopropane formulation is that the substituents on the olefinic carbons are expected to be bent back, as is shown in **90**. This is also expected to occur by looking from the π-olefin complex direction.

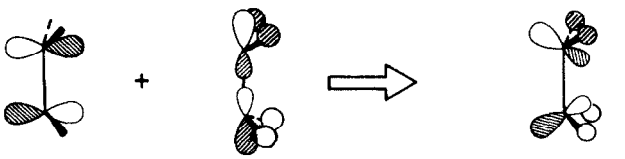

94 **95**

When the hydrogens in ethylene are pyramidalized π^* mixes in a higher lying σ^* orbital **94** so that the hydrogen s components (or hybrid components if the substituents are non-hydrogenic) are bonding with respect to π^*. This hybridizes π^* in the sense shown by **95**. It also lowers the energy of π^*. The hybridization in **95** and the lower energy make its interaction with b_2 stronger. Therefore, again there is no difference between the formulations. What does change, and is hard to quantify,[32] is the relative amount of $a_1 + \pi$ vs $b_2 + \pi^*$ interaction.

The amount of forward and back donation in metal olefin complexes can play a role in reactivity questions. Take, for example, nucleophilic attack on coordinated olefins.[50] Our generalized bonding

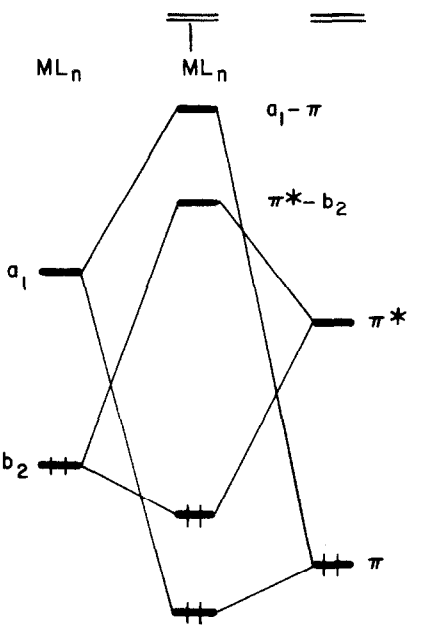

96

model for olefin–ML_n complexes is presented again in **96**. A nucleophile will have a filled, high-lying orbital. It will seek maximal bonding with the LUMO of olefin–ML_n. One can see from **96** that the LUMO will be the antibonding combination of π^* with ML_n b_2, π^*–b_2. That orbital is concentrated on the olefinic portion of the molecule. The antibonding $a_1 - \pi$ level will, in general, lie at higher energies and be concentrated at the metal. It is clear that the less destabilized $\pi^* - b_2$ is (the lower it lies in energy) the greater will be its interaction with the attacking nucleophile. Therefore, the more active an olefin–ML_n complex will be one where the ML_n b_2 orbital interacts less with π^*. There are rather obvious ways to accomplish this by perturbations within the ML_n unit; however, it would also seem to be clear that nucleophilic attack on olefin–ML_n complexes should never be more facile than attack on the uncoordinated olefins. The ML_n b_2 orbital will always destabilize π^* to some extent. Actually, a number of ML_n groups facilitate nucleophilic attack.[2] The point we have missed is that the ML_n will need to slip from η^2 coordination to an η^1 geometry in the product, **97** to **98**. It is this slipping motion that activates the olefin.[50a] **99** shows $\pi^* - b_2$ interacting with the nucleophile's lone-pair orbital at some geometry

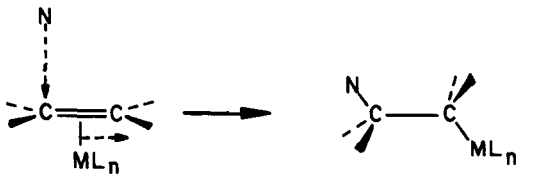

97 98

intermediate between **97** and **98**. The local symmetry about the olefin–metal region has been lowered by

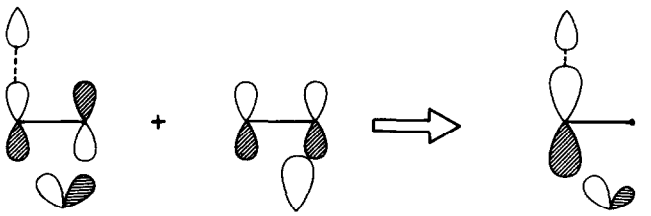

99 100 101

the slipping motion and so the higher-lying $a_1 - \pi$ orbital will mix into **99**. It will do so in a bonding way with respect to the incoming nucleophile as shown in **100**. The resultant orbital is diagrammed by **101**. There are two factors which are in operation here. Firstly, **99** is lowered in energy by slipping from η^2 since the overlap between b_2 and π^* is decreased. **99** is further lowered in energy by mixing **100** into itself. Secondly, the mixing of **100** induces a polarization in $\pi^* - b_2$. The atomic p coefficient at the carbon atom being attacked increases—see **101**. That results in a greater overlap to the lone-pair orbital. Therefore, the slipping motion activates attack both by energy-gap and overlap factors. What has been described is the general essence of the problem. The number and kinds of ligands in olefin–ML_n complexes will set the relative energies of $\pi^* - b_2$ and $a_1 - \pi$ and their composition. This varies the extent of **99–100** intermixing and, consequently, the propensity toward nuclephilic addition.[50a] Nucleophiles will preferentially add to certain cyclic polyenes over others and attack at selected positions in acyclic polyenes. A set of rules to determine these regiospecificity problems has been developed.[50b]

A point was made at the beginning of this section about the electronically anisotropic environment of the $C_{2v}ML_4$ fragment. This carries through to the $C_{2v}ML_2$ fragment and is a result of the $b_2 - b_1$ differences in energy and hybridization. The ML_4 group can get itself out of potential problems by distorting to C_{4v} symmetry, but not so with ML_2. This can cause interesting geometrical deformations in polyene–ML_2 complexes. A case in point are 18 electron, d^8 benzene–ML_2 compounds. Structures of substituted benzene–$Ni(C_6F_5)_2$ molecules show[51] an interesting boat deformation of the arene ring indicated by **102**. Note that it is the two *para* carbons which lie perpendicular to the ML_2 that move

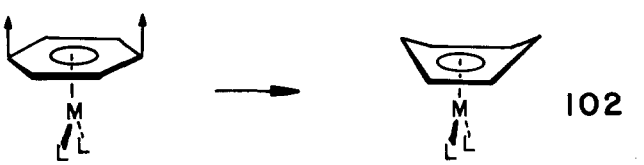

102

out of the ring, away from the metal. A steric interaction between L and the ring causing this distortion would be most unlikely. There is an electronic driving force behind this.[51a] Figure 11 shows an orbital interaction diagram for a d^8 benzene–ML_2 complex where the benzene ligand has been kept planar. The π orbitals of benzene are displayed on the left side of this Figure. The lowest π orbital of a_1 symmetry, forms a three orbital interaction with $1a_1$ and $3a_1$ of ML_2. The lowest two molecular orbitals, which are shown in Fig. 11, are filled. The $2a_1$ and a_2 fragment orbitals are of δ symmetry so they will be stabilized by the π^* orbitals shown in the upper left corner of Fig. 11. They are also destabilized by two relatively high-lying benzene ring orbitals which are also of δ symmetry. That leaves us with b_2 and b_1 of ML_2 and two π orbitals. b_2 of ML_2 forms a very strong interaction with the b_2 π orbital. The bonding combination is filled. Finally, and most importantly to our discussion, ML_2 b_1 and benzene b_1 form a bonding and antibonding combination *both* of which are filled. The antibonding b_1 orbital is shown in **103**.

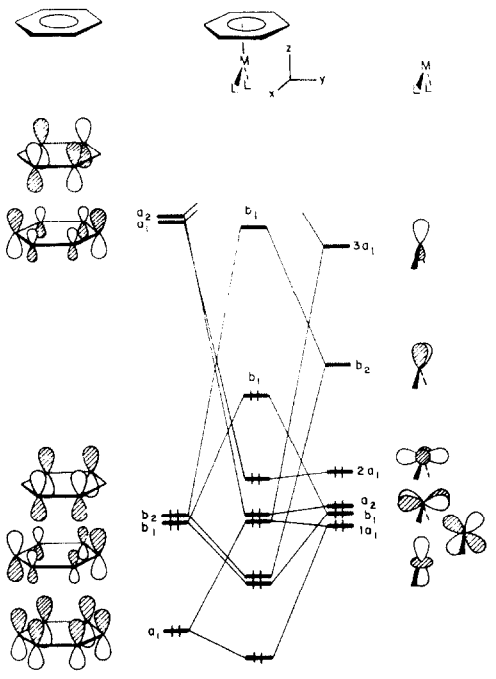

Fig. 11. Orbital interaction diagram for a d^8 benzene-ML_2 complex.

The antibonding to the two *para* carbons can be relieved by puckering the benzene ring as in **102**. The occupation of **103** also causes a discernible lengthening of the metal–benzene carbon lengths and is

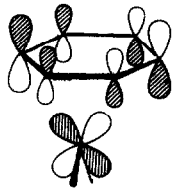

103

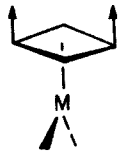

104

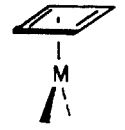

105

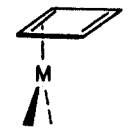

106

probably in back of the rapid arene exchange reactions that these complexes undergo.[51] A related example is an 18 electron, d^{10} cyclobutadiene-ML_2 complex. Several examples are known.[52] In this case, the degenerate π set which interacts with b_1 and b_2 lies at higher energy and again an antibonding interaction to b_1 is filled. That molecular orbital is expected to be at a very high energy and consequently signals instability.[53] If the ML_2 remains η^4, two conformations are possible, **104** and **105**. It can be shown[47] that when the ML_2 group eclipses two carbon atoms, **104**, the two staggered carbon atoms should move up out of the plane to a butterfly structure. Alternatively, the ML_2 group may eclipse carbon–carbon bonds, **105**. Those two bonds should lengthen and the two staggered bonds should shorten. The two structures will be relatively close in energy. A third possibility would be an η^2 structure, **106**. **104** or **105** may then serve as transition states for ring-whizzing. Other 18 electron polyene-ML_2 complexes such as cyclopentadienyl-$Co(CO)_2$,[54] trimethylenemethane-$Pt(PR_3)_2$,[55] substituted cyclopentadienyl-ML_2,[56] and carborane-ML_2[57] also have been shown to have slipped and/or distorted structures with similar arguments given.

Sixteen electron cyclic polyene-ML_2 complexes like cyclopentadienyl-$Mn(CO)_2$ or benzene-$Cr(CO)_2$ are interesting because they are intermediates in dissociative ligand exchange reactions of polyene-ML_3

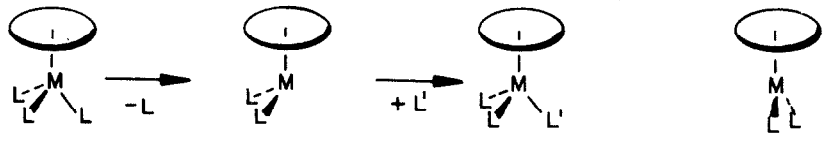

107 108 109 110

complexes. **107–109** shows a typical reaction sequence.[58] Removing one ligand from an 18 electron polyene–ML_3 complex, **107**, generates a coordinatively unsaturated 16 electron intermediate, **108**. Is the structure of the intermediate pyramidal, as in **108**, or trigonal, **110**? When all three ligands of the tripod are different the 18 electron complex is chiral. The **107–109** reaction is found to precede *without* racemization and, therefore, the intermediate must be pyramidal with a significant inversion barrier.[58] Why **108** is more stable than **110** has been treated in some depth by Hofmann.[59] In **110**, for a 16 electron complex, that antibonding orbital labelled b_1 in Fig. 11 is the LUMO. Notice that the nonbonding $2a_1$ is close to it in energy. Pyramidalization lowers the symmetry of the complex from a (maximum) of C_{2v} to C_S. That means that the two orbitals have the same symmetry and they mix. That lowers the energy of the HOMO and sends the LUMO to higher energy. The gain in energy by the HOMO is sensitive to the nature of the polyene and electronic properties of the L groups, but for the benzene and cyclopentadienyl cases the barrier for inversion (from **108** to **110**) is quite large.[59b] There is an amusing antithetic relationship here between organometallic and organic compounds. Consider the polyene to be one ligand. The coordinatively unsaturated complexes are pyramidal, **108**. Filling the molecular b_1 level in Fig. 11 causes the 18 electron, saturated complexes to be trigonal, **109**. On the other hand, unsaturated 6 electron molecules like BR_3 are trigonal while the saturated 8 electron ones are pyramidal.[60]

Theoretical investigations of fluxionality in polyene–ML_2 complexes have also been initiated. Examples include η^3-pentadienyl–ML_2,[61] η^3-trimethylenemethane–ML_2,[55] and η^2-cyclopropenium–ML_2.[62] The dominant mode of bonding in these complexes occurs between a polyene π level and ML_2 b_2. How the overlap in that combination evolves as a function of the reaction parth sets the barrier size. Therefore, the topology of the π system will have a direct bearing on the activation energy for these intramolecular rearrangements and barriers from very low to high activation energies are anticipated.[63,64]

These interrelationships between orbitals of different systems which have been stressed can be used in a variety of ways. The electronic requirements for reductive elimination[65] is one such case. In this reaction a dialkyl transition metal complex, **111**, decomposes into an alkane and a coordinatively

111

unsaturated complex. The reaction offers a way to couple two alkyl groups together and, therefore, much work has been done to exploit the reaction in catalytic[1] and stoichiometric[2] manners. In **111** there are a total of four electrons in the two M–R bonds. We would formally assign them to the R groups. Two electrons are used to form the carbon–carbon bond and the remaining two electrons are left at the metal. The most common situations start from d^8 ML_2R_2 complexes of **111**, e.g. Pd(II), Ni(II), Au(III), which decompose to d^{10} systems, but d^6 ML_4R_2 complexes are also known to undergo the reaction.

Let us start the discussion by looking at the reaction in a generalized sense. Taking linear combinations of the two M–C bonds in **111** generate orbitals of a_1, **112**, and b_2, **113**, symmetry. The

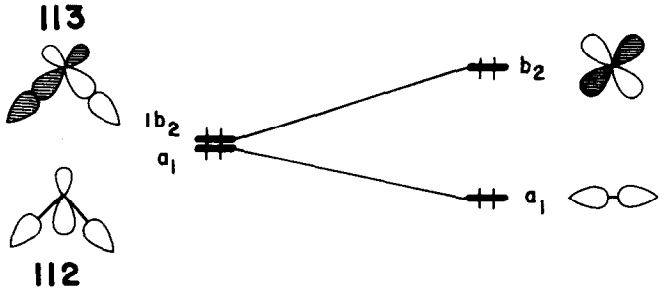

splitting between **112** and **113** will be small. Both are expected to be comprised of mainly alkyl group lone pair character with some metal p and d mixed in. As the two alkyl groups are coupled the a_1 combination smoothly correlates to the σ C–C bond while $1b_2$ evolves into a nonbonding metal d function. The metal then serves two functions: it provides a template, holding the two alkyl groups in close proximity, and it also serves as a repository for the two extra electrons in a d orbital of b_2 symmetry. If the latter function was inoperative for some reason, then the two electrons in $1b_2$, **113**,

would correlate to the σ^* C–C orbital, or at the very best, a very high-lying p orbital of b_2 symmetry at the metal (e.g. starting from a d^{10} R_2ML_n or main group compound). But how, really, does $1b_2$ become a metal d orbital? That might seem a bit mysterious because $1b_2$, **113**, is expected to be heavily concentrated at the alkyl groups. At some point along the reaction path the electron density in $1b_2$ must shift towards the metal if only to relieve the incipient antibonding between the two alkyl groups as they move closer together. The problem with our analysis has been that we have made it too simple. There have been a goodly number of orbitals that have been conveniently left out. Let us look at the reaction in more detail starting from MR_2 which decomposes to a naked metal atom and R–R. That is not a likely event to be observed, but all of the elements of the analysis are contained within it. The evolution of the molecular orbitals along the reaction coordinate is plotted in Fig. 12. The nature of the R groups doesn't really matter, those in Fig. 12 are CH_3 groups.[65b] On the left side of Fig. 12 are charted the relevant

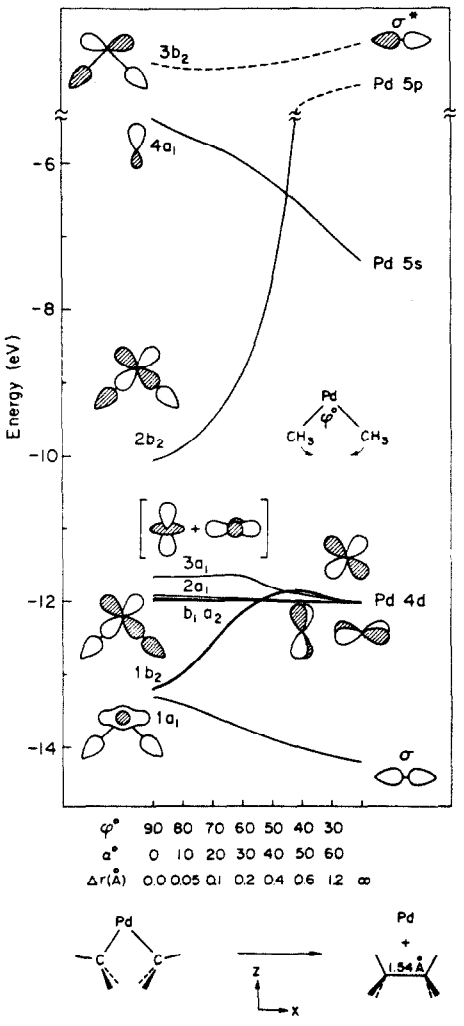

Fig. 12. A Walsh diagram for reductive elimination in $Pd(CH_3)_2$. Here φ is defined as the C–Pd–C angle and α is the rocking angle between the local three-fold axis of the methyl group and the Pd–C bond extension. These were varied simultaneously with stretching the Pd–C bonds, Δr.

levels for a d^8 complex. The orbitals are exactly the same as those for the ML_2 fragment in Fig. 10 only they have been redrawn so that the MR_2 group lies in the plane of the paper. The lower two bonding M–R orbitals have also been included which correspond to **112** and **113**. The d block contains four orbitals at low energy followed by our familiar b_2 orbital, **114**. Recall that the constitution of $2b_2$, **114**, is given by mixing the two lone pairs with the metal d orbital in an antibonding way and metal p mixes in a bonding manner (with respect to the lone pairs), **115**. In **113**, the M–R bond, the metal d and p interact with the one pairs in-phase. Finally, there is a much higher orbital shown at the top if Fig. 12, **116**. It is

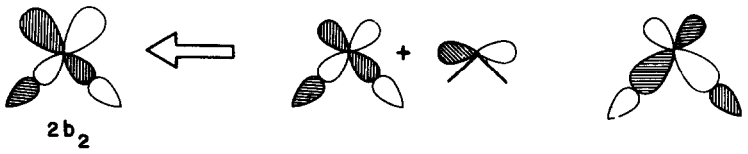

114 115 116

the fully antibonding counterpart of **113**. That orbital is at too high of an energy and we shall disregard it in the following analysis. A d^8 MR_2 molecule will have $3a_1$ as the HOMO and $2b_2$ as the LUMO.

When the R–M–R angle, φ, decreases and the two alkyl groups pivot towards another, α, (the coordinate plotted in Fig. 12) the energy of the lowest MR_2 bonding orbital, $1a_1$—**112**, goes down. It will smoothly pass to the σ C–C bond. The energy of $1b_2$, **113**, rises. Metal–carbon bonding is lost and some antibonding between the two alkyl carbons introduced. Nothing much happens to the four lower d block orbitals; they are essentially non-bonding with respect to the alkyl groups. The next orbital, $2b_2$—**114**, will behave differently. It is primarily of d character. Initially as the two alkyl groups move towards each other some antibonding from them to metal d is lost. The orbital may stay relatively constant or, perhaps, even go down in energy. In a way there is a natural correlation between $1b_2$ and σ^* of the alkane along with $2b_2$ descending to the d block of the metal. This is illustrated in **117** by the dashed line.

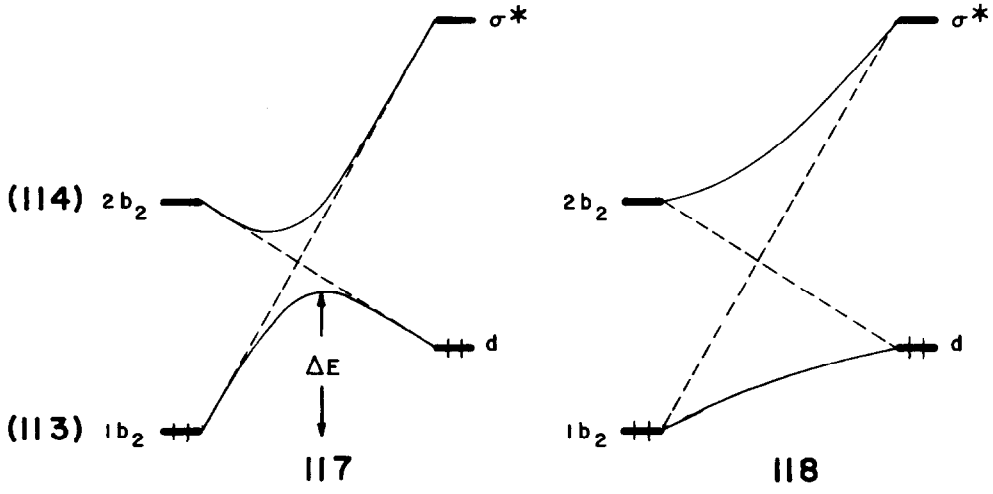

117 118

However, two orbitals of the same symmetry may never cross.[66] At some point along the reaction path there is an intermixing of molecular $1b_2$ and $2b_2$. An avoided crossing[67] occurs and $1b_2$ becomes a metal d orbital. How much mixing occurs can be treated in a typical perturbation mode—depending on how much overlap is introduced between the two orbitals during the distortion. ΔE in **117** is related, in one electron sense, to the origin of an activation barrier. Its magnitude is dependent on how avoided the crossing is. **117** is a case of a weakly avoided crossing. There is not much mixing until just before the crossing would have taken place. For a strongly avoided crossing there is a good bit of overlap between the two molecular levels at the beginning of the reaction path and a diagram like **118** would be more appropriate. The situation in Fig. 12 is somewhere between these two extremes perhpas closer to **117** and complicated a little by the highest b_2 level, **116**. At any rate, the $2b_2$ level will mix into $1b_2$. The phase relationship of the mixing is determined by the major constituents of each molecular orbital—the alkyl lone pairs on $1b_2$ and metal d on $2b_2$. Since $2b_2$ lies higher in energy than $1b_2$ does, $2b_2$ will mix into $1b_2$ in a net bonding manner with the phase shown in **119**. The resultant molecular orbital **120** will increase its d

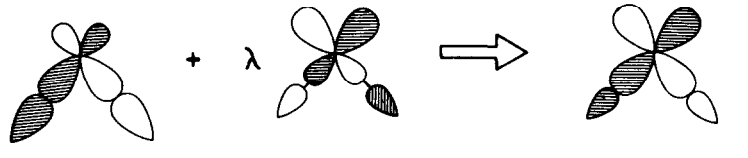

119 120

character *and* decrease the amount of lone pair character. This process continues until **120** becomes a purely metal d orbital at the right side of Fig. 12. $1b_2$ will mix into $2b_2$ with the opposite phase relationship which ultimately yields σ^* (neglecting **116**). Allowing for the fact that this will be a very endothermic reaction, there is not much of an activation barrier.

Let us now turn to a couple of more realistic models, reductive elimination in a trigonal $L-MR_2$, **121**, and square-planar L_2MR_2, **122**, complex. L here is taken as any two electron donor group (e.g. PR_3).

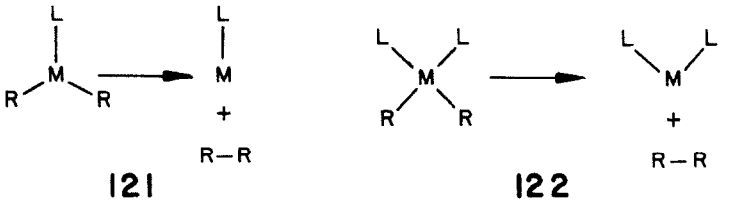

Walsh diagrams are shown for these examples in Fig. 13. On the left is the case for the trigonal $L-MR_2$

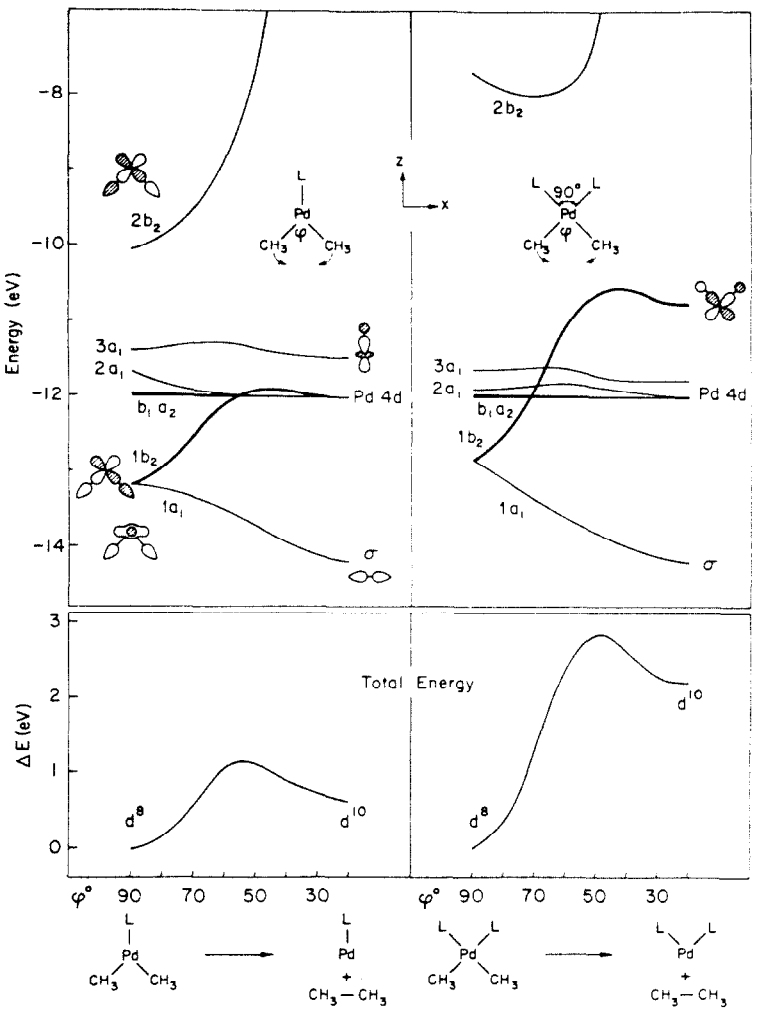

Fig. 13. Walsh diagrams for reductive elimination in a three coordinate L-Pd$(CH_3)_2$ and four coordinate $L_2Pd(CH_3)_2$ complex. The energy and reaction path coordinates are identical to those in Fig. 12. For simplicity the L groups were taken to be H^- with their valence state ionization potentials adjusted to match the one pair orbital of PH_3.

complex. It is totally analogous to MR_2 in Fig. 12. The extra ligand L with its donor orbital of a_1 symmetry cannot mix with any of the crucial b_2 orbitals. The activation energy is again expected to be small. A plot of the calculated total energy is given at the bottom left of this Figure. The L_2MR_2 case on the right side of Fig. 12 is different. One combination of L lone pair orbitals will be of b_2 symmetry. That

will *destabilize* $2b_2$ greatly and restore a square-planar splitting pattern ($2b_2$ now corresponds to $2b_{1g}$ in Fig. 3). **123** shows again the essential details of the avoided crossing between $1b_2$ and $2b_2$ in the $L-MR_2$

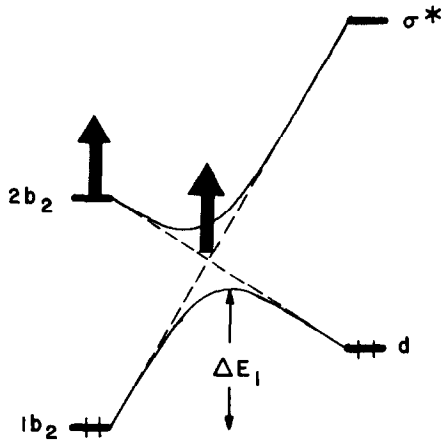

123

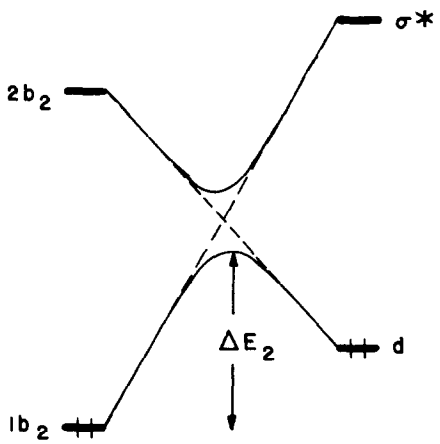

124

(or MR_2) model. If the energy of $2b_2$ is raised, then the intersection of the two dashed lines in **123** will also go up as the arrows are taken to indicate. Now the situation is approximated by **124** and is appropriate for the square-planar L_2MR_2 example at the right of Fig. 13. $1b_2$ must go higher in energy before the avoided crossing occurs and, consequently, the process will require a greater activation energy. ΔE_2 in **124** is guaranteed to be larger than ΔE_1 provided that there is approximately equal intermixing of $1b_2$ and $2b_2$ along the reaction path (which is the case here) for the two systems. Also the crossing cannot be of the strongly avoided type, **118**, for the two reactions (then equivalent activation energies would be predicted). Allowing the L–M–L angle to open up along the reaction path to a linear L_2M product does not change any of the qualitative details.[65a] A large activation barrier is still obtained.

These results would seem to be counter-intuitive. What we have shown is that starting from a 16 electron square-planar L_2MR_2 complex, it is easier to undergo the reductive elimination step by prior dissocation to a 14 electron intermediate than a direct parth from L_2MR_2. Experimentally this is observed for a number of systems.[68] The prior dissocation of one ligand must be an endothermic process so that there can be a delicate balance at work here. If the crossing in **124** can be made more strongly avoided (or if ligand dissociation becomes too endothermic), the direct elimination from a four-coordinate complex will be more favorable. Ni(II) complexes fall into this domain and direct reductive elimination from four coordinate, as well as prior dissocation to a three coordinate complex have been observed. On the other hand Pd(II) species uniformly favor the latter reaction path. In agreement with these facts calculations[65a] on L_2NiR_2 give a significantly smaller activation energy for a direct reductive elimination route than that calculated for L_2PdR_2. One way to look at this is that Ni is more electronegative than Pd. Therefore, $2b_2$ for Ni is shifted down in energy closer to the predominantly lone pair orbital, $1b_2$ (which stays at relatively constant energy for the two calculations). So this electronegativity effect will push the situation from **124** back towards **123**. Also because of the greater electronegativity of Ni there will be a greater portion of metal d character in $1b_2$ and less lone-pair character. $1b_2$ becomes more delocalized (recall the lesson from **19** and **20**). This translates into a stronger intermixing of $1b_2$ and $2b_2$ at the early stages of reaction, i.e. the situation shifts more towards the strongly avoided type in **118**. There are very similar ways that the electronic effects of L can influence the reaction barrier in either the three or four coordinate cases.[65a]

There has been learned a good bit more about the dynamics and actual geometries of these compounds.[65] We could have started from a $d^6C_{2v}L_2MR_2$ fragment **125**. Those orbitals are *equivalent* to the

125

$d^8C_{2v}MR_2$ set of Fig. 12. Extra ligands could be added and we would again come to the prediction that reductive elimination is more facile for a coordinately unsaturated five coordinate L_3MR_2 complex than for a saturated octahedral L_4MR_2 compound. In a later section we shall return to an example of reductive elimination where a real level crossing occurs and the reaction is then symmetry forbidden.

VI. THE $C_{3v}ML_3$ FRAGMENT

The derivation of the fragment orbitals for a $C_{3v}ML_3$ unit[22,69,70] is complicated a little by the need to change the coordinate system of the starting octahedral ML_6 complex. The octahedron at the top left of Fig. 14 has been tipped onto its site and the z axis intersects two of the three-fold faces. We have

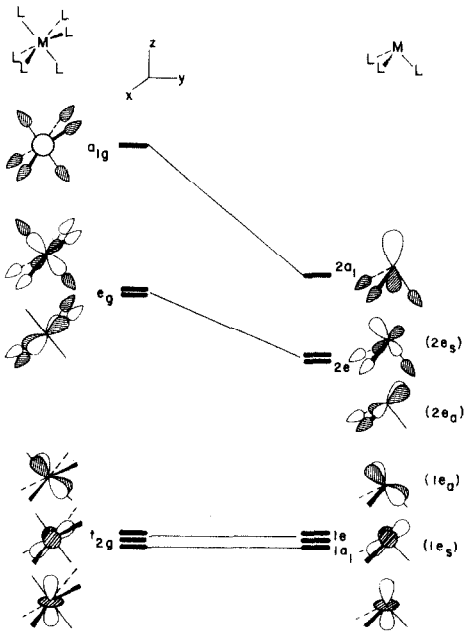

Fig. 14. Derivation of the fragment orbitals for a $C_{3v}ML_3$ unit.

exactly the same orbitals as before in Fig. 2 but their *atomic* constitution has changed.[71] One member of the t_{2g} set is z^2. The others are predominantly x^2-y^2 and zy with some yz and xz, respectively, mixed into them. This reorients x^2-y^2 and xy so that they lie in between the M–L bonds. Likewise e_g is now mainly yz and xz with some x^2-y^2 and xy mixed in to provide maximal antibonding to the ligand lone pairs. Finally, a_{1g} has the same atomic composition as before. This bothersome intermixing of atomic functions is, of course, nothing more than a consequence of change in coordinate system. Now removing three *fac* ligands does nothing to the t_{2g} set. If the ligands were carbonyls the three levels would rise slightly in energy but their composition would still be unchanged. The orbitals shall be labelled in C_{3v} symmetry now as $1a_1$ and 1e (the s and a subscripts for the e sets refer to whether they are symmetric or antisymmetric with respect to the plane of the paper). The e_g levels of the octahedron are stabilized greatly by removing three ligands. Half of the antibonding from the ligand lone pairs has been removed. Also, since the symmetry has been lowered from O_h to C_{3v} metal p can and does mix into 2e. It does so in a way which is bonding to the remaining ligand set. Not only does that stabilize 2e more but it also hybridizes 2e, as one can see from Fig. 14, toward the missing ligands. The hybridization and moderate energy will make the 2e the dominant source of interaction when we combine ML_3 with a polyene. Lastly, the octahedral a_{1g} is also lowered in energy by removing three *fac* ligands. The resulting orbital, $2a_1$, is hybridized in a manner identical to what we have seen for the analogous a_1 orbital in $C_{4v}ML_5$ or $C_{2v}ML_4$. Our peculiar coordinate system choice for the octahedron has led to a simple analysis when the perturbation occurs. That intermixing of x^2-y^2 with yz and xy with xz can be derived along other lines.[22] It is also sensitive to the pyramidality of the ML_3 group. But for almost all cases of interest where the fragment orbitals of ML_3 are to be used, the L–M–L angles are close to 90°. Thus, derivation from the octahedron is appropriate. Notice also that the orbitals of the 1e and 2e sets are "tilted". In other words, they are not displaced uniformly around the z axis (see Fig. 14). Instead they are tilted in

either the $+y$ or $-y$ directions. This tilting, which is a natural consequence of the aforementioned mixing of atomic functions, will be of importance in the following discussion of rotational barriers.

Trimethylenemethane (TMM) is an exceedingly reactive compound. Yet $Fe(CO)_3$ complexes of it are insoluble and perfectly stable. Besides constructing the molecular orbitals for this complex we shall also examine a conformational question. TMM–$Fe(CO)_3$ exists in staggered conformation **126**. It requires

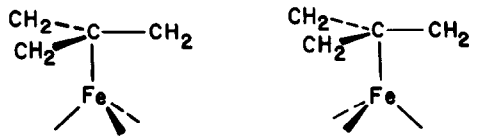

126 **127**

approximately 20 kcal/mol to rotate the $Fe(CO)_3$ group to the eclipsed conformation **127**.[72] Molecular orbital calculations[69] also give a barrier of this magnitude. Figure 15 depicts an interaction diagram for

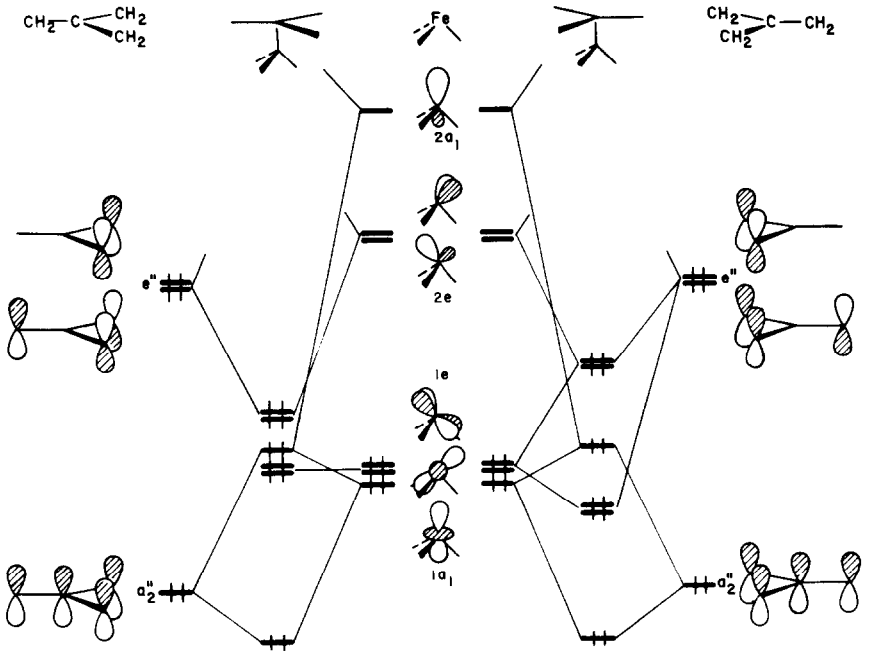

Fig. 15. Interaction diagrams for TMM–$Fe(CO)_3$ in the staggered (left) and eclipsed (right) conformations.

TMM–Fe $(CO)_3$ in both conformations. The TMM ligand has been taken to be a dianionic, six electron ligand. This requires a_2'' and e″ to be filled. Such a molecule has been prepared and is insoluble.[73] A neutral TMM molecule with two electrons less would leave e″ half-filled and this is at the heart of the parent molecule's reactivity. Counting TMM as dianionic makes $Fe(CO)_3^{2+}$ to be d^6. Therefore, $1a_1$ and 1e are filled and 2e is empty. In the staggered conformation a_2'', $1a_1$, and $2a_1$ combine to produce a typical three orbital pattern. The lower two molecular levels are filled. Those molecular orbitals are at the same energy in the eclipsed geometry. The three fragment orbitals are cylindrically symmetric and so their overlaps will be invariant to the conformation. In the staggered geometry 1e is mainly nonbonding. There is some overlap, for example, between $1e_a$ and the antisymmetric component of e″ on TMM. But that overlap is small because $1e_a$ is tilted to the right and the appropriate member of e″ has its atomic coefficients on the left side of the molecule. On the other hand, the overlap between 2e and e″ is very strong. The tilting and hybridization make it so. A bonding and antibonding combination results from the union and the former is filled. In the eclipsed geometry the overlap between 1e and e″ is turned on and that between 2e and e″ is diminished. The former interaction is a repulsive one, so that both effects conspire to give preference to the staggered geometry. Notice that it was the tilting of the e sets in $Fe(CO)_3$—this electronic asymmetry—that when matched with the same pattern in TMM gave rise to a

large barrier. If the ML_3 group was not tilted, then there could never be a significant rotational barrier except for steric reasons.

A corollary of this is that the polyene π orbitals must also be tilted, or put another way, have a left-right asymmetry. e″ in TMM and the π levels in the cyclopropenium ligand share this feature and large rotational barriers in ML_3 complexes of them ensue. On the other hand, if the polyene has two perpendicular mirror planes (or at least effective mirror planes), then the barriers will be small. The cyclobutadiene, cyclopentadienyl, benzene, etc. ligands are examples, ML_3 complexes of them will have small rotational barriers. The electronic structure of $CpML_3$ complexes has been put into a thorough, coherent picture from the photoelectron spectroscopy work of Lichtenberger and Fenske.[70a,74] There are ways to maximize rotational barriers in these cyclic-polyene complexes.[56,69,75] The easiest way to see how to do this is by taking a combination $2a_1$ and 2e. This produces for a d^6 complex three empty hybrid orbitals whose spatial distribution are indicated in **128a**. The hybrids point toward the three missing

128a **128b** **129**

ligands in an octahedral complex. A combination of $1e + 1a_1$ produces the three hybrids in **128b** which are filled. Next let the TMM^{2-} ligand be represented by **129**. There are three lone-pairs pointing towards the metal and an empty hybrid at the center. The three lone-pairs of TMM will want to maximize their overlap with **128a** and minimize it with **128b**. That occurs in the staggered geometry. What we have done is to force the molecule into an octahedral framework. Rotation could be viewed as a conversion from a d^6 octahedral complex, **130**, to a trigonal-prismatic one, **131**. This trigonal twist mechanism requires high

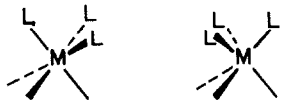

130 **131**

energies. A theoretical description of the **130–131** conversion has been viewed from a slightly different perspective along with other distortions in ML_6 compounds.[76] But it is clear that the more a polyene resembles the *fac* ligand set in **130**, the higher will be the rotational barrier for the complex. If one could somehow localize benzene into alternating C–C double and single bonds, then benzene–$Cr(CO)_3$ would have a very large rotational barrier.[69] In a similar vein it is easy to see that the way to maximize a barrier in benzene–$Cr(CO)_3$ is to put substituents of the electron donating or electron withdrawing type in a 1, 3, 5 substitution pattern. That perturbs the carbons given by closed circles in **132** relative to the open

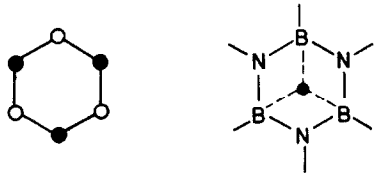

132 **133**

ones. Even better would be to change the electronegativity of the atoms at the closed circles by replacing CH groups for more electronegative N atoms. The ultimate perturbation would make the atoms at the closed circles more electronegative and the open circle atoms less electronegative than carbon. Such is the case for borazine. $Cr(CO)_3$ complexes of borazine are predicted to have high barriers[69] and a conformation given in **133**. The acceptor orbitals of $Cr(CO)_3$, **128a**, are then oriented toward the more electronegative nitrogens and the electron donor trio, **128b** are directed toward electropositive boron atoms.

A simple extension of this analysis shows[69] why the syn-eclipsed conformation **134** is found for

134 **135**

arenes with an electron donating substituent. The acceptor trio **128a** are pointed towards the electron rich *ortho* and *para* positions. Likewise an acceptor substituted arene–$Cr(CO)_3$ complex will have an anti-eclipsed orientation **135**. Now the donor trio **128b** are directed at the electron deficient *ortho* and *para* carbons. One thing that should be kept in mind for all of this is that the $Cr(CO)_3$ withdraws more electron density from benzene than it donates back. Remember that the acceptor trio was derived from $2e + 2a_1$ in Fig. 14. The 2e set is hybridized towards the benzene and overlaps in a π fashion. The donor trio is $1e + 1a_1$. 1e is not hybridized and will overlap in primarily a δ fashion. The overlap with 2e wins out on both accounts, so the ring in benzene–$Cr(CO)_3$ is electron deficient. It is no wonder then that aromatic nucleophilic substitution is greatly facilitated and synthetically useful[77] in arene–$Cr(CO)_3$ complexes. The way to approach this problem theoretically[78] would be to focus on the interaction of the HOMO of a nucleophile, a lone pair, with the LUMO of the arene–$Cr(CO)_3$. The LUMO will be the out-of-phase interaction of arene π^* with 1e on $Cr(CO)_3$. An interesting question arises about how the $Cr(CO)_3$ group withdraws electron density from the ring. Initially one might think that it does so in an isotropic fashion, i.e. equally from all six carbons. This is true only for a staggered geometry **136**. Then

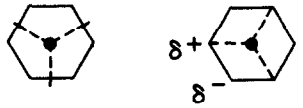

136 **137**

all six carbons are identical by symmetry (but the C–C bonds are not). But if the conformation is the eclipsed one **137** then this is not the case. A calculation[78] on eclipsed benzene–$Cr(CO)_3$ shows that the $Cr(CO)_3$ group polarizes the electron density in ring to that in **137**. Carbons which eclipse Cr–CO bonds are electron deficient compared to the staggered ones. The polarization can be traced using perturbation theory (just as the slight alternation in C–C bond lengths can be analyzed for **136**[79]), but there is an easier way to do this. A top view of the acceptor and donor trios of the $Cr(CO)_3$ group are shown in **138** relative to the benzene ring. The acceptors are again shown as being unshaded and the donors as shaded.

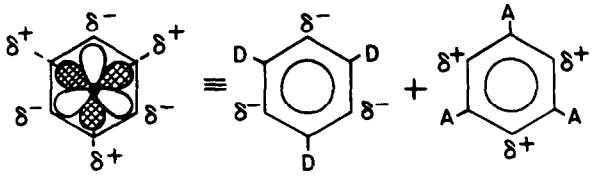

138 **140** **139**

The conformation of the $Cr(CO)_3$ is fixed to conform to that in **137**. The positioning of the acceptor trio is electronically equivalent to putting three π-electron withdrawing groups on **139**. The donor trio is analogous to **140**. The charge distribution in **137** then can be viewed as the superposition of **139** and **140**. Let's say that there is an electron accepting substituent on the benzene ring. The favored conformation is **135**. This conformation of the $Cr(CO)_3$ group as well as the acceptor itself will favor nucleophilic substitution at the para and ortho positions. If a π-donating group was the substituent, then conformation **134** is favored and both effects favor meta substitution. But is the conformational effect of the $Cr(CO)_3$ group, in **137**, greater than that of typical substituents? That is hard to probe experimentally. Theoretical calculations[78] indicate that it may be, but this should not be taken as the final word on the problem. What is known[80] is that toluene and ethyl benzene–$Cr(CO)_3$ direct nucleophilic substitution meta, but the predominant attack on t-butyl benzene–$Cr(CO)_3$ occurs at the para position. Likewise *electrophilic* aromatic substitution[81] on toluene and ethyl benzene–$Cr(CO)_3$ occurs at primarily the ortho

and para positions, as expected, but t-butylbenzene–$Cr(CO)_3$ is attacked at the meta position almost exclusively. The peculiar substituent effects of the t-butyl group can be rationalized by noting that the electronically preferred conformation of the complex should be the syn-eclipsed form, **134**. However, there may be enough of a steric interaction between the carbonyls and the t-butyl group to favor an anti-eclipsed conformation, **135**. There is actually indirect structural evidence for this happening.[78] Now in **135** the $Cr(CO)_3$ group will produce partial positive charges at the ortho and para positions so that if this polarization is larger than the hyperconjugative donating effect of the t-butyl group, then para attack will be favored for nucleophiles. Likewise, in **135** the induced negative charges at the meta carbons will favor substitution of electrophiles at this position.

The conformational preferences and bonding in any polyene–ML_3 complex can be elaborated in a way like we have done for TMM–$Fe(CO)_3$. The principal source of bonding between the polyene and ML_3 fragments are derived from the interaction of 2e (see Fig. 14) with two π orbitals. There will also be a nest of three levels, derived from $1e + 1a_1$, which will be at moderate energy. For example, in butadiene–$Fe(CO)_3$ we could treat the butadiene as a neutral, $4e^-$ donor. This makes $Fe(CO)_3$ a d^8 system, so that 2 electrons would be placed in the 2e set. 2e will then interact with the HOMO and LUMO of butadiene, **141**. In a sense electron density is removed from the π orbital and transferred to

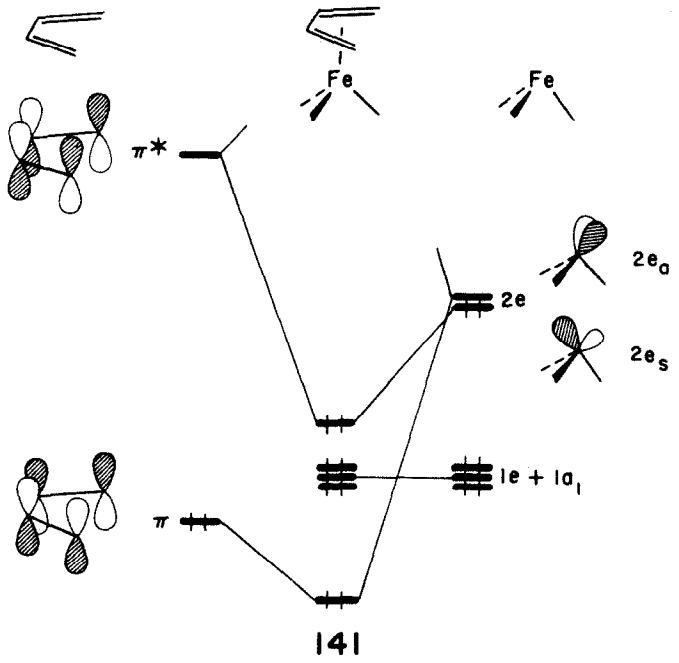

141

$2e_a$. But there is again the back donation of electron density from $2e_s$ to π^*. It is easy to see from the nodal structure of π and π^* in **141** that decreased occupation of π and increased occupation of π^* will tend to lengthen the C_1–C_2 and C_3–C_4 bonds and shorten the C_2–C_3 bond in the butadiene ligand.[82] In cyclobutadiene–$Fe(CO)_3$ the π and π^* levels (with the same nodal properties as shown in **141**) become degenerate. So the $2e_a + \pi$ molecular level will rise in energy and $\pi^* + 2e_s$ is lowered compared to that in **141**. The two molecular orbitals will be very close in energy, in the vicinity of the three non-bonding levels, $1e + 1a_1$.[84] Recall that $1e + 1a_1$ are the remnants of octahedral t_{2g}. They provide a girdle of electron density around the metal. This is why protonation occurs first at the metal in a polyene–ML_3 complex.[2] In a subsequent step the proton is transferred to the polyene.

It can also be shown[69] that any acyclic polyene–ML_3 complex will prefer geometry **142a** over **142b**

142a **142b**

for normal 18 electron complexes. The magnitude of the energy difference is variable and depends upon the energy difference between $2e_s$ and the π orbital which interacts with it. An interesting twist to this analysis is that 16 electron complexes are predicted to have **142b** as the favored orientation.[84] There is some experimental support for this idea.[84,85]

VII. METALLOCENES AND THE ISOLOBAL THEORY

In the preceding sections we have developed a catalog of orbitals for various ML_n fragments. Typical, but in no way comprehensive, structural and reactivity problems for each class has been analyzed. A recurring theme among what seems to be a myriad of fragment orbitals is that there exists relationships between them. That has paired the $C_{4v}ML_5$ fragment with $C_{2v}ML_3$ and $C_{2v}ML_4$ with $C_{2v}ML_2$. There exist many more which we will develop in a generalized way. This relationship is called the isolobal analogy.[86] This means that the number, symmetry properties, and energy of the *frontier* orbitals of the fragments are similar. The idea had its origins in Halpern's[87] perceptive comments about the similarities that exist between organic and transition metal intermediates. The structural and stability patterns in boranes and organometallic compounds developed by Wade[88] and Mingos[89] also played a role. The idea behind the isolobal analogy is outlined in Chart II. Let us start with a saturated 8 electron compound, **143**. Breaking one C–H bond in a homolytic manner generates the methyl radical,

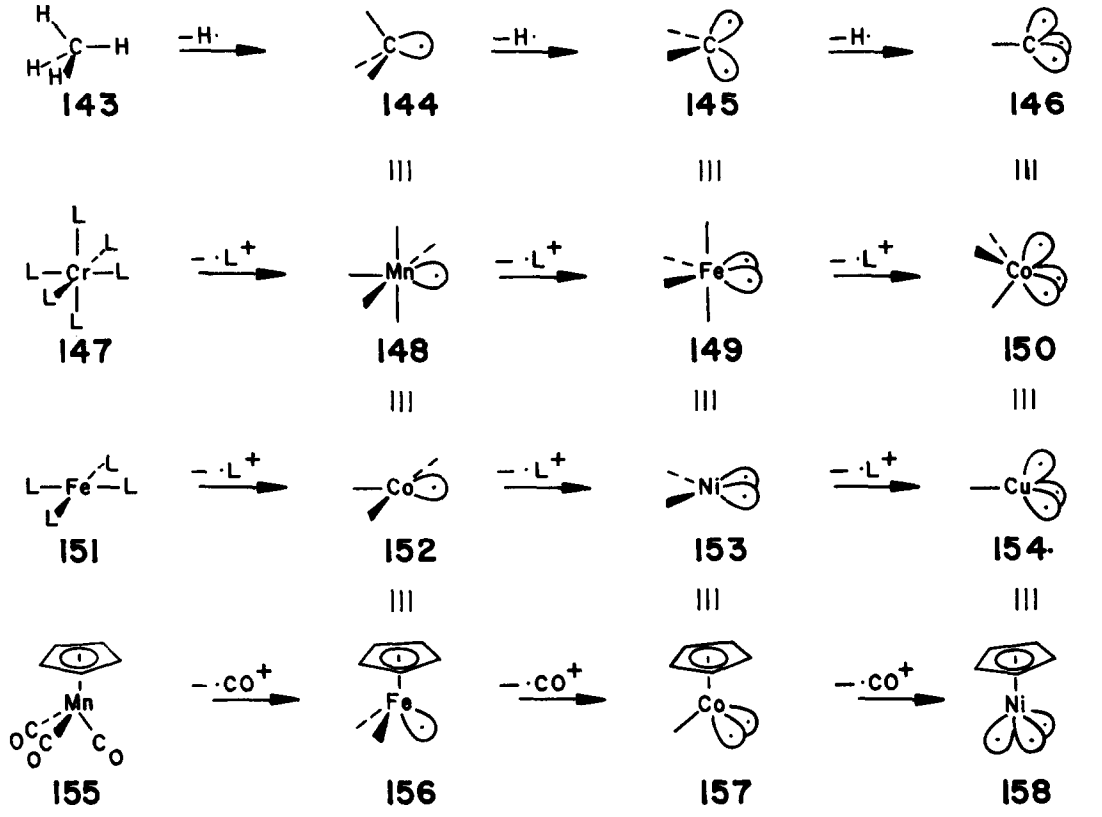

Chart II.

144. It will have one frontier orbital pointed in the direction of the missing hydrogen atom with one electron in it. Removing another hydrogen creates methylene, **145**. There are now two hybrid orbitals which in a localized sense point toward the two missing hydrogens. Removing still another hydrogen generates **146** which has three frontier orbitals with three electrons partitioned in them in some manner. **144–146** are the three archetypical fragment orbitals of organic chemistry or, to be more precise, all of chemistry which uses s and p functions for the dominant source of bonding. **147** represents another starting point. Here the use of Cr as a transition metal is purely arbitrary. What is important is that there are six two electron ligands coordinated in an octahedral arrangement to a d^6 metal. Therefore, **147** could just as well be W(0), Fe(+2), or V(−1)—all are d^6 and make a saturated, 18 electron complex. We now will break one Cr–L bond in a *homolytic* manner. For simplicity let L be a neutral ligand, e.g. a carbonyl

or phosphine. In the coordinate bond those two electrons are assigned to L. When the bond is homolytically broken one electron leaves with L and the other is now assigned to Cr. Therefore, a L_5Cr^- fragment is formed and L^+ is lost. In order to make the number of charges manageable, let us move one element to the right in the periodic table. That resulting fragment is a neutral one—L_5Mn, **148**. Here again what is important is that the fragment is a C_{4v}, d^7ML_5 type. **148** will have one frontier orbital pointed towards the missing ligand with one electron. It is clear that the orbital is a_1 in Fig. 4. We have dealt with its composition (mainly metal d with some s and p character) at some length in Section IV. The frontier orbital of the methyl radical will be composed of something like sp^3 character. It is also of a_1 symmetry. So both CH_3 and MnL_5 have one frontier orbital of a_1 symmetry with one electron in them. That means CH_3 and MnL_5 are isolobal. We shall cover the ways in which the isolobal analogy can be used shortly. For now let us just note that CH_3 and d^7–ML_5 are both intermediates which can be trapped in a low temperature matrix and display very similar types of reactions.[87] Removing another ligand (and moving one element to the right in the periodic table to keep the charge on the molecule neutral) generates a $C_{2v}FeL_4$ fragment, **149**. That will be isolobal with CH_2, **145**. Removing a third ligand generates CoL_3, **150**, which is isolated to CH, **146**. A d^8-square planar ML_4 complex **151** was the other origin that we used. **152–154** are the three fragments that are generated by sequential removal of ligands. But there are other starting points that could be used. For example, $CpMn(CO)_3$, **155**, is a saturated $18e^-$ complex. Removal of one CO^+ ligand creates the $CpFe(CO)_2$ fragment, **156**, which is also isolobal to CH_3, MnL_5, etc. Likewise, CpCo(CO) **157** is isolobal to CH_2 and CpNi **158** is isolobal to CH. One could have equally well started from benzene–$Cr(CO)_3$ or cyclobutadiene–$Fe(CO)_3$. Adjustments in the electron count can also be made. CH_3^+ will be isolobal to MnL_5^+ (or neutral CrL_5) and $CpMn(CO)_2$. CH_3^- is isolobal to $CpCo(CO)_2$. There may be some relaxation of the geometry for the compounds themselves in Scheme II. CH_3^+ is trigonal while $CpMn(CO)_2$, as explained at the end of Section V, is pyramidal and CH_3^- is pyramidal but $CpCo(CO)_2$ is trigonal. But these differences are minor. **145**, **149**, **153**, and **157** will have singlet and triplet electronic states. Which is the ground state and the singlet–triplet energy difference for CH_2 has been the subject of a great deal of research. But either nothing or very little is known (experimentally or theoretically) about this for **149**, **153**, and **157**. Moreover, one can easily write down many other examples which would be isolobal to CH_2. So the isolobal analogy can be used to anticipate the behavior of these reactive molecules themselves.

One needs to be a little careful about the fragments for which two or three ligands (or hydrogen atoms) have been removed. The orbitals which are displayed in Scheme II for these cases are localized and not symmetry correct. Symmetry correct orbitals can easily be generated by linear combinations of the localized ones.[13b,18] For two localized orbitals in-phase and out-of-phase combinations of them will give two symmetry correct orbitals. Those are shown for the four fragments of this type that we have covered in **159**. Each fragment will have an orbital of a_1 and b_2 symmetry. For the CH_2 group[90] that b_2

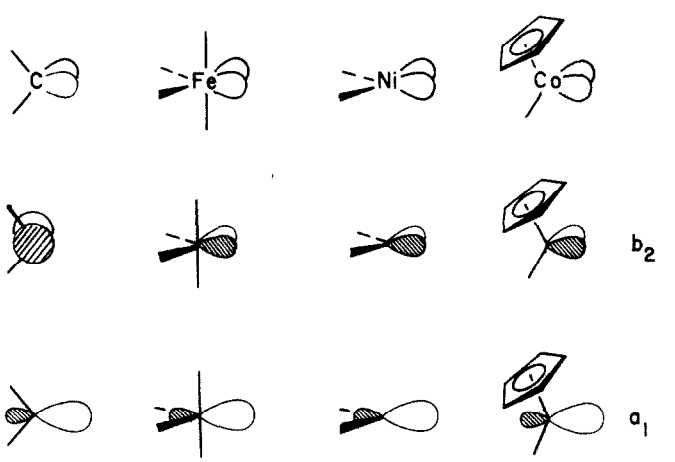

159

orbital will be a p orbital. In the transition metal fragments it will primarily metal d with some p character mixed in. The radial difference between CH_2 and the others is somewhat misleading. A d function is more "outward" pointing but it is also more diffuse than a p orbital. Therefore, both types

will have similar overlaps with another b_2 orbital. Linear combinations of the three hybrids in **146** generate orbitals of $a_1 + e$ symmetry—equivalent to those we have labeled $2a_1$ and 2e in Fig. 14 for the ML_3 fragment. Later we shall look more closely at the ML_3 vs MCp situation.

One way this relationship is useful is by replacing a fragment with its isolobal analog in a molecule. Some theoretical work has been initiated in this direction.[91] Replacing one or both methyl groups in ethane by $Mn(CO)_5$ creates $CH_3Mn(CO)_5$ and $Mn_2(CO)_{10}$, respectively, both of which are known. In Section IV a bridging hydride dimer, **160**, was discussed. Replacing each $Cr(CO)_5$ group by a methyl

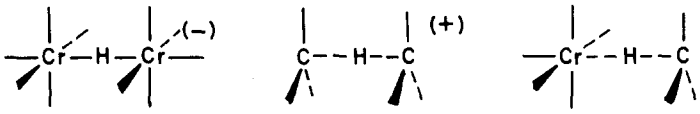

160 **161** **162**

cation and adjusting the charge yields **161**. A cyclic derivative of **161** has just recently been uncovered.[92] It would be interesting to find conditions to stabilize **162**. Isoelectronic, monodentate BH_4^- complexes are known.[93] Still more unusual organic compounds can be formulated. A $Mn(CO)_3$ group is isolobal to CH^{2+}. Replacement of $Mn(CO)_3$ in $CpMn(CO)_3$ (**155**) creates the nonclassical derivatives of **163** which have

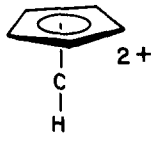

163

been prepared by Kwant and Hogeveen.[94,95] The bonding in **163** can be described in a fashion completely analogous to $CpMn(CO)_3$. The replacement of one methylene in cyclopropane by CpCo(CO) gives **164**.

164 **165**

That is just the metallocyclopropane formulation of ethylene–CpCo(CO). If two CH_2 units are replaced by CpCo(CO), then the methylene bridged dimer **165** is formed. These compounds have been recently prepared[96] and a theoretical study of them commenced.[97] There is actually a good deal of similarity between the electronic structure of cyclopropane and **165**.

There are two pitfalls that may be encountered in this isolobal replacement. Especially when one goes from an organometallic compound to an organic one, the latter species may be kinetically unstable and rearrange (if it could be formed at all) to a more stable molecule. One example of this problem is given by TMM–$Fe(CO)_3$ **126**. The $Fe(CO)_3$ fragment is isolobal to CH^+. Therefore, one might expect **166a**, more conventionally written as **166b**, to also be stable. At both the *ab initio* and MINDO/3 levels[91c]

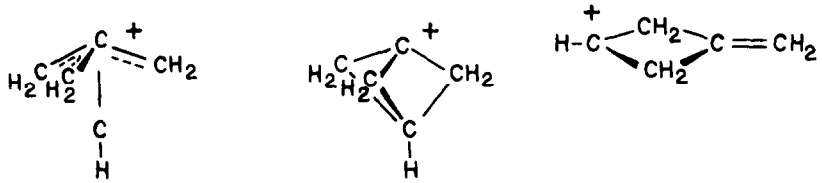

166a **166b** **167**

166 *is a local minimum* on the $C_5H_7^+$ energy surface. However, **166** rearranges to the less strained **167** with a very small energy barrier. Secondly, there may be geometrical changes associated when two or

more organic pieces are replaced by organometallic analogs particularly when the organometallic fragments have carbonyl ligands. In transition metal dimers and clusters carbonyls frequently bridge two or even three metal atoms instead of remaining terminal. The bridging-terminal interchange is commonly very facile.[98] For example, replacement of the three methylenes in cyclopropane with $Fe(CO)_4$ groups would lead to a structure of $Fe_3(CO)_{12}$ as in **168**. The solid state structure is actually **169** where two

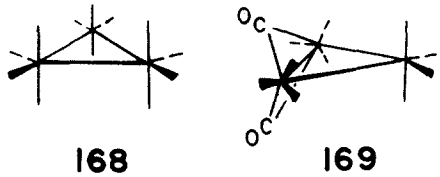

168 **169**

carbonyls bridge. However, the isoelectronic $Os_3(CO)_{12}$ does have structure **168** so there must not be much of an energy difference between them. There has been some theoretical work initiated on bridging-terminal exchange.[99] But this is a problem which is difficult to treat theoretically and much more needs to be done. Changes occur in the pattern of "non-bonding" metal centered orbitals on going from a terminal to bridging carbonyl structure. These changes will obviously be different for bridging carbonyls than for hydrides or phosphido ligands. The nature of the direct metal–metal bonding also is perturbed on going from a terminal to bridging environment.[100] Finally, the electronic details of the process will be dependent on the number, types, and geometrical disposition of the auxiliary ligands.

It should be remembered that the "basis-set" of orbitals that were constructed in Scheme II is small. Only the frontier orbitals—those which will play the dominant role in the reconstruction of an octahedron or square-planar splitting pattern—are illustrated. For example, compare ML_4 and ML_2 in **159** with Figs. 8 and 10 respectively. The set of metal-centered lone-pairs has been left out. There will be three orbitals of this type for the fragments which originate from the octahedron (including the $CpML_n$ system, etc.) and four orbitals from the equare-planar derivatives. They can play a very important electronic role. One especially noteworthy example is provided by nucleophilic attack on CpMo(CO)(NO)(allyl)$^+$. It has been shown[101] that in **170**, nucleophiles should preferentially attack *trans* to the

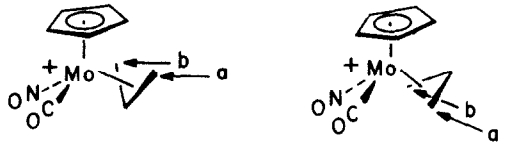

170 **171**

mitrosyl ligand—path a. On the other hand, in conformation **171** nucleophiles attack via paths a and b. More than the single a_1 orbital of **156** (Scheme II) must be used. In this case it is the perturbation of an orbital equivalent to $1e_a$ (Fig. 14) by the nitrosyl which causes an asymmetry in the $CpMo(CO)(NO)^{2+}$ fragment. That asymmetry is then translated to the π orbitals of the allyl group.[101]

Before we leave the isolobal analogy let us probe deeper into the similarities between the $C_{3v}ML_3$ and CpM fragments. The orbitals of a CpM fragment[102] are constructed in Fig. 16. The π and π^* orbitals of the cyclopentadienyl ligand are shown on the left side of the Figure. Notice that Cp is treated as anionic so that $a_1 + e_1$ (in C_{5v} symmetry) are filled. These are stabilized by metal *s* and *xz*, *yz* (the coordinate system is given at the top of Fig. 16). Metal z^2 is also of a_1 symmetry but it is not destabilized much by the lowest π level, because the overlap between them is small. The a_1 π orbital lies approximately on the node of z^2. Metal $x^2 - y^2$ and *xy* levels (e_2) are stabilized a little by $Cp\pi^*$. Here again because the overlap is small and two ring sigma orbitals of e_2 symmetry mix in an antibonding way; the molecular e_2 set stays at roughly the same energy. However, *xz* and *yz* are destabilized significantly by the $Cp\pi$ set of e_1 symmetry. What stops the molecular e_2 set from rising to very high energy is that metal *x* and *y* mix into it in a bonding fashion with respect to $Cp\pi$. The resultant shape of the molecular level labelled e_1 in Fig. 16 is shown in **172**. Finally molecular level $2a_1$ **173** is primarily metal *s* antibonding with respect to the lowest $Cp\pi$ orbital with some metal *z* mixed in a bonding fashion. For a d^6 fragment $e_2 + 1a_1$ would be filled and e_1 and $2a_1$ empty. Compare this with the d^6ML_3 fragment in Fig. 14. The two sets of fragment orbitals are essentially identical in shape. So $Cr(CO)_3$ is isolobal to MnCp (recall that we are taking Cp as

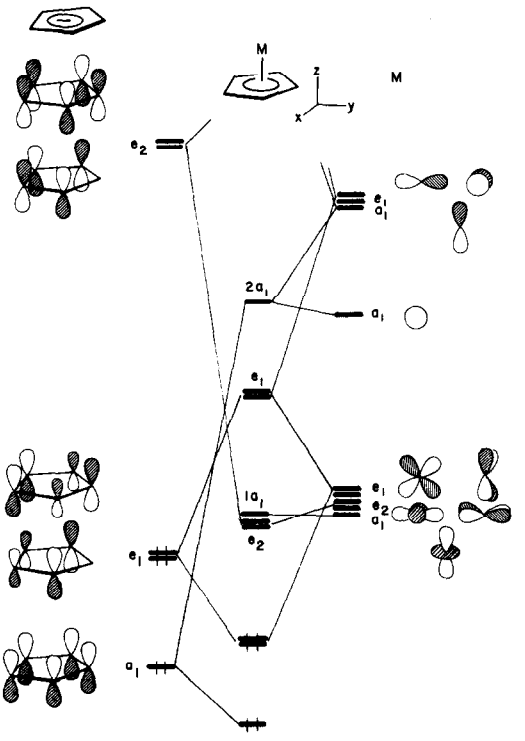

Fig. 16. Orbital interaction diagram for the MC_p fragment.

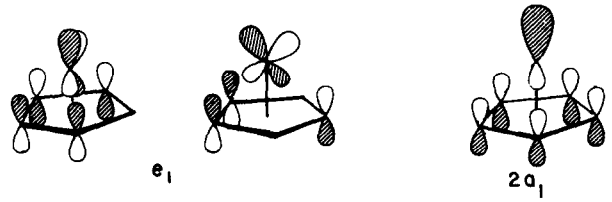

172 173

anionic, therefore, this is Mn(I)). Likewise, $Co(CO)_3$ in Scheme II with three electrons partitioned in some way between $2e + 2a_1$ is isolobal to NiCp where three electrons are in $e_1 + 2a_1$. The fragments are different in two relatively minor aspects. The orbitals of ML_3 are tilted, those of MCp are not. Therefore, large rotational barriers will not be found in polyene–MCp compounds. The replacement of three carbonyls for a Cp will also increase the electron density at the metal. The CO π^* orbitals are at an energy lower than that for Cp π^*. Furthermore, the disposition of CO π^* orbitals is ideally set up to interact with metal $1a_1 + 1e$ (or t_{2g} in an octahedral framework). Therefore, a $CpML_n$ anion will be more basic (and nucleophilic) than a $(CO)_3M'L_n$ anion. The orbitals of a benzene–M or any polyene–M fragment, for that matter, will be very similar to those developed for Cp–M.[102a]

What makes the valence orbitals of MCp so similar to ML_3 is that the three lone pairs of the ligands which form the M–L bonds are topologically equivalent to the three π levels of Cp^-. A *fac* L_3 set can then be replaced by Cp^- and the bonding in the molecule remains essentially the same. Starting with $Cr(CO)_6$, **174**, replacement of a Cp^- for three carbonyls gives $CpCr(CO)_3^-$ or $CpMn(CO)_3$, **175**. Another

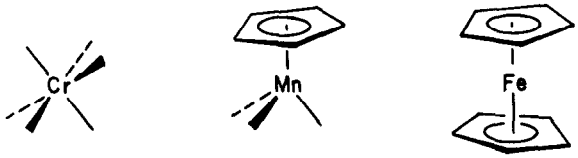

174 175 176

substitution leads to ferrocene **176**. The six (localized) Cr–CO bonds in $Cr(CO)_6$ are obvious. As

mentioned in the introduction there also should be six in ferrocene. That is difficult to see in a localized sense. Figure 17 shows an interaction diagram for ferrocene starting from Cp_2^{2-} and Fe^{2+}. In and out-of-phase combinations of the Cpπ levels are shown on the left side. A short-hand notation has been

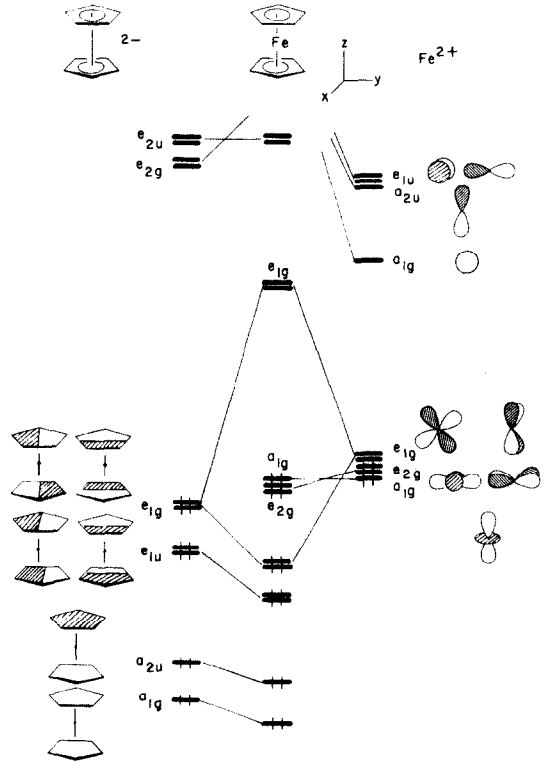

Fig. 17. Construction of the molecular orbitals of ferrocene.

used here which indicates only the nodal properties and relative phases for the π orbitals. a_{1g} and a_{2u} are the bonding and antibonding combinations, respectively, of the lowest Cpπ level (that was labeled a_1 on the left side of Fig. 16). The former orbital is stabilized by metal *s* the latter by metal *z*. e_{1u} and e_{1g} are the combinations of Cp π (e_1 in Fig. 16) which form bonding interactions with *z*, *y* and *zy*, *yz*, respectively. We have just gone through a total of six orbitals which are bonding between Fe and the Cp rings. They are related to $1a_{1g}$, $1t_{1u}$, and $1e_g$M–L bonding orbitals for ML_6 in Fig. 2. At moderate energy are the molecular levels labeled e_{2g} and a_{1g}. They are basically nonbonding x^2-y^2, *xy*, and z^2. Finally at higher energy is e_{1g}. This is the antibonding combination of metal *xz*, *yz* with the Cp_2 e_{1g} set. Notice that the octahedral splitting pattern is again formed. $e_{2g}+a_{1g}$ are analogous to t_{2g} in ML_6 and e_{1g} is similar to $2e_g$ (see Fig. 2). Ferrocene, an 18 electron complex, fills the bottom nine levels through a_{1g}. Actually, compounds having fewer electrons exist. Cp_2V with 15 electrons and Cp_2Cr with 16 electrons are known. Cp_2Co with 19 electrons and Cp_2Ni with 20 electrons also have been prepared. For Cp_2Ni the extra two electrons will go into the molecular e_{1g} set, which means that the molecule will have a triplet ground state. Recall that e_{1g} is an antibonding orbital between Fe and the Cp rings. Therefore, occupation should cause the metal–carbon bond distance to increase. This is experimentally true; the average Fe–C distance in Cp_2Fe is 2.05 Å[6] while that in Cp_2Ni is 2.19 Å.[103] What geometrically happens in metallocenes with partially filled e sets has been elegantly described by Ammeter and coworkers.[104] Photoelectron spectra of the series from Cp_2V to Cp_2Ni have also been obtained and analyzed with great care.[105] Interaction diagrams for other sandwich compounds, like bis(benzene)Cr, could also be constructed. They will show very similar patterns. The orbitals for ferrocene were labeled in Fig. 17 for a staggered, D_{5d}, molecule. Rotation to the eclipsed, D_{5h}, geometry does not alter their energies. Even the highest quality *ab initio* calculation has given a rotational barrier in ferrocene that is miniscule.[106]

A technical point needs to be brought up here. In all of the interaction diagrams that were presented the real symmetry of the fragments was always greater than or equal to the symmetry of the molecule. Had the orbitals of ferrocene been constructed from $CpFe^+ + Cp^-$ fragments this would not be true (the symmetry of ferrocene is D_{5d} or D_{5h} whereas that for $CpFe^+$ is C_{5v}) and we would have trouble. For

example, we would be led to believe that molecular e_{1g} in ferrocene could be constructed from the antibonding combination of e_1, **172**, and the Cpπ set. Yet, e_{1g} by symmetry cannot contain any metal p character and e_1 does have x and y character mixed into it as a fragment. If an actual fragment molecular orbital calculation[14,15] was carried out with this fragmentation mode, then we would see other orbitals of e_1 symmetry mix into this molecular orbital in such a way so that the metal p character vanishes. It is easier to choose the way outlined in Fig. 17. But sometimes although the real symmetry of the molecule is low, the apparent symmetry is higher. The situation for η^5–indenyl–FeCp[107] is one such example. The maximum symmetry of the molecule is C_S. A straightforward way to construct the orbitals might then be from the π orbitals of indenyl$^-$ and FeCp$^+$. The bothersome intermixing of e_1 orbitals in FeCp still occurs because the metal centered orbitals partition themselves to be ferrocene-like (forming a combination of indenyl + Cpπ orbitals is not much help either in this case). It is almost as if symmetry has conspired against us to make a problem more difficult than it should be. But in actual fact, symmetry is more often a time-shaving device.

The advantages of a symmetry-based, delocalized analysis is clear for a consideration of the bonding in triple-decker sandwich complexes, **177**.[108] The three Cp's each have six π electrons and a stable metal

177

configuration, on the basis of our experience with ferrocene, should be d^6 (the orbitals analogous to $a_{1g} + e_g$ in Fig. 17 would be filled). Our prediction would be then that a 30 electron complex should be stable. And indeed they are.[108] But systems with up to four more electrons are also stable. To see how this comes about, the orbitals of **177** can be developed[102b] by first taking plus and minus combinations of the two outer MCp fragments. One will get a total of six closely spaced levels from the $a_{1g} + e_g$ combinations (the two MCp fragments are separated from each other by a large distance so there will not be much overlap between them). The in-phase **178** and out-of-phase **179** interactions of e_1 will also be

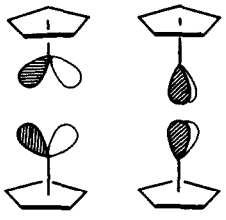

178

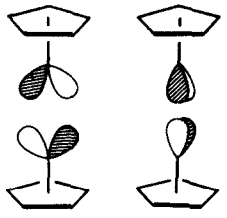

179

at moderate energy. When the π orbitals of the central Cp are interacted with the CpM–MCp fragment **179** will have a large overlap with the e_1 Cp set (see Fig. 16). But **178** does not find a symmetry match and stays nonbonding. Therefore, this e set will house the "extra" four electrons. To be sure, there will be a good energy difference between the lower d block of six and **178**, so both 30 and 34 electron families will be stable. Another situation somewhat like this occurs in tris(acetylene)W(CO). When both π faces of an acetylene are used it would be a four electron donor. That makes tris(acetylene)W(CO) a 20 electron complex. However, if one takes linear combinations of the acetylene π orbitals, it turns out that one combination does not match any tungsten orbital of the d, s, or p type.[109] Therefore, that orbital is not used by the metal and the complex is really of the 18 electron type.

VIII. Cp_2ML_n COMPLEXES

A last fragment that we shall look at in some depth is a bent Cp_2M one. There exist a vast number of Cp_2ML_n compounds where $n = 1-3$ and M is one of the early transition metals. There have been a

number of theoretical treatments of those molecules,[110] the approach that we will take follows that of Lauher and Hoffmann.[111] The molecular e_{2g} and a_{1g} orbitals of Fig. 17 will be exclusively used in the bent Cp_2M fragment. The other orbitals will either be Cp centered or lie at too high of an energy (for example, molecular e_{1g}). These three starting orbitals for a "linear" Cp_2M system are shown of the left side of Fig. 18. It really makes no difference whether the Cp's are staggered or eclipsed when they are bent back.

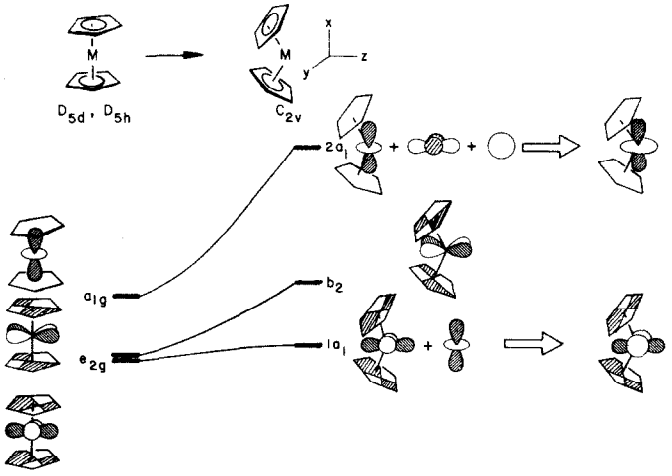

Fig. 18. A Walsh diagram for the valence orbitals of a Cp_2M fragment as a function of the bending angle.

For convenience the orbitals will be labelled in C_{2v} symmetry as if the rings were eclipsed. The e_g levels (e_2' in the eclipsed, D_{5h}, geometry) split into nondegenerate orbitals of b_2 and a_1 symmetry. b_2 rises in energy on bending the Cp's back. It loses some of the δ bonding to Cp π^* and, more importantly, there is increased antibonding from Cp σ orbitals. The same would happen with $1a_1$, however, it and what was a_{1g}—now $2a_1$—intermix. The mixing of $2a_1$ into $1a_1$ is shown on the right side of Fig. 18. This intermixing stabilizes $1a_1$ so that it stays at relatively constant energy. $2a_1$, on the other hand, rises rapidly in energy. Some metal s character also mixes into $2a_1$. A top view of these three orbitals in the *yz* plane (see top of Fig. 18) is shown in **180**. Since the ligands will coordinate to Cp_2M in the *yz* plane, we shall use the

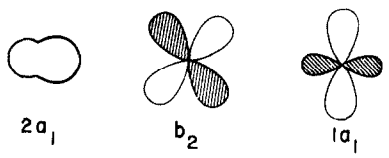

180

representations in **180**. When three ligands are brought into the coordination plane they bring with them three donor functions. Linear combinations of the three lone pairs are shown in **181–183**. They match

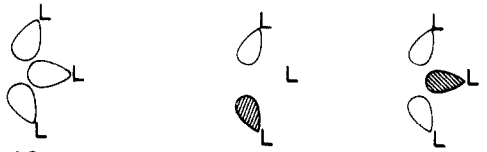

181 **182** **183**

nicely the nodal properties of **180**; **181** with $2a_1$, **182** with b_2, and **183** with $1a_1$. So all three metal levels are destabilized and a d^0 complex is anticipated to be stable. The two Cp's contribute 12 electrons and three ligands 6 electrons, so a d^0 complex is of the saturated 18 electron type. There are obvious steric prohibitions at work here as well.

Construction of the molecular orbitals for a Cp_2ML_2 complex yields a similar pattern with one important difference. The ligand set will have donor functions of a_1 and b_2 symmetry, shown at the right of **184**. The b_2 function will interact strongly with the Cp_2M b_2 orbital. The a_1 donor will overlap most

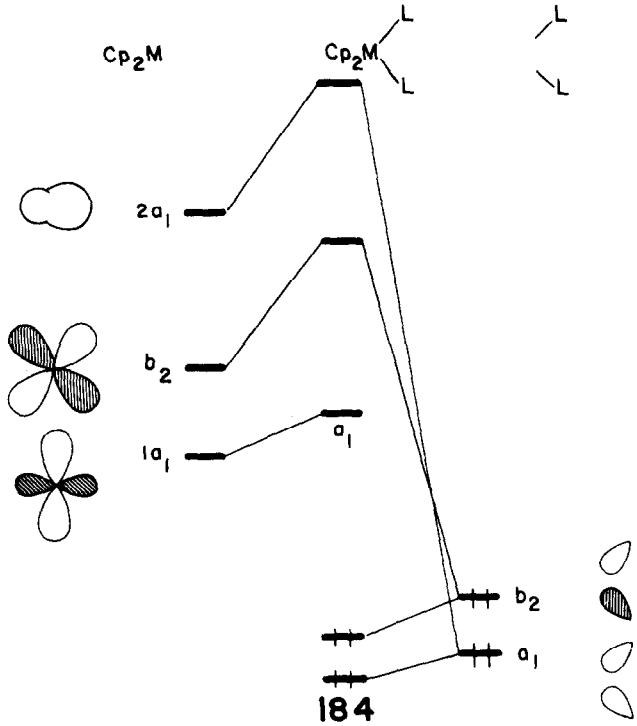

184

strongly with $2a_1$. The lone pairs will lie almost on the nodal plane of $1a_1$ and the resultant overlap will be small. Therefore, Cp_2M $1a_1$, labeled a_1 in **184**, remains essentially nonbonding. A d^2 complex with a_1 filled is expected to be stable by the 18 electron rule. However, a_1 is well separated from the two M–L bonding orbitals and the two metal centered antibonding levels. Therefore, a 16 electron, d^0 complex with a_1 empty should also be stable. In fact, this electron count is very common for the system. One can see important reactivity differences emerging on the basis whether $2a_1$ is filled or empty.

Consider reductive elimination in dialkyl substituted complexes. In **185** the orbitals of $d^0Cp_2MR_2$ are listed. They were constructed in **184**. **186** shows the three valence orbitals of d^2Cp_2M along with the σ

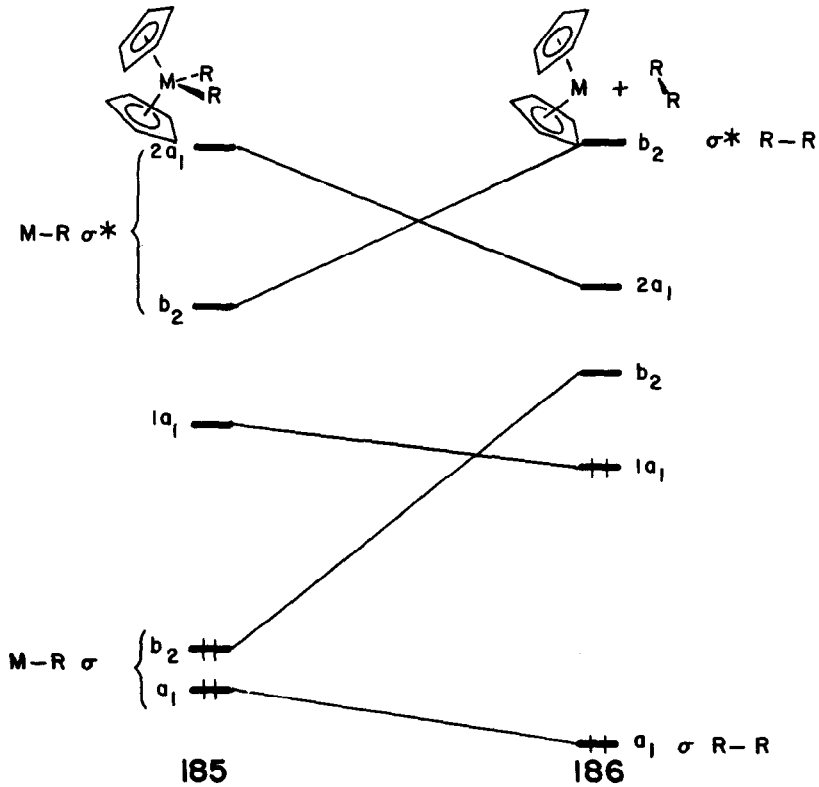

185 186

and σ^* levels of the alkane formed. The correlation is drawn for a least motion pathway which, therefore, maintains C_{2v} symmetry. That reaction is symmetry forbidden.[111] A non-least motion pathway would have to be followed. Notice also that this symmetry prohibition would be removed for a $d^2Cp_2MR_2$ complex. In that case $1a_1$ is filled in **185** and a d^4Cp_2M species (with b_2 occupied in **186**) is formed. The reaction is now symmetry allowed. But, the reductive elimination pathway may require high activation energies. The MR_2 bonding orbital must rise to the nonbonding b_2 Cp_2M level. The reverse pathway, insertion of d^4Cp_2M into a C–C (or C–H) bond is expected to be more favorbale. There is some evidence for this reaction.[112]

A key intermediate for olefin polymerization using homogeneous Ziegler–Natta catalysts are (alkyl)(olefin)Cp_2M complexes.[7,113] The electronic structure for them will be very similar to the previous example. The alkyl group presents a lone pair and ethylene a π orbital to be used as donors. Combinations of the two will find symmetry matches with $2a_1$ and b_2 of Cp_2M. The $1a_1$ orbital instead of being nonbonding will overlap substantially with ethylene π^*—**187**. That will stabilize $1a_1$. On going from

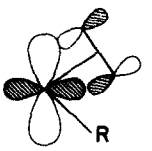

187

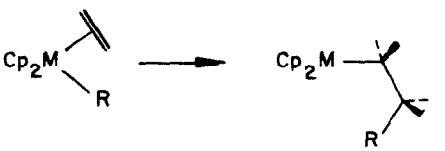

188 **189**

188 to **189** the two donor combinations smoothly transform into the R–C and M–C bonds. A potential problem is that $1a_1$ in **189** is also no longer nonbonding. The one pair of the newly formed alkyl group will overlap with *both* $1a_1$ and $2a_1$. Both are destabilized and so **187** correlates to an orbital which lies much higher in energy. The moral of this story is that for the **188** to **189** process, $1a_1$ (**187**) should be empty. In other words, a coordinatively unsaturated d^0 system is expected to undergo the reaction with an activation energy lower than that in a saturated d^2 complex.[111]

A different twist on these kinds of reactions is provided by the oxidative coupling of bis(ethylene)Cp_2Ti to a titanacyclopentane complex, **190–191**. The orbitals of **190** are constructed in Fig. 19.[111]

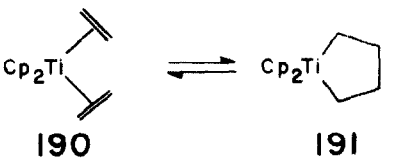

190 **191**

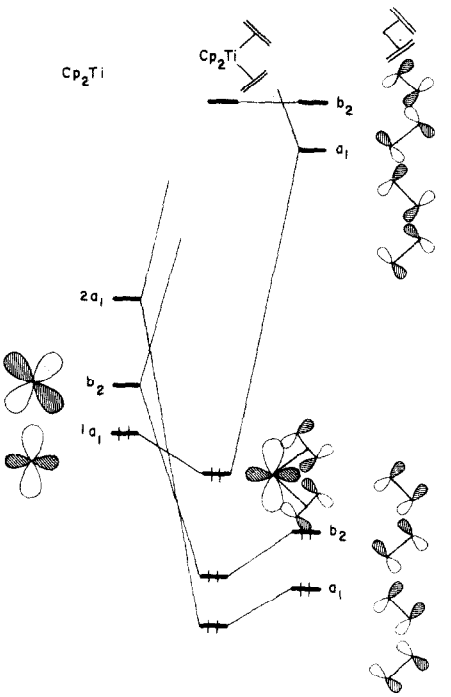

Fig. 19. Interaction diagram for bis(ethylene)Cp_2Ti.

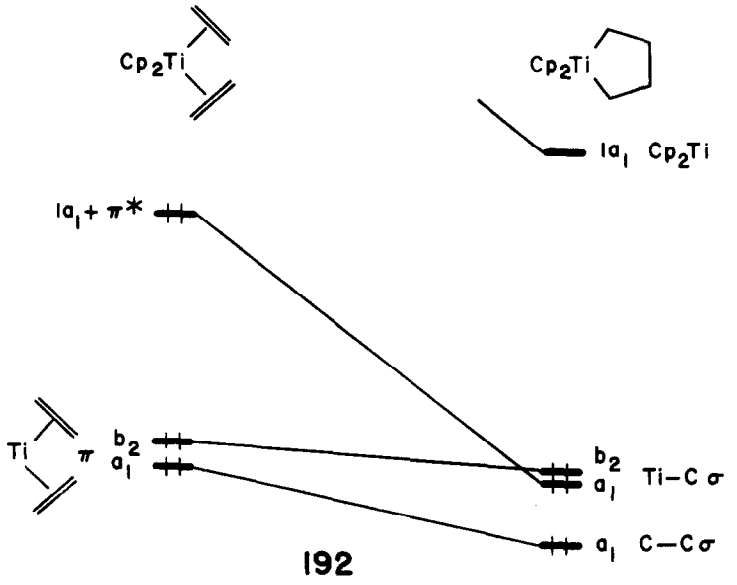

192

In-phase and out-of-phase combinations of the ethylene π orbitals are of a_1 and b_2 symmetry. They interact with $2a_1$ and b_2 of Cp_2Ti. The $1a_1$ Cp_2Ti level is now especially stabilized by the in-phase combination of the ethylene π^* set. It is drawn out explicitly in the center of this Figure. On going to **191** there have been two Ti–C bonds formed. The electronic structure will strongly resemble that for Cp_2ML_2 in **184**. It is a d^0 complex so that $1a_1$ is empty. Additionally, one C–C bond has been formed. A partial correlation diagram for a least motion pathway from **190** to **191** which maintains C_{2v} symmetry is shown in **192**.[111] The reaction is symmetry allowed. The $1a_1$ level in the bis-ethylene complex goes down in energy to become one of the Ti–C σ orbitals. The oxidative coupling reaction has also been theoretically studied for a number of other systems.[65g,114] The electronic details are very strongly influenced not only by the number of electrons at the metal but also the number and geometrical position of the other ligands. One must not forget that the remaining ligands, be they multidentate like Cp or of the single σ donor type, tailor the metal orbitals to specific shapes and energy patterns.

IX. FUTURE DEVELOPMENTS AND METHODS

We have spent considerable time delineating the valence orbitals of ML_n fragments. This was done to highlight the interrelationships between the two families of fragments which originate from the octahedron and square-plane. Also, those fragments along with Cp_2M are the most common ones in complexes which contain a single transition metal. Other groups of fragments, for example those given by **155–158** in Chart II, could have been utilized. The large field of metalloboranes and carboranes has not been represented in this review. Many interesting parallels can be found here, as well. For example, Hawthorne first reported[115] that the $C_2B_9H_{11}^{2-}$ cage was equivalent to Cp^-. This basically has been borne out by calculations.[116] We also have not spent much time with transition metal dimers and clusters. This is one area where a good bit of theoretical work needs to be done. The fragment molecular orbital methodology can be used just as easily here. A little more care must be taken to develop the fragment orbitals. For example, the M_2L_6—sawhorse fragment **193** has been constructed[117] by combining two ML_3

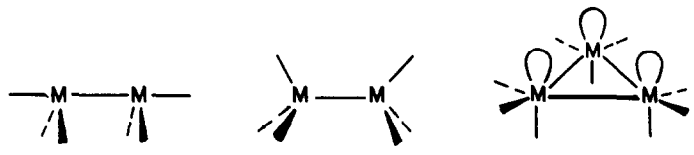

193 194 195

fragments to give **194**. The ML_3 units are then bent back to the geometry in **193**. Recall from Fig. 14 that the ML_3 fragment has six valence orbitals. The 12 in **193** become cumbersome. A simplification can often be made by neglecting those which are derived from relatively low-lying combinations—$1a_1$ and 1e in ML_3. Actually in **193** there are five orbitals which form the dominant bonding contributions to

coordinated polyenes. Extensive use of the M_3L_9 fragment has also been made[118] to study the electronic structure of metal clusters. A difficult way to develop the valence orbitals of **195** would be to combine three ML_3 units. It is easier to take three $C_{2v}ML_4$ fragments and build the orbitals of M_3L_{12}, **168**. Then three *cis*, axial ligands are removed to give **195**. It is easy to see that there will be formed three hybrid orbitals of $a_1 + e$ symmetry pointing toward the missing ligands.

It is usual for the symmetry-based arguments presented in this review to be buttressed by molecular orbital calculations. But it is important to realize that this strategy for analyzing the electronic structure is very powerful. It is based only on symmetry properties and the elementary perturbation ideas expressed in Section II. Therefore, calculations at any level (within reason) should show these patterns. The *magnitudes* of the effects may be method dependent, however. The extended Hückel method[119] is the most elementary. Because of its transparency it presents the clearest picture of how the electronic structure, orbital by orbital, varies with respect to the structure of the molecule or reacting system. Angular variations are normally well-described and bond-length variations are not.[120] At an intermediate level are the Fenske-Hall[121] and CNDO/INDO[122] methods. The former cannot be used for geometrical optimizations but does an admirable job in the calculation of spectroscopic quantities. The latter method exists in many parameterization schemes. It is difficult to make a decision on which form is the most accurate one in the transition metal field. There seem to be problems with any of the CNDO/INDO schemes in giving correct geometries. For example, ethylene-$Fe(CO)_4$ is predicted to be more stable in conformation **64** rather than **63**.[123] In fact, the opposite geometry is more stable and calculated to be so by ~30 kcal/mol at the extended Hückel[32a] and *ab initio*[42] levels. Such conformational questions can be of importance in reactions, but that does not mean that the results of calculations at this level cannot be trusted for an analysis of reactions or calculations of spectroscopic properties. One must be aware of potential problems. Nor are calculations at the $\chi\alpha$[124] or *ab initio* SCF levels problem-free, even though they are at the highest level of sophistication. $\chi\alpha$ calculations are very useful for the calculation of ionization potentials and excitation energies. Problems which involve bond-length, bond-angle or conformational variations cannot be treated in a direct fashion. Therefore, reactions cannot be studied with $\chi\alpha$. There have been several revealing studies of geometrical optimizations at the *ab initio* level. The optimum Fe–C distances in ferrocene were found[125] to be 1.93 and 1.94 Å, depending upon the basis set size. Whereas, the experimental distance is 1.65 Å. One might have expected a result like this from extended Hückel! It has been shown by Kirschenbaum, Howell and Rossi[126] that the calculated optimum Ni–C bond distance in $Ni(CO)_4$ is sensitive to the orbital exponents chosen for the 4s and 4p orbitals. The relative ordering of molecular orbitals at the *ab initio* level is sometimes nonintuitive. Bursten, Fenske *et al.*[127] have indicated that the reason why $\chi\alpha$, the Fenske–Hall method, or extended Hückel give results superior in this regard to *ab initio* calculations for transition metal complexes is that spherical averaging of the potential about the metal atom has been included for the former three methods. This, of course, also has a bearing on the interpretation of photoelectron spectra in organometallic compounds[128] and the validity of Koopman's theorem.[129] In this reviewer's mind both the size of the basis set and the values of the orbital exponents, particularly of the $(n + 1)$ s and p type need to be investigated at the *ab initio* level before configurational interaction and other treatments beyond the Hartree–Fock level are called into action. One would like to see a basis set development done along the lines of the Pople group for the first and second row atoms[130] extended to the transition metal series.[131] It is not my intent in this discussion to deprecate any method. Many successes have been garnered in each. But as consumers of molecular orbital theory, we should not put blind faith in the actual numbers of calculations. These in my mind are not so important. What should be of primary concern is how did the numbers come about. A clear, logical framework for analyzing the results must be established. It is here where the most important business of extrapolation and prediction can begin.

A number of typical reactions in organometallic chemistry were covered in this review. Actually the vast majority of theoretical work has been directed toward an understanding of the geometrical and electronic structures of organo-metallic molecules. The study of reaction mechanisms has just begun and there is much work to do here. A study of the bonding, structures, and reactions in transition metal clusters was another area previously mentioned. Extending this leads to the study of surfaces and solid-state structures. These are infinite systems in one to three dimensions and different methods where periodic boundary conditions must be applied. A pictorial description of molecular orbital interactions, etc. becomes difficult. Burdett and coworkers[132] in particular have initiated research in this direction. Here, too, there is much to be learned.

Acknowledgements—I wish to thank Professors J. Burdett, B. E. Bursten, A. Dedieu, R. Gleiter, M. B. Hall, R. Hoffmann, and P. Hofmann in particular, for many private communications and preprints of their work, and to J. Richard Keistler for typing the manuscript. Much of our work described here was generously supported by the Robert A. Welch Foundation and the Camille and Henry Dreyfus Foundation for a Teacher–Scholar award.

REFERENCES

[1a]G. W. Parshall, *Homogeneous Catalysis.* Wiley, New York (1980); [b]A. Nakamura and M. Tsutsui, *Principles and Applications of Homogeneous Catalysis.* Wiley, New York (1980); [c]G. Henrici-Olive and S. Olive, *Coordination and Catalysis.* Verlag-Chemie, Weinheim (1977); [d]A. E. Martell and T. Kham, *Homogeneous Catalysis*, Vols. I and II. Academic Press, New York (1973).

[2a]J. P. Collman and L. S. Hegedus, *Principles and Applications of Organotransition Metal Chemistry.* University Science Books, Mill Valley (1980); [b]R. F. Heck, *Organotransition Metal Chemistry.* Academic Press, New York (1974).

[3]T. J. Kealy and P. J. Pauson, *Nature (London)* **168**, 1039 (1951).

[4]G. Wilkinson, M. Rosenblum, M. C. Whiting and R. B. Woodward, *J. Am. Chem. Soc.* **74**, 2125 (1952).

[5]E. O. Fischer and W. Pfab, *Z. Naturforsch.* **7b**, 377 (1952).

[6]P. Seiler and J. D. Dunitz, *Acta Cryst.* **B35**, 2020 (1979) and Refs. therein.

[7]J. Boor, *Ziegler–Natta Catalysts and Polymerizations.* Academic Press, New York (1979); K. Ziegler, *Adv. Organomet. Chem.* **6**, 1 (1968).

[8]J. Schwartz and J. A. Labinger, *Angew. Chem. Int. Ed. Engl.* **15**, 333 (1976).

[9]W. C. Zeiss, *Ann. Phys.* **9**, 932 (1827).

[10]C. E. Holloway, G. Hulley, B. F. G. Johnson and J. Lewis, *J. Chem. Soc. A*, 53 (1969); 1653 (1970); J. Ashley-Smith, Z. Douek, B. F. G. Johnson and J. Lewis, *J. Chem. Soc. Dalton Trans.* 128 (1974); J. Ashley-Smith, I. Douek, B. F. G. Johnson and J. Lewis, *Ibid.* 1776 (1972).

[11]K. Kawakami, K. Ishii and T. Tanaka, *Bull. Chem. Soc. Jpn.* **48**, 105 (1975).

[12]D. J. Bauer and C. Krüger, *J. Organomet. Chem.* 77, 423 (1974); C. D. Cook and K. Y. Wan, *Inorg. Chem.* **10**, 2696 (1971).

[13]For recent reviews see: [a]D. M. P. Mingos, *Adv. Organomet. Chem.* **15**, 1 (1977); [b]R. Hoffmann, *Science*, **211**, 995 (1981); [c]J. K. Burdett, *Molecular Shapes.* Wiley, New York (1980).

[14]The theoretical underpinnings have been developed in H. Fujimoto and R. Hoffmann, *J. Phys. Chem.* **78**, 1167 (1974); R. Hoffmann, H. Fujimoto, J. R. Swenson and C.-C. Wan, *J. Am. Chem. Soc.* **95**, 7644 (1973).

[15]The decomposition of the molecular orbitals of a molecule in terms of the molecular orbitals of fragments can be done in an exact way within the extended Hückel method. An approximate method for this analytical procedure at the *ab initio* level and its use in organic chemistry has been developed by Whangbo and Wolfe, see M.-H. Whangbo, H. B. Schlegel and S. Wolfe, *J. Am. Chem. Soc.* **99**, 1296 (1977); M.-H. Whangbo and S. Wolfe, *Isr. J. Chem.* **20**, 36 (1980).

[16]An excellent discussion on the interaction of orbitals as applied to organic chemistry is to be found in R. Hoffmann, *Accts. Chem. Res.* **4**, 1 (1971).

[17]See for example, K. Müller, *Helv. Chim. Acta*, **53**, 1112 (1970); L. Salem, *J. Am. Chem. Soc.* **90**, 543 (1968).

[18]For an excellent guide to group theory, see F. A. Cotton, *Chemical Applications of Group Theory*, 2nd Edn. Wiley, New York (1971).

[19]F. A. Cotton and G. Wilkinson, *Advanced Inorganic Chemistry*, 4th Edn. Interscience, New York (1980); K. F. Purcell and J. C. Kotz, *Inorganic Chemistry.* Saunders, Philadelphia (1977).

[20]R. J. Goddard, R. Hoffmann and E. D. Jemmis, *J. Am. Chem. Soc.* **102**, 7667 (1980).

[21]T. Ziegler and A. Rauk, *Inorg. Chem.* **18**, 1755 (1979).

[22]M. Elian and R. Hoffmann, *Ibid.* **14**, 1058 (1975); J. K. Burdett, *J. Chem. Soc. Faraday Trans.* 2 **70**, 1599 (1974); *Inorg. Chem.* **14**, 375 (1975).

[23]R. N. Perutz and J. J. Turner, *J. Am. Chem. Soc.* **97**, 4791, 4805 (1975); *Inorg. Chem.* **14**, 262 (1975); J. K. Burdett, J. M. Gryzbowski, R. N. Perutz, M. Poliakoff, J. J. Turner and R. F. Turner, *Ibid.* **17**, 147 (1978).

[24]P. J. Hay, *J. Am. Chem. Soc.* **100**, 2411 (1978).

[25]D. L. Lichtenberger and T. L. Brown, *Ibid.* **100**, 366 (1978).

[26]H. Huber, E. P. Kundig, G. A. Ozin and A. J. Poe, *Ibid.* **95**, 308 (1975).

[27]For reviews of matrix isolation of metal carbonyls see: J. K. Burdett, *Coord. Chem. Rev.* **27**, 1 (1978); J. J. Turner, J. K. Burdett, R. N. Perutz and M. Poliakoff, *Pure Appl. Chem.* **49**, 271 (1977); *Cryogenic Chemistry* (Edited by G. A. Ozin and M. Moskovitz). Wiley, New York (1976).

[28]For reviews, see F. Calderazzo, *Angew, Chem.* **89**, 305 (1977); G. Henrici-Olive and S. Olive, *Ibid.* **88**, 144 (1976); see also Refs. 1 and 2.

[29]H. Berke and R. Hoffmann, *J. Am. Chem. Soc.* **100**, 7224 (1978); M. E. Ruiz, A. Flores-Riveras and O. Novaro, *J. Catal.* **64**, 1 (1980).

[30]J. L. Petersen, R. K. Brown and J. M. Williams, *Inorg. Chem.* **20**, 158 (1981); J. Roziere, J. M. Williams, R. P. Steward, Jr., J. L. Petersen and L. F. Dahl, *J. Am. Chem. Soc.* **99**, 4497 (1977); R. D. Wilson, S. A. Graham and R. Bau, *J. Organomet. Chem.* **91**, C49 (1975); R. Bau, R. G. Teller, S. W. Kirtley and T. F. Koetzle, *Accts. Chem. Res.* **12**, 176 (1979); J. L. Petersen, P. L. Johnson, J. O'Connor, L. F. Dahl and J. M. Williams, *Inorg. Chem.* **17**, 3460 (1978); J. L. Petersen, R. K. Brown, J. M. Williams and R. K. McMullan, *Ibid.* **18**, 3493 (1979).

[31]J. K. Burdett, *Inorg. Chem.* **17**, 2537 (1978).

[32a]T. A. Albright, R. Hoffmann, J. C. Thibeault and D. L. Thorn, *J. Am. Chem. Soc.* **101**, 3801 (1979); [b]P. J. Hay, *Ibid.* **103**, 1390 (1981). [c]T. Ziegler and A. Rauk, *Inorg. Chem.* **18**, 1558 (1979).

[33]M. J. S. Dewar, *Bull. Soc. Chim. Fr.* **18**, C79 (1951); J. Chatt and L. A. Duncanson, *J. Chem. Soc.* 2939 (1953).

[34]L. L. Wright, R. M. Wing, M. F. Rettig and G. R. Wiger, *J. Am. Chem. Soc.* **102**, 5949 (1980).

[35]C. E. Hollaway, G. Hulley, B. F. G. Johnson and J. Lewis, *J. Chem. Soc.* (*A*), 53 (1969). For a full listing see Ref. 32[a].

[36]C. Bachmann, J. Demuynck and A. Veillard, *J. Am. Chem. Soc.* **100**, 2366 (1978).

[37]J. K. Burdett and T. A. Albright, *Inorg. Chem.* **18**, 2112 (1979).

[38]D. L. Thorn and R. Hoffmann, *J. Am. Chem. Soc.* **100**, 2079 (1978).

[39]A. Dedieu, *Inorg. Chem.* **19**, 375 (1980); **20**, 2803 (1981).

[40]E. O. Fischer, *Adv. Organomet. Chem.* **14**, 1 (1976); D. J. Cardin, B. Cetinkaya, M. J. Doyle and M. F. Lappert, *Chem. Rev.* **72**, 545 (1972); *Chem. Soc. Rev.* **2**, 99 (1973).

[41]W. M. Butler and J. H. Enemark, *Inorg. Chem.* **12**, 540 (1973); O. P. Anderson and A. B. Packard, *Ibid.* **17**, 1333 (1978); D. J. Cardin, B. Cetinkaya, M. F. Lappart, L. J. Manojlovic-Muir and K. W. Muir, *Chem. Commun.* 400 (1971).

[42]J. Demuynck, A. Strich and A. Veillard, *Nouveau J. Chim.* **1**, 217 (1977).

[43]A review of the structures of olefin-ML_n complexes may be found in S. D. Ittel and J. A. Ibers, *Adv. Organomet. Chem.* **14**, 33 (1976). A complete listing may be found in Ref. 32[a].
[44]Walsh diagrams have been beautifully elaborated for organic and main group systems in B. M. Gimarc, *Molecular Structure and Bonding*. Academic, New York (1979) and J. K. Burdett for inorganic systems—see Ref. 13[c].
[45]G. Del Piero, G. Perego and M. Cesari, *Cryst. Struct. Commun.* **3**, 15 (1974); C. Nave and M. R. Truter, *J. Chem. Soc. Dalton Trans.* 2202 (1973); K. van Putte and A. van der Ent, *Inorg. Chim. Acta* **7**, 497 (1973).
[46]See, for example, J. A. Segal and B. F. G. Johnson, *J. Chem. Soc. Dalton Trans* **677**, 1990 (1975); L. Kruczynski, L. K. K. LiShingMan and J. Takats, *J. Am. Chem. Soc.* **96**, 4006 (1974); S. T. Wilson, N. J. Coville, J. R. Shapley and J. A. Osborn, *Ibid.* **96**, 4038 (1974).
[47]T. A. Albright, R. Hoffmann, Y.-C. Tse and T. D'Ottavio, *J. Am. Chem. Soc.* **101**, 3812 (1979).
[48]R. Ben-Shoshan and R. Pettit, *Ibid.* **89**, 2231 (1967).
[49]T. A. Albright, to be published.
[50a]O. Eisenstein and R. Hoffmann, *Ibid.* **102**, 6148 (1980); **103**, 4308 (1981); [b]For a general theoretical analysis and review of nucleophilic addition to polyene-ML_n complexes, see: S. G. Davies, M. L. H. Green and D. M. P. Mingos, *Tetrahedron*, **34**, 3047 (1978); *Nouv. J. Chim.* **1**, 445 (1977); see also S. Sakaki, M. Nishikawa and A. Ohyoshi, *J. Am. Chem. Soc.* **102**, 4062 (1980).
[51a]L. J. Radonovich, F. J. Koch and T. A. Albright, *Inorg. Chem.* **19**, 3373 (1980); [b]L. J. Radonovich, K. J. Klabunde, C. B. Behrens, D. P. McCollar and B. B. Anderson, *Ibid.* **19**, 1221 (1980); K. J. Klabunde, B. B. Anderson, M. Bader and L. J. Radonovich, *J. Am. Chem. Soc.* **100**, 1313 (1978); [c]For related cases see M. J. Nolte, G. Gafner and L. Haines, *Chem. Commun.* 1406 (1969); M. J. Nolte and G. Gafner, *Acta Crystallogr. Sect. B.* **30**, 738 (1974).
[52]U. Griebsch and H. Hoberg, *Angew. Chem.* **90**, 1014 (1978); H. Hoberg and C. Frohlich, *Ibid.* **92**, 131 (1980); H. Hoberg and W. Richter, *J. Organomet. Chem.* **195**, 347, 355 (1980).
[53]B. E. Bursten and R. F. Fenske, *Inorg. Chem.* **18**, 1760 (1979).
[54]L. R. Byers and L. F. Dahl, *Ibid.* **19**, 277 (1980).
[55]T. A. Albright, *J. Organomet. Chem.* **198**, 159 (1980).
[56]T. A. Albright and R. Hoffmann, *Chem. Ber.* **111**, 1578 (1978).
[57]D. M. P. Mingos, *J. Chem. Soc. Dalton Trans.* 602 (1977); D. M. P. Mingos, M. I. Forsyth and A. J. Welch, *Ibid.* 1363 (1978); D. M. P. Mingos and A. J. Welch, *Ibid.* 1674 (1980).
[58]H. Brunner, *Forschr. Chem. Forsch.* **56**, 67 (1975).
[59a]P. Hofmann, *Angew. Chem.* **89**, 551 (1977); [b]P. Hofmann, Habilitationschrift, Uni. Erlangen (1978).
[60]An excellent theoretical discussion of inversion barriers has been given by C. C. Levin, *J. Am. Chem. Soc.* **97**, 5649 (1975); see also Ref. 44.
[61]D. M. P. Mingos and C. R. Nurse, *J. Organomet. Chem.* **184**, 281 (1980).
[62]C. Mealli, S. Midollini, S. Moneti, L. Sacconi, J. Silvestre and T. A. Albright, *J. Am. Chem. Soc.* **104**, 95 (1982).
[63]T. A. Albright, to be published.
[64]D. M. P. Mingos, *J. Chem. Soc. Dalton Trans.* **31** (1977).
[65a]K. Tatsumi, R. Hoffmann, A. Yamamoto and J. K. Stille, *Bull. Chem. Soc. Jpn.* **54**, 1857 (1981); [b]R. Hoffmann, *Pure and Applied Chem.* in press; [c]S. Kominya, T. A. Albright, R. Hoffmann and J. K. Kochi, *J. Am. Chem. Soc.* **98**, 7255 (1976); [d]S. Kominya, T. A. Albright, R. Hoffmann and J. K. Kochi, *J. Am. Chem. Soc.* **99**, 8440 (1977); [e]R. G. Pearson, *Symmetry Rules for Chemical Reactions*, pp. 286, 405. Wiley-Interscience, New York (1976); [f]B. Åkermark and A. Ljungqvist, *J. Organomet. Chem.* **182**, 59 (1979); B. Akermark, H. Johansen, B. Roos and U. Wahlgen, *J. Am. Chem. Soc.* **101**, 5876 (1979); [g]R. J. McKinney, D. L. Thorn, R. Hoffmann and A. Stokis, *J. Am. Chem. Soc.* **103**, 2595 (1981); [h]K. Kitaura, S. Obara and K. Morokuma, *Ibid.* **103**, 2891 (1981).
[66]See, for example C. A. Coulson, *Valence*, 2nd Edn, p. 65. Oxford University Press, Oxford (1961).
[67]For excellent discussions of avoided crossings in organic chemistry particularly at the state, rather than orbital level, see L. Salem, C. Leforestier, G. Segal and R. Wetmore, *J. Am. Chem. Soc.* **97**, 479 (1975); A. Devaguet, *Pure Appl. Chem.* **41**, 455 (1975).
[68]For reviews of the experimental literature, see Ref. 65[a-d].
[69]T. A. Albright, P. Hofmann and R. Hoffmann, *J. Am. Chem. Soc.* **99**, 7546 (1977).
[70a]D. L. Lichtenberger and R. F. Fenske, *J. Am. Chem. Soc.* **98**, 50 (1976); [b]T. H. Whitesides, D. L. Lichtenberger and R. A. Budnik, *Inorg. Chem.* **14**, 68 (1975).
[71]L. E. Orgel, *An Introduction to Transition Metal Chemistry*, p. 174. Wiley, New York (1960).
[72]E. S. Magyar and C. P. Lillya, *J. Organomet. Chem.* **116**, 99 (1976).
[73]R. B. Bates, W. A. Beavers, B. Gordon III and N. S. Mills, *J. Org. Chem.* **44**, 3800 (1979); J. J. Bahl, R. B. Bates, W. A. Beavers and N. S. Mills, *Ibid.* **41**, 1620 (1976).
[74]D. L. Lichtenberger and R. F. Fenske, *J. Organomet. Chem.* **117**, 253 (1976); *Inorg. Chem.* **15**, 2015 (1976); J. L. Hubbard and D. L. Lichtenberger, *Ibid.* **19**, 1388 (1980).
[75]T. A. Albright, *Trans. Am. Crystallogr. Ass.* **16**, 35 (1980).
[76]R. Hoffmann, J. M. Howell and A. R. Rossi, *J. Am. Chem. Soc.* **98**, 2484 (1976); for similar work on ML_5, ML_7 and ML_8 complexes see A. R. Rossi and R. Hoffmann, *Inorg. Chem.* **14**, 365 (1975); R. Hoffmann, B. F. Beier, E. L. Muetterties and A. R. Rossi, *Ibid.* **16**, 511 (1977); J. K. Burdett, R. Hoffmann and R. C. Fay, *Ibid.* **17**, 2553 (1978).
[77]For a review see M. F. Semmelhack, *Ann. N.Y. Acad. Sci.* **295**, 66 (1977).
[78]T. A. Albright and B. K. Carpenter, *Inorg. Chem.* **19**, 3092 (1980).
[79]M. B. Hall, to be submitted.
[80]M. F. Semmelhack, G. Clark, R. Farina and M. Saeman, *J. Am. Chem. Soc.* **101**, 217 (1979).
[81]W. R. Jackson and W. B. Jennings, *Chem. Commun.* 824 (1966).
[82]For a review of these structural patterns see F. H. Herbstein and M. G. Reisner, *Acta Crystallogr.* **B33**, 3304 (1977).
[83]The p.e. spectra for butadiene and cyclobutadiene-$Fe(CO)_3$ derivatives have been discussed by S. D. Worley, T. R. Webb, D. H. Gibson and T. S. Ong, *J. Organomet. Chem.* **168**, C16 (1979); *J. Electron Spectr.* **18**, 189 (1980); J. C. Green, P. Powell and J. van Tilborg, *J. Chem. Soc. Dalton Trans.* 1974 (1976); M. C. Böhm and R. Gleiter, *J. Comput. Chem.* **1**, 407 (1980).
[84]T. A. Albright, R. Hoffmann and P. Hofmann, *Chem. Ber.* **111**, 1591 (1978).
[85a]M. Brookhart, private communication; [b]R. L. Harlow, R. J. McKinney and S. D. Ittel, *J. Am. Chem. Soc.* **101**, 7476 (1979).
[86]M. Elian, M. M. L. Chen, D. M. P. Mingos and R. Hoffmann, *Inorg. Chem.* **15**, 1148 (1979).
[87]J. Halpern, *Advances in Chemistry: Homogeneous Catalysis*, No. 70, pp. 1–24. American Chemical Society, Washington, D.C. (1968).
[88]K. Wade, *Chem. Commun.* 792 (1971); *Inorg. Nucl. Chem. Letts.* **8**, 559, 563 (1972); *Adv. Inorg. Radiochem.* **18**, 1 (1976).
[89]D. M. P. Mingos, *Nature (London), Phys. Sci.* **236**, 99 (1972).

[90]A good introduction to the shapes of the orbitals in organic fragments and molecules may be found in W. L. Jorgensen and L. Salem, *The Organic Chemist's Book of Orbitals*. Academic Press, New York (1973).
[91a]P. Brint, K. Pelin and T. R. Spalding, *Inorg. Nucl. Chem. Letts.* **16**, 391 (1980); *J. Chem. Soc. Dalton Trans.* 546 (1981); [b]A. Sevin and A. Devaquet, *Nouv. J. Chim.* **1**, 357 (1977); [c]J. Chandrasekhar, P. V. R. Schleyer and H. B. Schlegel, *Tetrahedron Letters* 3393 (1978); [d]V. I. Minkin and R. M. Minyaev, *Zh. Org. Khim.* **15**, 1569 (1979); R. M. Minyaev, V. I. Minkin, N. S. Zefirov and Yu. A. Zhdanov, *Ibid.* **15**, 2009 (1979); [e]T. Clark and P. V. R. Schleyer, *Nouv. J. Chim.* **2**, 665 (1978); [f]K. Krogh-Jespersen, D. Cremer, D. Poppinger, J. A. Pople, P. V. R. Schleyer and J. Chandrasekhar, *J. Am. Chem. Soc.* **101**, 4843 (1979); [g]J. A. Ulman, E. L. Andersen and T. P. Fehlner, *Ibid.* **100**, 456 (1978).
[92]R. P. Kirchen, K. Ranganayakulu, A. Rauk, B. P. Singh and T. S. Sorensen, *Ibid.* **103**, 588 (1981); R. P. Kirchen, N. Okazawa, K. Ranganyakulu, A. Rauk and T. S. Sorensen, *Ibid.* **103**, 597 (1981).
[93]T. J. Marks and J. R. Kolb, *Chem. Rev.* **77**, 263 (1977).
[94]H. Hogeveen and P. W. Kwant, *Acc. Chem. Res.* **8**, 413 (1975); H. Hogeveen and E. M. G. A. van Kruchten, *J. Org. Chem.* **46**, 1350 (1981).
[95]Equivalent main group analogs, $Me_5C_5Sn^+$ and $Me_5C_5Ge^+$ are also known and have been the subject of theoretical studies; P. Jutzi, F. Kohl, P. Hofmann, C. Krüger and Y.-H. Tsay, *Chem. Ber.* **113**, 757 (1980).
[96]For a review see W. Herrmann, *Angew. Chem.* **90**, 855 (1978).
[97]P. Hofmann, *Angew. Chem.* **91**, 591 (1979); B. E. R. Schilling and P. Hofmann, to be published.
[98]E. Band and E. L. Muetterties, *Chem. Rev.* **78**, 639 (1978); J. Evans, *Adv. Organomet. Chem.* **16**, 319 (1977); R. E. Benfield and B. F. G. Johnson, *J. Chem. Soc. Dalton Trans.* 1554 (1978); *Ibid.* 1743 (1980).
[99a]A. R. Pinhas, T. A. Albright, P. Hofmann and R. Hoffmann, *Helv. Chim. Acta* **63**, 29 (1980); [b]S. Shaik and R. Hoffmann, *J. Am. Chem. Soc.* **102**, 1194 (1980); S. Shaik, R. Hoffmann, C. R. Fisel and R. H. Summerville, *Ibid.* **102**, 4555 (1980); [c]E. D. Jemmis, A. R. Pinhas and R. Hoffmann, *Ibid.* **102**, 2576 (1980); [d]B. E. R. Schilling and P. Hofmann, to be published. [e]V. Bellagamba and A. Gamba, *J. Organomet. Chem.* **212**, 125 (1981).
[100a]M. Bernard, *Inorg. Chem.* **18**, 2782 (1979); [b]R. H. Summerville and R. Hoffmann, *J. Am. Chem. Soc.* **101**, 3821 (1979); **98**, 7240 (1976); R. Hoffmann, B. E. R. Schilling, R. Bav, H. D. Kaesz and D. M. P. Mingos, *Ibid.* **100**, 6088 (1978); [c]J. Evans, *J. Chem. Soc. Dalton Trans.* 1005 (1980); [d] D. L. DuBois, W. K. Miller and M. Rakowski DuBois, *J. Am. Chem. Soc.* **103**, 3429 (1981).
[101]B. E. R. Schilling, R. Hoffmann and J. W. Faller, *Ibid.* **101**, 592 (1979); for a general analysis of the $CpML_2$ fragment and its bonding requirements see B. E. R. Schilling, R. Hoffmann and D. L. Lichtenberger, *Ibid.* **101**, 585 (1979).
[102a]M. Elain, M. M. L. Chen, D. M. P. Mingos and R. Hoffmann, *Inorg. Chem.* **15**, 1148 (1976); [b]J. Lauher, M. Elian, R. H. Summerville and R. Hoffmann, *J. Am. Chem. Soc.* **98**, 3219 (1976).
[103]P. Seiler and J. D. Dunitz, *Acta Cryst.* **B36**, 2255 (1980).
[104]J. H. Ammeter, N. Oswald and R. Bucher, *Helv. Chim. Acta*, **58**, 671 (1975); J. H. Ammeter, *Nouv. J. Chim.* **4**, 631 (1980) and Refs. therein.
[105]For a review see J. C. Green, *Structure and Bonding* **43**, 37–112 (1981).
[106]P. S. Bagus, U. I. Wahlgren and J. Almlöf, *J. Chem. Phys.* **64**, 2324 (1976).
[107]T. A. Albright, R. Hoffmann, C. P. Lillya, P. Dobosh and P. Hofmann, to be submitted for publication.
[108]A review of these compounds may be found in W. Siebert, *Adv. Organomet. Chem.* **18**, 301 (1980).
[109]R. B. King, *Inorg. Chem.* **7**, 1044 (1968); see also Ref. 13[c], pp. 224–225.
[110a]J. L. Petersen, D. L. Lichtenberger, R. F. Fenske and M. B. Hall, *J. Am. Chem. Soc.* **97**, 6433 (1975); J. L. Petersen and L. F. Dahl, *Ibid.* **96**, 2248 (1974); **97**, 6416, 6422 (1975); [b]H. H. Brintzinger, *J. Organomet. Chem.* **171**, 337 (1979); [c]H. H. Brintzinger, L. L. Lorh, Jr. and K. L. T. Wong, *J. Am. Chem. Soc.* **97**, 5146 (1975); [d]C. Balhausen and J. P. Dahl, *Acta Chem. Scand.* **15**, 1333 (1961); [e]N. W. Alcock, *J. Chem. Soc. A*, 2001 (1967); [f]For photoelectron studies see: C. Cauletti, J. P. Clark, J. C. Green, S. E. Jackson, I. L. Fragala, E. Ciliberto and A. W. Coleman, *J. Electron Spectr.* **18**, 61 (1980); J. C. Green, S. E. Jackson and B. Higginson, *J. Chem. Soc. Dalton Trans.* 403 (1975); H. van Dam, A. Terpstra, A. Oskam and J. H. Teuben, *Z. Naturforsch.* **36b**, 420 (1981) and Refs. therein.
[111]J. W. Lauher and R. Hoffmann, *J. Am. Chem. Soc.* **98**, 1729 (1976).
[112]C. Giannotti and M. L. H. Green, *J. Chem. Soc. Chem. Commun.* 1114 (1972); K. Elmitt, M. L. H. Green, R. A. Forder, I. Jefferson and K. Prout, *Ibid.* 747 (1974); G. P. Pez, *J. Am. Chem. Soc.* **98**, 8072 (1976) and Refs. therein.
[113]For calculations on the $TiCl_4$/alane system in regard to Ziegler–Natta polymerization see: O. Novaro, E. Blaisten-Barojas, E. Clementi, G. Giunchi and M. E. Ruiz-Vizcaya, *J. Chem. Phys.* **68**, 2337 (1978); R. McKinney, *J. Chem. Soc. Chem. Commun.* 490 (1980).
[114a]P. S. Braterman, *J. Chem. Soc. Chem. Commun.* 70 (1979); [b]Y. Wakatsuki, O. Nomura. H. Tone and H. Yamazaki, *J. Chem. Soc. Perkin II* 1344 (1980); [c]A. Stockis and R. Hoffmann, *J. Am. Chem. Soc.* **102**, 2952 (1980).
[115]M. F. Hawthorne and R. L. Pilling, *J. Am. Chem. Soc.* **87**, 3987 (1965); M. F. Hawthorne, D. C. Young, T. D. Andrews, D. V. Howe, R. L. Pilling, A. D. Pitts, M. Reintjes, L. F. Warren Jr. and P. A. Wegner, *Ibid.* **90**, 879 (1968).
[116]D. A. Brown, M. O. Fanning and N. J. Fitzpatrick, *Inorg. Chem.* **17**, 1620 (1978); **19**, 1822 (1980).
[117]D. L. Thorn and R. Hoffmann, *Inorg. Chem.* **17**, 126 (1978).
[118]B. E. R. Schilling and R. Hoffmann, *J. Am. Chem. Soc.* **101**, 3456 (1979); **100**, 6274 (1978); *Acta Chem. Scand.* **B33**, 231 (1979).
[119]R. Hoffmann and W. N. Lipscomb, *J. Chem. Phys.* **36**, 2179, 3489 (1962).
[120]See, however, an adaptation of the extended Hückel method which compensates for this A. B. Anderson, *J. Chem. Phys.* **62**, 1187 (1975); D. A. Pensak and R. J. McKinney, *Inorg. Chem.* **18**, 3407 (1979); R. J. McKinney and D. A. Pensak, *Ibid.* **18**, 3413 (1979).
[121]M. B. Hall and R. F. Fenske, *Inorg. Chem.* **11**, 768 (1972).
[122]J. A. Pople and D. A. Beveridge, *Approximate Molecular Orbital Theory*. McGraw-Hill, New York (1970); V. I. Baranovskii, O. V. Sizova and N. V. Ivanova, *Zh. Strukt. Khim.* **17**, 549 (1976); M. C. Böhm and R. Gleiter, *Theoret. Chim. Acta* **59**, 127, 153 (1981).
[123a]P. Mehotra, private communication; [b]R. Gleiter, private communication; [c]J. Ph. Grima, F. Choplin and G. Kaufmann, *J. Organomet. Chem.* **129**, 221 (1977); [d]The rotational barrier in TMM–$Fe(CO)_3$ is calculated to be less than 1 kcal/mol when in fact it is 20 kcal/mol—see J.-M. Savariault and J.-F. Labarre, *Inorg. Chim. Acta* **19**, L53 (1976).
[124]J. C. Slater, *Quantum Theory for Molecules and Solids: The Self-Consistent Field for Molecules and Solids*, Vol. 4. McGraw-Hill, New York (1974); K. H. Johnson, *Ann. Rev. Phys. Chem.* **26**, 39 (1975).
[125]H. P. Lüthi, J. Ammeter, J. Almlöf and K. Korsell, *Chem. Phys. Letters* **69**, 540 (1980).
[126]L. J. Kirschenbaum, J. M. Howell and A. R. Rossi, *J. Phys. Chem.* **85**, 17 (1981).
[127]B. E. Bursten, J. R. Jensen, D. J. Gordon, P. M. Treichel and R. F. Fenske, *J. Am. Chem. Soc.* **103**, 5226 (1981).
[128]For reviews see Ref. 105 and: [a]A. H. Cowley, *Prog. Inorg. Chem.* **26**, 46 (1979); [b]R. F. Fenske, *Ibid.* **21**, 179 (1976); [c]R. L. Dekock

and D. R. Lloyd, *Adv. Inorg. Chem. and Radiochem.* **16**, 65 (1974); [d]R. L. Dekock, *Electron Spectroscopy*, Vol. 1, pp. 293–353. (Edited by C. R. Brundle and A. D. Baker). Academic Press, New York (1977); [e]I. H. Hillier, *Pure Applied Chem.* **51**, 2183 (1979).
[129]See D. C. Calabro and D. L. Lichtenberger, *Inorg. Chem.* **19**, 1732 (1980); M. C. Bohm, R. Gleiter and C. D. Batich, *Helv. Chim. Acta* **63**, 990 (1980); and Refs. therein.
[130]W. J. Hehre, R. F. Stewart and J. A. Pople, *J. Chem. Phys.* **51**, 2657 (1969); R. Ditchfield, W. J. Hehre and J. A. Pople, *Ibid.* **54**, 724 (1971). See Ref. 126 for a start in this direction.
[131]In this regard, note that any molecular orbital method uses parameters.
[132]J. K. Burdett, *Nature* **279**, 121 (1979); *J. Am. Chem. Soc.* **102**, 450, 5458 (1980); J. K. Burdett *et al.*, submitted for publication.